NATIONAL AERONAUTICS AND SPACE ADMINISTRATION

Technical Memorandum 33-338

The Applications Technology Satellite Apogee Rocket Motor: A Summary Report

R. G. Anderson

JET PROPULSION LABORATORY
CALIFORNIA INSTITUTE OF TECHNOLOGY
PASADENA, CALIFORNIA

February 1, 1970

TECHNICAL REPORT STANDARD TITLE PAGE

1. Report No. 33-338	2. Government Accession No.	3. Recipient's Catalog No.
4. Title and Subtitle THE APPLICATIONS TECHNOLOGY SATELLITE APOGEE ROCKET MOTOR: A SUMMARY REPORT		5. Report Date February 1, 1970 6. Performing Organization Code
7. Author(s) R. G. Anderson		8. Performing Organization Report No.
9. Performing Organization Name and Address JET PROPULSION LABORATORY California Institute of Technology 4800 Oak Grove Drive Pasadena, California 91103		10. Work Unit No. 11. Contract or Grant No. NAS 7-100 13. Type of Report and Period Covered Technical Memorandum
12. Sponsoring Agency Name and Address NATIONAL AERONAUTICS AND SPACE ADMINISTRATION Washington, D.C. 20546		14. Sponsoring Agency Code

15. Supplementary Notes

16. Abstract

This report documents the design, development, qualification testing, and flights of a spacecraft-stage solid propellant rocket motor that was used to transfer the NASA Goddard Space Flight Center Applications Technology Satellite from its initial elliptical trajectory to a near-synchronous earth orbit. The motor fires at the apogee position of a highly elliptical transfer orbit to place the spacecraft in a circular orbit at synchronous altitude (22,300 miles). The mission requirements for precise motor thrust vector alignment during the burn phase and for dynamic balance before, during, and after burning are unique and stringent; therefore, the Development Phase has focused on producing precision components. Most developmental tests used chambers fabricated from AISI 410 stainless steel; however, a later program requirement for nonmagnetic materials caused a change to chambers of 6Al-4V titanium alloy. Several Development tests, all Qualification units, and all Flight motors have used the titanium chamber. The motor Development Phase consisted of a logical sequence of testing to confirm processing, component design, and survival ability in simulated booster and space environments, and to establish preliminary performance characteristics. The Qualification Phase, which consisted of testing eight units at simulated altitude while spinning at 100 rev/min with propellant grains conditioned to 40° or 100°F, established the exact performance characteristics of the motor.

17. Key Words (Selected by Author(s))	18. Distribution Statement
Propulsion, Solid	Unclassified -- Unlimited

19. Security Classif. (of this report)	20. Security Classif. (of this page)	21. No. of Pages	22. Price
Unclassified	Unclassified	51	

HOW TO FILL OUT THE TECHNICAL REPORT STANDARD TITLE PAGE

Make items 1, 4, 5, 9, 12, and 13 agree with the corresponding information on the report cover. Use all capital letters for title (item 4). Leave items 2, 6, and 14 blank. Complete the remaining items as follows:

3. Recipient's Catalog No. Reserved for use by report recipients.

7. Author(s). Include corresponding information from the report cover. In addition, list the affiliation of an author if it differs from that of the performing organization.

8. Performing Organization Report No. Insert if performing organization wishes to assign this number.

10. Work Unit No. Use the agency-wide code (for example, 923-50-10-06-72), which uniquely identifies the work unit under which the work was authorized. Non-NASA performing organizations will leave this blank.

11. Insert the number of the contract or grant under which the report was prepared.

15. Supplementary Notes. Enter information not included elsewhere but useful, such as: Prepared in cooperation with... Translation of (or by)... Presented at conference of... To be published in...

16. Abstract. Include a brief (not to exceed 200 words) factual summary of the most significant information contained in the report. If possible, the abstract of a classified report should be unclassified. If the report contains a significant bibliography or literature survey, mention it here.

17. Key Words. Insert terms or short phrases selected by the author that identify the principal subjects covered in the report, and that are sufficiently specific and precise to be used for cataloging.

18. Distribution Statement. Enter one of the authorized statements used to denote releasability to the public or a limitation on dissemination for reasons other than security of defense information. Authorized statements are "Unclassified–Unlimited," "U. S. Government and Contractors only," "U. S. Government Agencies only," and "NASA and NASA Contractors only."

19. Security Classification (of report). NOTE: Reports carrying a security classification will require additional markings giving security and downgrading information as specified by the Security Requirements Checklist and the DoD Industrial Security Manual (DoD 5220.22-M).

20. Security Classification (of this page). NOTE: Because this page may be used in preparing announcements, bibliographies, and data banks, it should be unclassified if possible. If a classification is required, indicate separately the classification of the title and the abstract by following these items with either "(U)" for unclassified, or "(C)" or "(S)" as applicable for classified items.

21. No. of Pages. Insert the number of pages.

22. Price. Insert the price set by the Clearinghouse for Federal Scientific and Technical Information or the Government Printing Office, if known.

NATIONAL AERONAUTICS AND SPACE ADMINISTRATION

Technical Memorandum 33-338

The Applications Technology Satellite Apogee Rocket Motor: A Summary Report

R. G. Anderson

JET PROPULSION LABORATORY
CALIFORNIA INSTITUTE OF TECHNOLOGY
PASADENA, CALIFORNIA
February 1, 1970

Preface

The work described in this report was performed by the Propulsion Division of the Jet Propulsion Laboratory.

Contents

Contents (contd)

Tables

Contents (contd)

Tables (contd)

Figures

Contents (contd)

Figures (contd)

Abstract

This report documents the design, development, qualification testing, and flights of a spacecraft-stage solid propellant rocket motor that was used to transfer the NASA Goddard Space Flight Center *Applications Technology Satellite* from its initial elliptical trajectory to a near-synchronous earth orbit. The motor fires at the apogee position of a highly elliptical transfer orbit to place the spacecraft in a circular orbit at synchronous altitude (22,300 miles). The mission requirements for precise motor thrust vector alignment during the burn phase and for dynamic balance before, during, and after burning are unique and stringent; therefore, the Development Phase has focused on producing precision components. Most developmental tests used chambers fabricated from AISI 410 stainless steel; however, a later program requirement for nonmagnetic materials caused a change to chambers of 6Al–4V titanium alloy. Several Development tests, all Qualification units, and all Flight motors have used the titanium chamber. The motor Development Phase consisted of a logical sequence of testing to confirm processing, component design, and survival ability in simulated booster and space environments, and to establish preliminary performance characteristics. The Qualification Phase, which consisted of testing eight units at simulated altitude while spinning at 100 rev/min with propellant grains conditioned to 40° or 100°F, established the exact performance characteristics of the motor.

The *Applications Technology Satellite* Apogee Rocket Motor: A Summary Report

I. Introduction

In January 1963, the Jet Propulsion Laboratory initiated a development program to provide a solid propellant apogee rocket motor (Fig. 1) for a second-generation SYNCOM (*Synchronous Communications Satellite*). This satellite, produced by Hughes Aircraft Company (HAC) under the management of Goddard Space Flight Center for the National Aeronautics and Space Administration, was designated Advanced SYNCOM. The design was that of a spin-stabilized, active repeater communications satellite weighing about 750 lb, which operated at synchronous altitude (22,300 mi) and handled voice communications, teletype, and monochrome and color television signals.

The Advanced SYNCOM program was expanded in January 1964 to include instrumentation for experiments in meteorology, communications, radiation, navigation, and gravity-gradient stabilization, as well as other engineering experiments. This redirected effort was designated the *Applications Technology Satellite* (ATS) program. Five launches, including two synchronous-altitude spin-stabilized (S/S; Fig. 2), two synchronous-altitude gravity-gradient-stabilized (S/G), and one medium-altitude gravity-gradient-stabilized (M/G) spacecraft, are planned. The *Atlas/Agena* was used to boost the synchronous-altitude spin-stabilized and the medium-altitude gravity-gradient spacecraft, and the *Atlas/Centaur* was used for the heavier synchronous-altitude gravity-gradient spacecraft. The medium-altitude gravity-gradient spacecraft did not require an apogee unit.

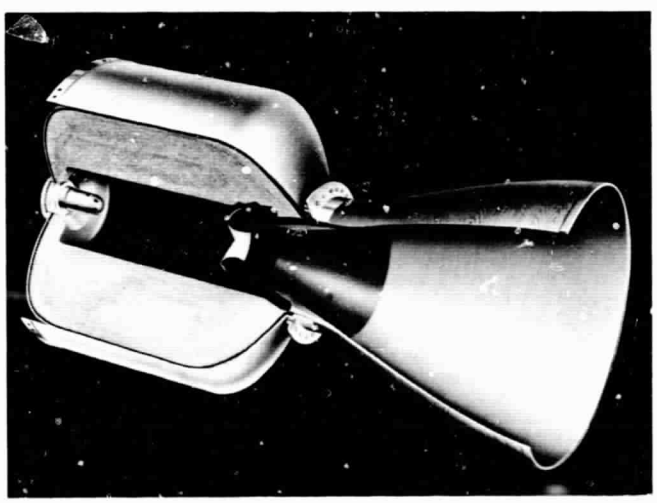

Fig. 1. *Applications Technology Satellite* apogee rocket motor

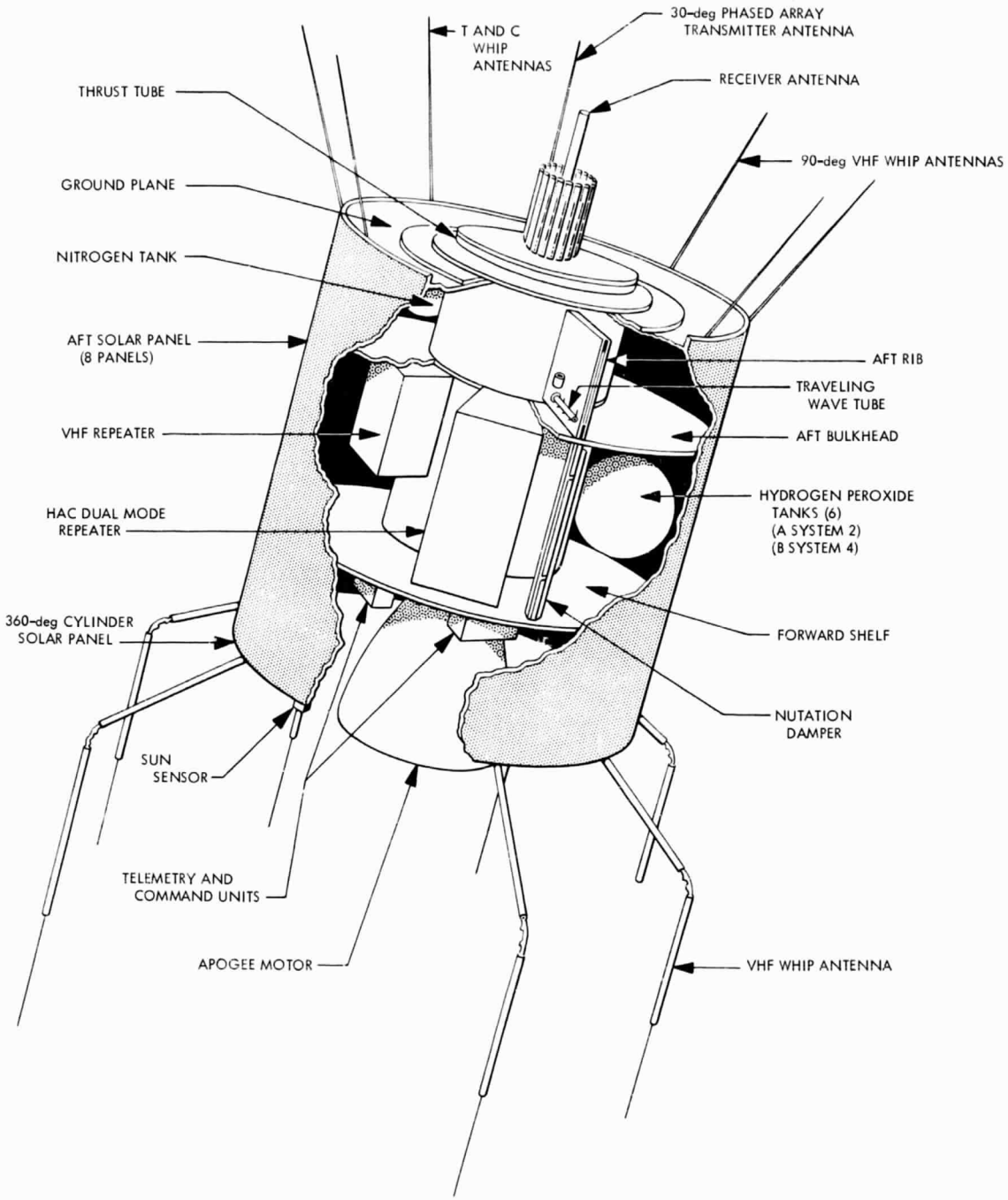

Fig. 2. Synchronous-altitude spin-stabilized spacecraft

Table 1 shows the basic parameters and payloads of the spacecraft.

To place the satellites into synchronous earth orbit, the Jet Propulsion Laboratory furnished the solid propellant rocket motor (JPL SR-28-3) for the final velocity increment at the apogee position of the highly elliptical transfer orbit. Six apogee units were delivered to the Air Force Eastern Test Range (AFETR) for flight support.

The Jet Propulsion Laboratory (JPL) has completed the design, development, and formal Qualification testing of the ATS apogee motor. This report describes these features and specifics related to the motor assembly and its

Table 1. *Applications Technology Satellite* Parameters

Physical configuration	S/S 57.6-in.-diam cylinder	M/G 56-in.-diam cylinder	S/G-1 56-in.-diam cylinder	S/G-2 56-in.-diam cylinder
Weight	1625 lb at launch; 775 lb in 24-h equatorial orbit	702 lb at launch and in orbit	1760 lb at launch; 808 lb in 24-h equatorial orbit	1895 lb at launch; 941 lb in 24-h equatorial orbit
Apogee motor	JPL SR-28-3	Not applicable	JPL SR-28-3	JPL SR-28-3
Control systems	5-lb thrust H_2O_2 system to get on station 5-lb thrust H_2O_2 system for stationkeeping east–west and north–south 5-lb thrust hydrazine (in addition to H_2O_2) for stationkeeping on ATS-C	5×10^{-4} lb thrust subliming solid system for inversion	5-lb thrust N_2H_4 system to get on station 5×10^{-4} lb thrust subliming solid system (inversion) 10^{-5} lb thrust resistojet system (east–west stationkeeping)	5-lb thrust N_2H_4 system to get on station 5×10^{-4} lb thrust subliming solid system (inversion) 10^{-5} lb thrust resistojet system (east–west stationkeeping)
Electrical power	*n–p* solar cell array 175 W initial Two 6-A-h batteries (22 cells each)	*n–p* solar cell array 130 W initial Two 6-A-h batteries (22 cells each)	*n–p* solar cell array 130 W initial Two 6-A-h batteries (22 cells each)	*n–p* solar cell array 130 W initial Two 6-A-h batteries (22 cells each)
Telemetry	Four 2.1-W transmitters; Two at 136.470 MHz Two at 137.350 MHz Two encoders, GSFC PCM standard	Four 2.1-W transmitters; Two at 136.470 MHz Two at 137.350 MHz Two encoders, GSFC PCM standard	Two 2.1-W transmitters; One at 136.470 MHz One at 137.350 MHz Two encoders, GSFC PCM standard	Four 2.1-W transmitters; Two at 136.470 MHz Two at 137.350 MHz Two encoders, GSFC PCM standard
Command	Two receivers at approximately 150 MHz Two decoders, GSFC FSK standard	Two receivers at approximately 150 MHz Two decoders, GSFC FSK standard	Two receivers at approximately 150 MHz Two decoders, GSFC FSK standard	Two receivers at approximately 150 MHz Two decoders, GSFC FSK standard
Communications	Two triple-mode repeaters 4- or 12-W TWT power amplifier 8- or 18-dB receiving antenna 18-dB transmitting antenna 6301- and 6212-MHz ground to spacecraft 4195- and 4120-MHz spacecraft to ground	Two triple-mode repeaters 4-W TWT power amplifier 10-dB transmitting and receiving antenna 6301- and 6212-MHz ground to spacecraft 4195- and 4120-MHz spacecraft to ground	Two triple-mode repeaters Four 4-W TWT power amplifiers Two 18-dB antennas—one transmitting and one receiving 6301- and 6212-MHz ground to spacecraft 4195- and 4120-MHz spacecraft to ground	Two triple-mode repeaters—one C-band and one L-band Two 4-W C-band and two 12-W L-band TWT power amplifiers Two receiving antennas—one 18 dB and one 0 dB Two transmitting antennas—one 18 dB and one 5 dB One 15-dB transmit/receive L-band antenna
Payloads S/S-1 S/S-2	Environmental measurement VHF repeater Resistojet Spin-scan cloud camera Nutation experiment Mechanical despun antenna Resistojet Image dissector camera Self-contained navigation experiment Reflectometer Multicolor spin-scan cloud camera VHF repeater Plume temperature measurement Solar cell radiation damage experiment Third harmonic generator	Environmental measurement Albedo experiment Meteorological package Gravity-gradient stabilization and instrumentation	Ion engine Gravity-gradient stabilization and instrumentation Image orthicon camera Magnetic control system	Gravity-gradient stabilization and instrumentation Ion engine Environmental measurement Solar cell radiation damage experiment Third harmonic generator Millimeter wave experiment Magnetic control system

Note
PCM—pulse code modulation
FSK —frequency shift keying
VHF—very high frequency
TWT—traveling wave tube
n–p —negative–positive

subcomponents. Additional data are presented in detail in several volumes of the Space Programs Summary (Ref. 1).

II. Milestones and Scheduling Events

The five ATS flights are covered in this report. The fifth, and final, flight (ATS-E) was launched on August 12, 1969. Figure 3 shows the milestones and scheduling events covering the four years from program award in January 1963 to delivery of the first flight units in late 1966. Flight operational support has extended the program into the second half of 1969.

The ATS apogee unit was basically designed as a scaled-up version (2.3×) of the SYNCOM apogee motor (Refs. 2 and 3) developed at JPL. The experience gained in this earlier motor program was extremely valuable during the later program and led to several hardware and material improvements in the larger ATS apogee unit.

The SYNCOM nozzle was attached to the motor chamber by a single, large thread. Both the chamber and nozzle attachment ring were fabricated from heat-treated 410 stainless steel. Because identical material was used to interface chamber and nozzle, several instances of material galling were encountered during SYNCOM nozzle placement and removal. The single-thread method of nozzle attachment also made any final nozzle alignment or offset adjustment impossible. Nozzles and chambers had to be matched in order to minimize thrust misalignment and offset of the motor assembly.

The ATS nozzle–motor chamber interface was an improvement of the SYNCOM unit. The ATS nozzle is attached to the motor chamber by a series of 36 high-strength screws whose symmetrical pattern allows the nozzle to be placed in any one of 36 angular positions. During the Qualification Phase of the motor, several units were assembled with the nozzle in different angular positions. Although it was found that nozzle alignment and offset data could be minimized by the correct positioning, the chamber and nozzle hardware are fabricated with sufficient precision to allow random nozzle placement and still maintain alignment and offset well within specification limits.

Galling problems at the nozzle–chamber interface were completely eliminated by the use of dissimilar materials. The motor chamber is made of heat-treated titanium (6Al–4V), the nozzle screws are heat-treated steel, and the nozzle attachment ring is an aluminum alloy. Steel screws placed through the aluminum nozzle ring and threaded into the titanium chamber preclude the chances of material galling.

The SYNCOM nozzle was compression-molded from a macerated carbon cloth and phenolic resin system. Several effective changes in design and material were incorporated into the larger ATS nozzle. These changes include a tape-wrapped nozzle body, a contoured expansion cone, and a cantilevered, high-density-graphite throat insert. The final nozzle configuration was accomplished by contour machining with diamond cutting tools.

A tapered layer of V-52, a rubber-like insulation material, protects the ATS apogee motor chamber internally from the hot combustion gases (5250°F) that are generated during propellant burning. Patterned pieces of uncured V-52 are positioned into the chamber and then cured to form the correct insulation configuration. The much smaller SYNCOM chamber was protected during motorburn by the same V-52 material. Precision insulation boots were fabricated with matched metal dies, and the pre-cured insulation was then bonded into the chamber.

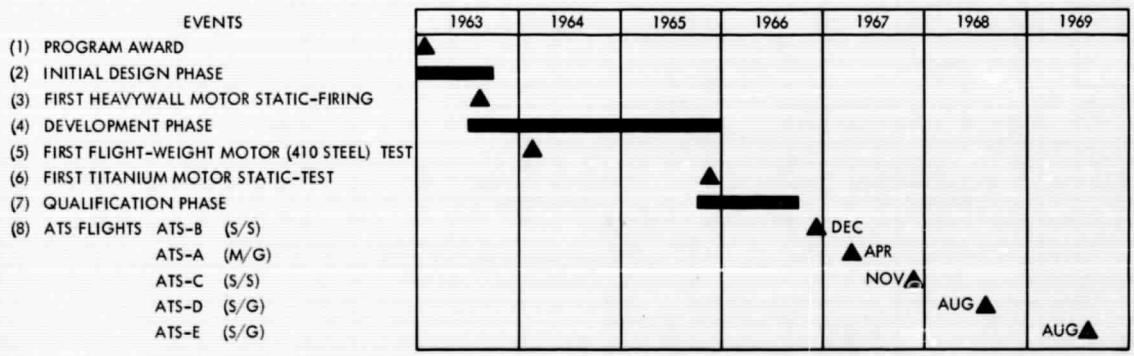

Fig. 3. Milestones and schedules of the ATS apogee motor program

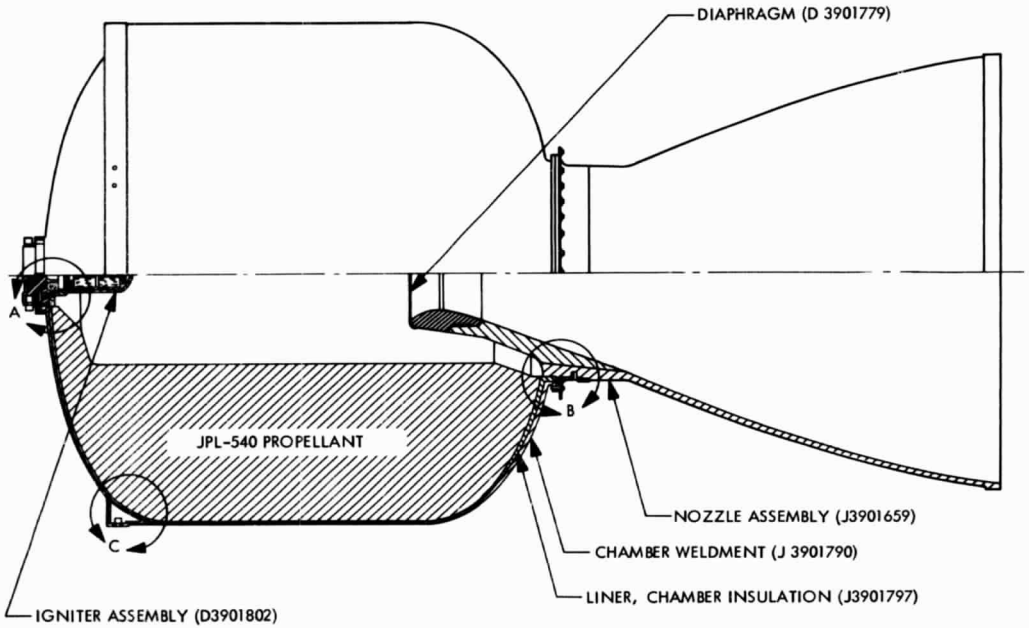

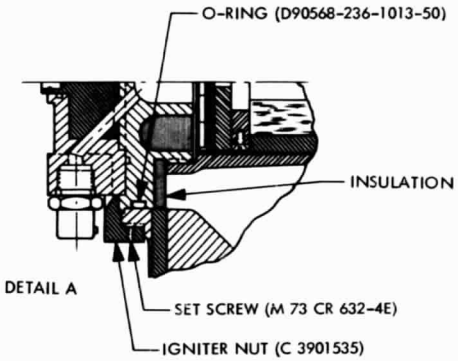

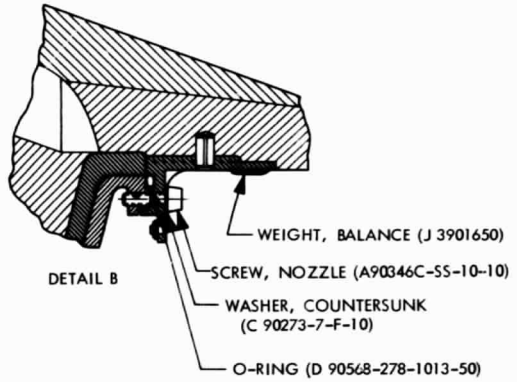

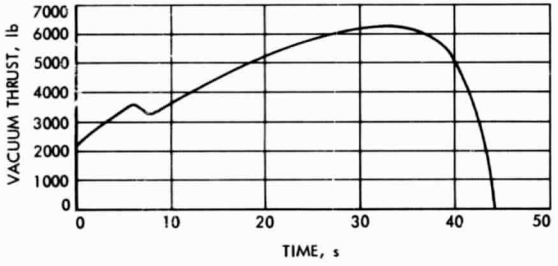

NOMINAL DATA (AT 60°F)

BURNING TIME	43.5	s
MAXIMUM CHAMBER PRESSURE	260	psia
MAXIMUM VACUUM THRUST	6250	lbf
TOTAL WEIGHT	840.7	lbm
PROPELLANT WEIGHT	760	lbm
PREFIRE INERT WEIGHT	80.7	lbm
MAXIMUM DIAMETER	28.2	in.
OVERALL LENGTH	54.6	in.
THROAT DIAMETER	4.08	in.
NOZZLE EXPANSION RATIO	35:1	

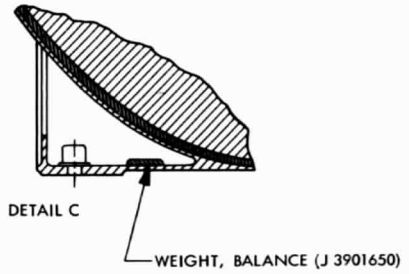

Fig. 4. Motor assembly

Matched metal dies for the ATS chamber insulation would have been extremely expensive because of their size. The ATS hand-lay-up insulation procedure proved efficient, reliable, and fairly inexpensive. Quality control of the weight and thickness of the ATS insulation proved to be no problem.

The igniter used for the ATS apogee unit was developed exclusively for the ATS program. Several early attempts at scaling up the SYNCOM igniter for ATS use proved fruitless. The ATS igniter, as developed, is of the controlled-pressure, or pyrogen, type. Reproducible motor ignition is achieved with this system.

Rather late in the motor Development Phase a requirement was made that the ignition system must be protected by a safe-and-arm device. The development of such a device and its integration into the ATS system was given to the Harry Diamond Laboratories (HDL) by Goddard Space Flight Center (GSFC). A safe-and-arm unit that meets the AFETR safety requirements has been successfully used on three ATS flights. The SYNCOM unit did not require a safe-and-arm device.

The propellant used in both the SYNCOM and the ATS motors is an aluminized polyurethane system. Propellant composition is the same for both units.

The original ATS motor design used a heat-treated 410 steel chamber. Material and method of construction were identical to the SYNCOM motor chamber. Thirty steel ATS chambers were fabricated and delivered to JPL. In September 1964 JPL was directed by GSFC to change the chamber from a magnetic to a nonmagnetic material. A titanium alloy, 6Al–4V, was selected and a total of 23 chambers have been fabricated and received at JPL. Because of this material change, the motor Development Phase used both steel and titanium chambers. The Qualification Phase and all flight units have used the titanium motor chamber.

The ATS apogee motor flight configuration is shown in Figs. 4 and 5. The complete flight unit, including the safe-and-arm device, weighs approximately 841 lb, contains 760 lb of an aluminized polyurethane propellant, has an overall length of 57 in., and has a diameter of approximately 28 in. The unit has been developed and qualified, and has three times successfully performed its function of spacecraft injection into a synchronous, equatorial, earth orbit.

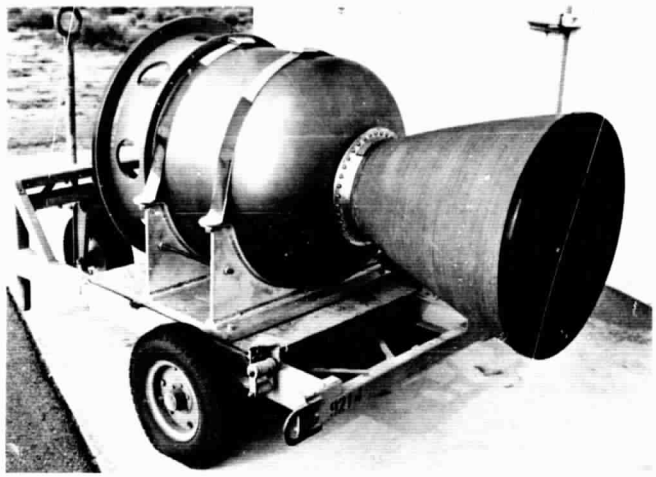

Fig. 5. Titanium chamber

III. Design Features

A. System Requirements

The apogee motor was designed, fabricated, and tested according to specification requirements established by GSFC (Ref. 4). Excerpts from this motor specification that describe the major system requirements are given as Table 2. (See also Table 3 and Fig. 6.)

B. Motor Component Description

The apogee motor assembly consists of the basic components of chamber, chamber insulation, nozzle, propellant, igniter and safe-and-arm assembly, and balance weights. Each of these will be described in some detail in the following sections. Each major component has also been documented by JPL in separate Technical Memorandums (see References).

1. Motor chamber

a. Material selection. The requirements for this task included the selection of a high-efficiency material for the chamber structure. Such a selection was based on the following material characteristics:

(1) High yield strength to density ratio.

(2) Strength retention at temperature.

(3) Performance reliability and reproducibility at selected working stress.

(4) Material and fabrication economy.

(5) High strength with minimum distortion.

Table 2. Excerpts from the ATS apogee motor specification

1. General Classification

The ATS apogee rocket motor shall be classified as a space vehicle rocket motor of the solid-propellant type. It is to be used for injection of the ATS spacecraft into a nominally circular equatorial orbit from the apogee of a transfer orbit. It must be capable of propellant offloading for use with spacecraft of varying weights.

2. Total Impulse

The nominal total impulse for the rocket motor in vacuo shall be such as to provide a velocity increment of 6100 ft/s to the spacecraft. The total impulse must be adjustable to provide the above velocity increment to a spacecraft assembly having a weight which may be of any of one of three specified values. These three values will lie in the region of 1300 to 1550 lb. At a given spacecraft weight the total impulse in vacuo, within the temperature range of 20 to 100°F, shall not exceed 1.5% (3σ) of the nominal value.

3. Thrust

The maximum thrust at 100°F and vacuum conditions shall not accelerate the payload by more than 9.0 g based on a 1550-lb spacecraft.

4. Spin Condition

The rocket motor shall function satisfactorily after being spun, and while spinning, at 100 $\pm$ 50 rev/min.

5. Time in Space

The rocket motor shall function satisfactorily after 30 h maximum of space exposure.

6. Vibration from Launch Vehicle

The rocket motor shall not be adversely affected from vibrations [listed in Table 3] which are applied separately at the engine mounts.

7. Temperature

The rocket engine shall function satisfactorily over the temperature range of 20 to 100°F. The engine shall also function satisfactorily with a 40°F temperature gradient across the grain.

8. Acceleration

The rocket motor shall not suffer any detrimental effects from static accelerations applied through the attachment fittings of 12 g for 10 min along the spin axis opposite the direction of thrust, 12 g for 10 min along the spin axis in the direction of thrust, and 2.3 g for 10 min perpendicular to the spin axis.

9. Moment of Inertia

The ratio of the roll moment to the pitch moment of the loaded apogee motor shall be approximately 1.0.

10. Thrust Misalignment

The misalignment between the thrust vector and the spin axis at any time during burning shall not exceed 0.001 in./in.

11. Thrust Offset

Projected thrust offset at the attachment plane of the rocket motor shall not exceed 0.030 in.

12. Balancing

All quality assurance tested and delivered apogee motors shall have the inert parts dynamically balanced about the spin axis. Balancing weights may be added (or material removed) at appropriate locations on the empty motor parts. No weight shall be added or removed from the inert parts after loading. The spin rate during dynamic balancing shall be a minimum of 75 rev/min. The static and dynamic unbalance of the assembled inert parts and loaded motor assembly shall not exceed that specified in Fig. 6.

13. Weight

The weight shall be specified on the applicable drawings. The maximum weight shall not exceed 850 lb.

14. Envelope Dimensions

The rocket motor shall not exceed the envelope defined by JPL.

(6) Fabrication ease.

(7) High weld-joint efficiency.

Candidate materials during the initial design phase included AISI 4340, 17-4 PH, AM 350, AISI 410, 17-7 PH, PH 15-7Mo, Ti–6Al–4V (annealed), Ti–6Al–4V (heat-treated), B120VCA titanium alloy, and 2014 aluminum alloy. Because of a good performance vs cost trade-off, AISI 410 stainless steel was first selected. Its efficiency, from a strength-to-weight standpoint, was lower than many of the other materials, but was considered adequate for this application. Fabrication on the steel chambers was started; however, redirection of the Advanced SYNCOM to the ATS precluded the use of AISI 410 steel for flight application. Because of the new instrumentation on board the satellite, it was necessary that the new material be nonmagnetic. Selection was based on the same materials characteristics, already listed, with the exception that the alloy had to be nonmagnetic; cost, although an important consideration, was not as great an influence as for Advanced SYNCOM, because materials meeting the high-efficiency and nonmagnetic requirements are more costly. Heat-treated Ti–6Al–4V was considered the outstanding material, as it was in the Advanced SYNCOM selection; however, it had been ruled out originally because of its higher cost.

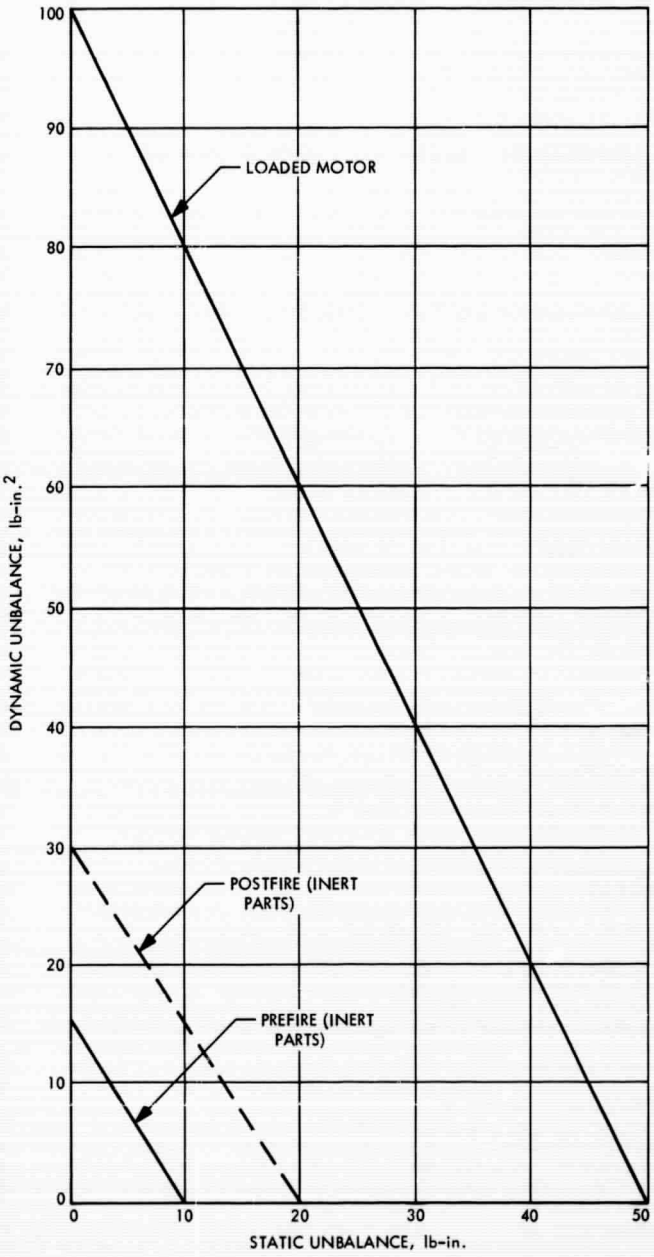

Fig. 6. Maximum allowable sum of static and dynamic unbalance

It was decided that the 30 already fabricated steel chambers could be used to demonstrate adequacy of the chamber design in certain parts of the Development program. The 23 chambers of Ti–6Al–4V were to be used for further Development and Qualification tests, and for Flight units.

b. Design. The ATS chamber was designed at JPL. The titanium alloy chamber consists basically of two half-shells and a mounting ring for attachment to the satellite structure. Each half-shell consists of a 2:1 ellipsoidal dome with a cylindrical skirt and requires only one girth weld for joining. At the apex of each dome are integral bosses for the igniter and nozzle assemblies. The nominal dimensions of the chamber are 28 in. in diameter by 29 in. in length. The following criteria provided the basis for the chamber design:

Maximum temperature	
End domes	200°F
Cylinder	110°F
Maximum operating pressure	270 psia
Minimum proof pressure at ambient temperature	285 psia
Minimum yield pressure at 110°F	300 psia
Minimum design allowable yield strength	
at ambient temperature	150,000 psi
at 110°F	144,000 psi
at 200°F	129,000 psi

Table 3. Required vibration input for apogee motor

Condition	Frequency range, Hz	Magnitude (1.5 × expected)	Parallel to thrust axis, g	Perpendicular to thrust axis, g
		Sinusoidal		
4.35-min logarithmic sweep at 2 octaves/min from 5 to 2000 Hz along thrust axis and 2 orthogonal axes	5–15	—	¼-in. double amplitude	¼-in. double amplitude
	15–250	—	3	3
	250–400	—	5	5
	400–2000	—	7.5	7.5
		Random		
6 min along each of 2 orthogonal axes in attachment plane	20–80	0.04 g^2/Hz	—	—
	80–1280	Increasing from 0.04 g^2/Hz to 0.07 g^2/Hz at 0.61 dB/octave		
	1280–2000	0.7 g^2/Hz		
6 min along thrust axis	20–1000	0.1 g^2/Hz	—	—

Minimum weld tensile strength at ambient temperature 140,000 psi

Minimum buckling pressure at 200°F 340 psi

Improvement due to biaxial stresses rather than uniaxial +10%

Material thickness, determined by the equation $t = Pr/\sigma$ for the cylindrical section, resulted in a calculated value of 0.0292 in. This is decreased to 0.0265 in. on the assumption of a biaxial strength increase of 10%. However, in the transition area between the cylinder and ellipsoidal ends, local bending occurs. An additional thickness of 0.0015 in., making a cylindrical section thickness of 0.028 in., would be necessary to accommodate this force. The minimum necessary thickness for the domes was calculated at 0.033 in. To prevent buckling in the transition from cylinder to dome, a 0.048-in. thickness was required. Consequently, the dome thickness varied from 0.033 to 0.048 to account for buckling. From this information, the following results were expected in hydrostatic burst testing of a minimum chamber at ambient temperature:

Proof pressure	285 psig
Yield pressure	312 psig
Buckling pressure	340 psig
Burst pressure	352 psig

The proof pressure selected for chamber qualification was actually 302 psi. Since the actual properties obtained exceed the design properties, 302-psi proof tests were considered to provide a greater margin.

c. Fabrication. The ATS chamber was fabricated under a fixed-price contract in accordance with JPL specification and drawings. The contract schedule called for one chamber every 15 days after receipt of the first ATS chamber in May 1965, and a completion date of April 1966. Chamber fabrication was completely successful. Delivery of the last unit was made in December 1965, four months ahead of schedule. Only 3 chambers were accepted in which discrepancies were noted; these were assigned to developmental tests. The remaining 20 chambers were acceptable for flight use.

The primary processing of the chambers consisted of die-forging the half-shells (Figs. 7 and 8) and ring-rolling the mounting ring from forged billet. The end forgings from each billet were designated for aft domes. The forward and aft domes for each chamber were made from the same heat of material, where possible; or, were matched as closely as possible according to chemical composition and mechanical properties. The forging operation was followed by machining, appropriate heat-treatment cycles, welding, aging, and finishing. All welding is done by the automatic TIG technique in a chamber capable of maintaining 99.9% pure inert atmosphere. No filler wire is used, since the joints to be welded are machined to provide their own filler.

The following list describes the general procedure in the fabrication and inspection of the titanium alloy chamber:

(1) Forge dome and mounting ring at 1725°F.

(2) Rough machine.

(3) Solution-treat 1 h at 1600–1750°F; water-quench.

(4) Stress-relieve 2 h at 950–1150°F; air-cool.

(5) Finish machine.

(6) Weld mounting ring to forward dome.

(7) Weld half-shells together.

(8) Age 2 h at 950–1150°F; air-cool.

(9) Proof-test at 302 psi.

(10) Package and ship to JPL.

Various inspection techniques are used throughout the fabrication of the chamber, including microstructural analysis, and ultrasonic, penetrant, radiographic, and dimensional inspection.

d. Qualification. Before and during the fabrication process, the forging, heating, and welding qualifications were conducted. Forging qualification was of two kinds—ring and dome.

Ring forging. One ring forging was selected at random for each heat used. One longitudinal and one transverse tensile specimen were taken from two diametrically opposed locations in the ring and tested after aging. The specifications required that the material meet the following properties:

Ultimate strength	160,000 to 175,000 psi
Yield strength	150,000 psi, minimum
Elongation	10%, minimum
Reduction in area	30%, minimum

Dome forging. One forging was taken from the center and two from the ends of each ingot for the purpose of qualification. Sectioning of the forging to provide seven tensile specimens from various locations resulted in destruction of the forging. From the end forgings, four tensile specimens were sectioned in a manner that permitted use of the forgings for fabrication of the chambers. The mechanical property requirements were as already specified. In addition, one tensile specimen was taken from each forging used to fabricate the 23 chambers, the mechanical property requirements being as specified previously. Microstructural analysis was also performed on each forging used for qualification or fabrication. Each sample must exhibit an equiaxed, fine-grained structure (less than ASTM No. 8 grain size) with a minimum of 30% primary α in an α–β matrix.

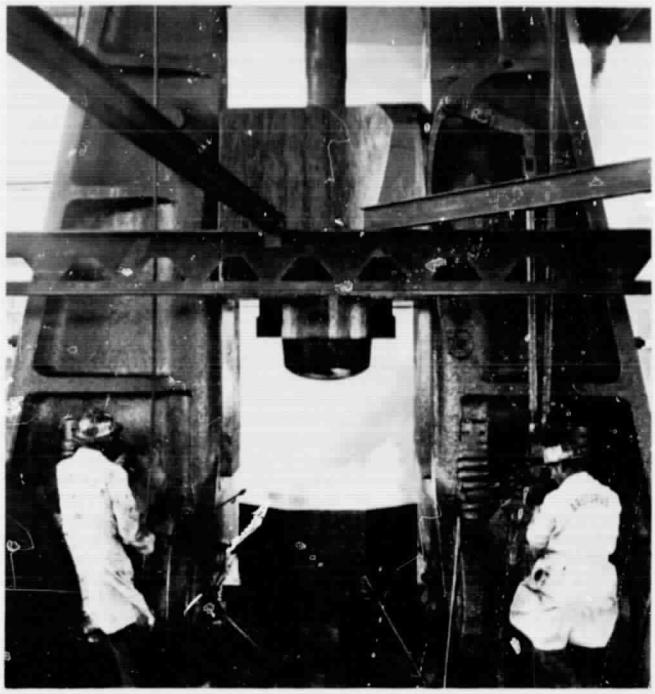

Fig. 7. Forging operation in progress

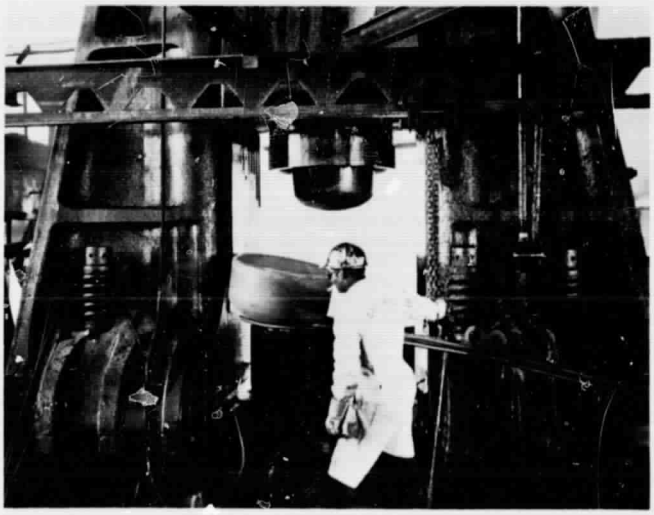

Fig. 8. Finished forging on removal from die

Weld qualification was conducted by simulating the two welds required in the process. Two weld specimens were taken from each of the simulated joints. The material used had undergone the same fabrication and inspection steps as had the chamber itself. The welded specimens were required to have an ultimate minimum strength of 140,000 psi. In addition, a microhardness survey was conducted for each specimen. The hardness of

the weld was not to exceed that of the parent metal by more than 30 diamond-hardness numbers.

e. Testing. Three titanium chambers were subjected to hydroburst tests. Pressure inside the chambers was built up slowly to 302 psi, held for 5 min, and resumed until failure occurred (Fig. 9). The fracture of all three chambers appeared essentially the same and no buckling was seen.

The following are data obtained as a result of the hydroburst tests:

Code	Chamber serial number	Proportional limit	Burst pressure
B-4T	T-1	355 psig	420 psig
B-5T	T-5	375 psig	420 psig
B-6TF	T-6	370 psig	428 psig

The proportional limit values are given as determined from the pressure volume curve. Chamber T-6 was static-fired before the hydroburst testing.

Chamber T-1 was tested by the manufacturer; the remaining two chambers were tested at JPL. Tensile specimens and metallographic samples were sectioned from all three chambers. Tests conducted on the sectioned samples indicate that the chambers were fabricated with accepted techniques according to the requirements set forth by JPL. A more detailed description of the ATS motor chamber is given in Ref. 5.

2. *Nozzle.* The ATS nozzle (Fig. 10) was designed to take advantage of numerous state-of-the-art improvements since the development of the earlier SYNCOM apogee motor. The principal changes include tape-wrapped construction, a silica exit cone, a partially unsupported or cantilevered graphite throat insert, an aluminum bolt-on attachment ring, and a contoured expansion cone. Basic design and fabrication procedures produced a precision nozzle with a minimum thrust vector misalignment.

Fig. 9. Chamber B-1T after hydrostatic burst test

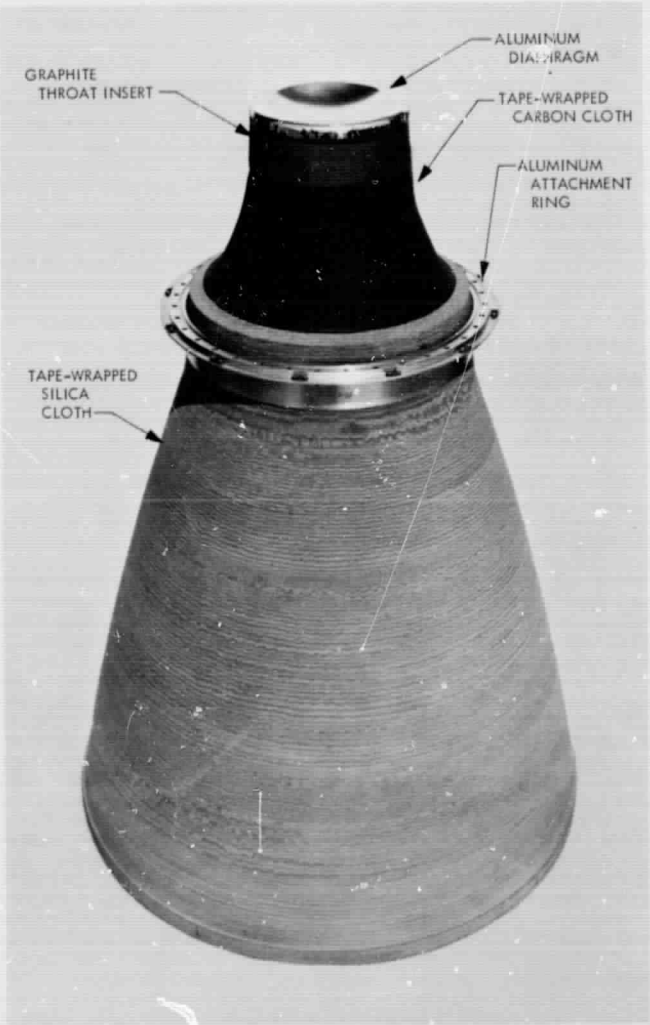

Fig. 10. Prefire nozzle assembly

a. Design features. To improve the pitch moment of inertia of the spacecraft–apogee motor combination, the nozzle is submerged into the motor chamber to an expansion ratio of 4.5:1. This design allows a greater reduction of heat transfer at the aft end of the motor case than does an external nozzle design. Two disadvantages arise, however: (1) some energy in the combustion gases is lost through flow reversal, and (2) the hot, submerged throat insert, after motorburn, radiates heat to the motor chamber, which in turn radiates heat to the spacecraft.

A contractor developed the ATS nozzle contour, using a two-phase (gaseous and solid particle) nozzle combustion gas flow computer program. The contour consists of a circular arc throat section joined smoothly 3 in. downstream of the throat to a 108-in. circular arc. The initial half-angle at the intersection of the arc is 26 deg, and the final exit cone angle is 10 deg. The computer program predicted an improvement of 2 s for specific impulse. Actually, the specific impulse improvement of the ATS motor over that of the SYNCOM motor is about 5 s. This upgraded performance is attributable to a combination of both nozzle contouring and motor scale-up.

The four-piece nozzle consists of an aluminum attachment ring, a high-density-graphite throat insert, a tape-wrapped carbon cloth throat section, and a tape-wrapped silica cloth exit cone. The carbon cloth is impregnated with a highly substituted ring structure phenyl-aldehyde condensation resin. The silica cloth is impregnated with a modified, filled phenolic resin. The threaded silica nozzle body and a matching threaded aluminum ring, bonded with an epoxy adhesive, constitute the nozzle attachment ring joint. Physical dimensions of the nozzle include an area expansion ratio of 35:1, a 4.08-in. throat diameter, and a 24.14-in. exit plane diameter. The sonic throat section and nozzle exit plane are 31.84 in. apart.

b. Fabrication. The nozzle body blank fabrication begins with the carbon cloth throat section being tape-wrapped (parallel to the centerline) on a contoured mandrel. An 8-deg angle is machined on the carbon cloth at an area ratio of 8:1, to maintain a realistic silica cloth bond line in the exit cone. Silica bias tape is next wrapped at an 8-deg angle to an area ratio of 26:1, then at a 4-deg angle. The unit is capsulated in a vacuum bag and receives the final cure at 300°F and 1000 psig in a hydroclave.

Final fabrication operations include contour-machining the outside surface of the nozzle body, threading the body to accept the aluminum attachment ring, and threading the carbon cloth throat section to mate with the graphite throat insert. The throat insert is threaded to provide a mechanical interlock after motor firing. An epoxy adhesive is used to bond both the throat insert and the precision attachment ring to the nozzle body. The unit is now ready for the final precision contour machining of the inside surface of the nozzle with a diamond tool. This procedure ensures maximum nozzle alignment, close dimensional control of the internal surface, and a precision surface finish. After fabrication is complete, the unit is inspected on a precision rotating fixture to determine the nozzle centerline misalignment and any out-of-roundness of the throat, exit cone, and other alignment surfaces.

To protect the interior of the motor from contamination, a nozzle diaphragm is installed over the leading edge of the throat insert. This diaphragm, fabricated from 0.004-in.-thick 1100-0 aluminum and pressure-formed from a precut disk, is bonded to the nozzle inlet with an epoxy adhesive. The diaphragm bursts at approximately 30 psig during the motor ignition phase.

Before a nozzle is assigned to a motor, it is weighed, x-rayed, and pressure-tested. The pressure test prevents two possible failure modes by confirming the integrity of the nozzle attachment O-ring surface, and by ensuring a gas-tight seal between the nozzle body and attachment ring. Typical misalignment for the 8-lb flight nozzle attached to a motor chamber is 0.002 in./in. with a 0.003-in. offset as projected to the motor attachment plane.

c. Testing. Before the ignition of the apogee motor, the spacecraft may complete one to five cycles in an elliptical orbit with the apogee position being at synchronous altitude. While the spacecraft is moving in these elliptical orbits, the nozzle exit cone, which extends out of the aft-section of the spacecraft, is rapidly cooled, thus establishing a nozzle exit cone temperature gradient (axial direction). To permit evaluation of the integrity of the exit cone under these low temperature conditions, a simulated temperature vacuum test was conducted at JPL. A thermocoupled nozzle was mated to a motor containing inert propellant so that heat transfer characteristics between nozzle and chamber could be maintained. The assembled unit was then positioned in an environmental test chamber (Figs. 11 and 12) and the pressure was reduced to 3×10^{-4} torr. Liquid nitrogen was circulated through the radiative shield until an average shield temperature of −300°F was established.

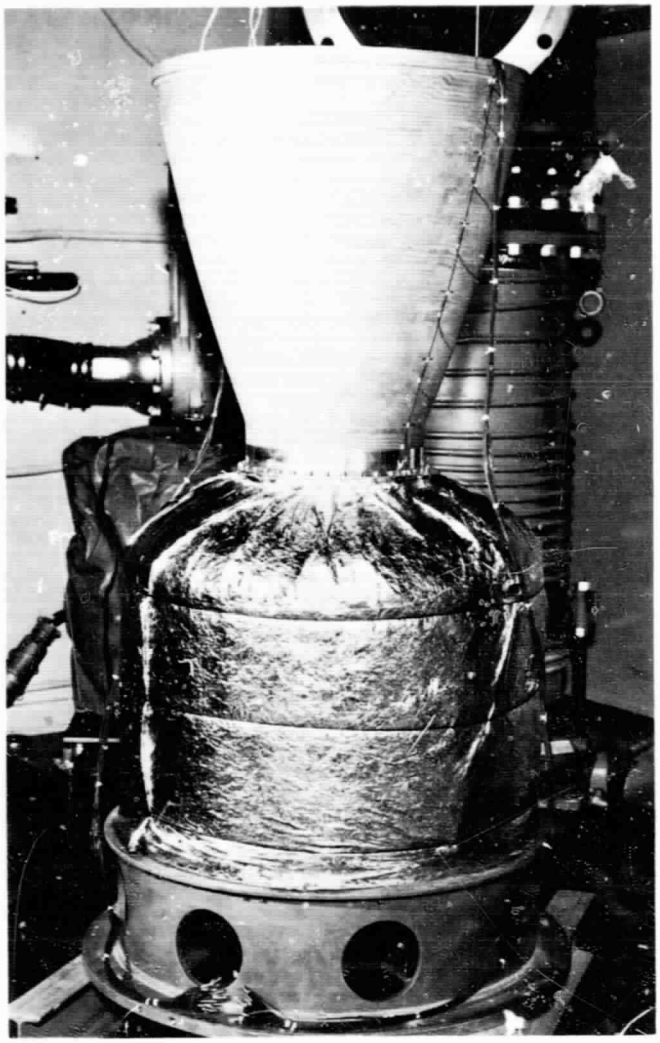

Fig. 11. Nozzle test setup for vacuum exposure

A 4-h low temperature cycle was established that is significantly more severe than flight environments. The cooling period required 3 h for the end of the exit cone to reach −190°F and 1 h for the exit cone to recover to ambient temperature (70°F). Upon completion of the five-cycle test the nozzle was removed from the chamber. Visual and radiographic inspections, and alignment checkout of the nozzle, revealed no deleterious effects from the temperature–vacuum environment. The nozzle was assigned to development code G-4 and static-fired at simulated altitude at Arnold Engineering Development Center (AEDC), Tullahoma, Tennessee.

All nozzles have performed successfully during motor firings, except for one early development unit that was tested in the JPL zero-flow diffuser facility at Edwards

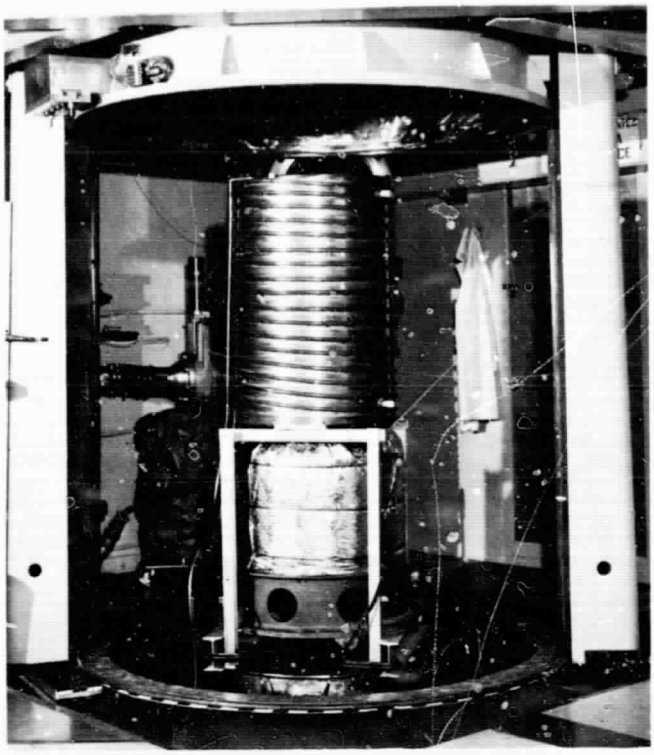

Fig. 12. Nozzle vacuum exposure with radiative shield in place

Test Station (ETS), Edwards Air Force Base, California.* After a 17-s motor operation, the nozzle body was expelled from the attachment ring because of the excessive heat loads radiated by the hot diffuser tube to the aluminum nozzle adapter ring. Four nozzles were tested during the Development Phase at simulated altitude at AEDC. In simulated altitude the exhaust gases undergo complete expansion in the nozzle, causing realistic heat flux loads, char, and erosion in the exit cone.

Two motors fired while spinning at 100 rev/min significantly affected the postfire condition of the nozzle when compared with nonspinning firings. There were noticeable changes: throat erosion was reduced, a minimum amount of aluminum oxide deposit remained on the submerged throat section, and rutting of the leading edge of the graphite throat was negligible. Both spinning motors were instrumented with thermocouples on the nozzle exit cone. The external temperatures of the exit cone were significantly below the degradation temperature of the resin binder system. Since motor balance after

*All reference in this report to JPL tests conducted at Edwards Test Station is intended to mean at the JPL area of ETS.

firing is important, the lower temperatures help maintain the structural integrity of the nozzle, and prevent excessive distortion that could effect motor imbalance and misalignment.

Before the disassembly of a spent motor, a mechanical inspection of the chamber and nozzle is performed to determine the geometric centers of the nozzle throat and exit plane. The geometric thrust vector misalignments and offsets are tabulated for three motors fired at simulated altitude (Table 4). The postfire alignment results may be considered greater than misalignment and offset that occur during actual motor firing, since the nozzle exit cone distorts during postfire heat-soak and subsequent cool-down.

Table 4. Alignment data from simulated altitude tests, Development Phase

Code	Misalignment, in./in.		Offset at attachment plane, in.	
	Prefire	Postfire	Prefire	Postfire
Specification GSFC/S2-0153	0.001	0.001	0.030	0.030
E-1	0.0003	0.0006	0.008	0.014
G-3	0.0001	0.0006	0.004	0.016
G-4	0.0001	O.0002	0.0005	0.005

Nozzle throat erosion and weight loss during altitude firings at AEDC are shown in Table 5. Two of these nozzles were sectioned to determine char depth of the ablative material. The submerged carbon cloth throat section chars completely, as a result of both firing and heat-soak loads. Char depth in the exit cone is usually 50% of the thickness, so that structural integrity is maintained for motor balance and thrust vector alignment.

Fifty nozzles were fabricated for the motor program, including the units assigned for flight application. Thirteen of these were fabricated with an area expansion of 8.5:1, the minimum ratio for the submerged nozzle; the remaining units were of flight configuration. The shorter nozzles were constructed as a cost-saving measure and were used on the Heavywall and Basic series atmospheric firings. The nozzle has been successfully developed and subjected to all flight environments, including those of shipping temperature, booster vibration, booster acceleration, temperature cycle, space temperature–vacuum exposure, and spin firing. Additional nozzle details are given in Ref. 6.

Table 5. Nozzle throat erosion and weight loss in simulated altitude tests, Development Phase

Code	Throat erosion (area), %	Weight loss, %	Condition
E-1	1.92	3.89[a]	Non-spinning
E-2	1.67	4.28	Non-spinning
G-3	1.33	4.35	Spinning
G-4	1.48	4.34	Spinning

[a]Heavyweight nozzle.

3. Chamber insulation. The motor case insulation is designed to protect the chamber from the hot combustion gases during propellant expulsion. The case is primarily designed to withstand only operating pressures, and not the heat flux loads and temperature (5250°F) at which the propellant front advances during motor operation. The chamber must, therefore, be thermally protected to avoid catastrophic failure modes such as a burn-through of the 0.028-in.-thick-titanium chamber wall. Each case is insulated with NBR Gen-Gard V-52 insulation.

a. Design features. The composition of V-52, which affects its performance during and after propellant expulsion, is that of a butadiene-acrylonitrile rubber, with the ingredients of silica, asbestos, a dehydrogenation catalyst, a plasticizer, curatives, and an antioxidant. Typical physical properties of vulcanized V-52 are shown in Table 6. This material has been specifically formulated to withstand the internal environments of high temperatures up to 7000°F and the erosive exhaust products of the solid propellant motor. The material can also accommodate long-term storage and low temperature environments.

Table 6. Physical properties of the V-52 insulating material

Property	Value	Test method
Hardness, shore A	82	ASTM D 676
Specific gravity	1.334	GTR 1762
Parallel tensile strength, psi	1600	ASTM D 412
Perpendicular tensile strength, psi	1600	ASTM D 412
Aged parallel tensile strength, psi	1800	ASTM D 412
Parallel elongation, %	400	ASTM D 412
Perpendicular elongation, %	500	ASTM D 412
Aged parallel elongation, %	200	ASTM D 412

The V-52 material, manufactured under conditions of strict quality control, was chosen because it was successfully used in the SYNCOM apogee motor and has been used in numerous other solid rocket programs. The property of the material to adhere to itself in a completely charred state and remain in position after motor burnout constituted the final reason for the choice. This adhesion characteristic helps to maintain both static and dynamic motor balance after propellant expulsion, an important factor in preserving the spin stability of the spacecraft throughout its life span.

The internal surface of the chamber requires special preparation before the insulation is installed. The first operation is a light bead blast to remove surface contaminants. Next, the case is cleaned with solvent, then wiped with a sodium hydroxide alkaline solution to remove any remaining contaminants. The final cleaning procedure is the chemical etching of two critical insulation bonding surfaces. A solution of nitric acid and hydrofluoric acid is used to etch the surfaces adjacent to the chamber openings, thereby ensuring optimum bonding surfaces. The internal surface of the chamber receives two coats of a vulcanizing rubber primer and one coat of a vulcanizing cement. Each coat of primer or cement is allowed to dry thoroughly after its application.

The insulation is purchased in calendered, unvulcanized, 36-in.-wide rolls in thicknesses of 0.030 in. and 0.080 in. Pieces resembling semicircles (Fig. 13) are cut with the use of precision templates and then positioned in sequence inside the chamber to build up the required thicknesses. To ensure complete lamination of the layered material, a standard vacuum bagging technique is used to remove entrapped air between the layers. The insulated unit is then placed in an autoclave and pressurized to 100 psig minimum, after which the temperature is gradually increased for vulcanizing (325°F for 2 h). Before the pressure is released, the unit is allowed to cool gradually so that maximum bond strength is ensured between chamber and insulation.

Fig. 13. Chamber insulation pattern pieces

The final operations include trimming excess insulation at the chamber openings and abrading the interior surface of the vulcanized insulation to improve the propellant bonding surface. The insulation at the nozzle opening is precision-trimmed to an 11.40-in. inside diameter to accept the submerged nozzle. Minimum clearance between the insulation and the nozzle decreases the circumferential gap by which hot combustion gases can gain access to the aluminum nozzle attachment ring.

b. Component development. For the four static firings in the motor development Heavyweight series, an excess amount of insulation was installed into the motor chambers. The reasons for this overage were (1) to ensure successful operation of the motor during static firing and (2) to provide sufficient virgin insulation material after propellant expulsion so that insulation char-depths could be determined. The insulation configuration for the 410 steel case was completed according to char data obtained from Heavyweight firings.

The igniter and nozzle opening insulation thickness begins at 0.140 in. and tapers to 0.080 in. where the cylindrical case section is met. The cylindrical section is covered by one layer of 0.030-in. insulation; less insulation is required here because this section does not receive the heat flux load until late in the motor run at motor tailoff. This design (configuration 1), developed for the stainless steel motor chamber, has been used successfully on 22 motors in the Development Phase. The configuration has an average weight of 10.3 lb, including 1 lb of primer and vulcanizing adhesive.

Four steel motor chambers—two in the Basic series fired at ETS at ambient conditions, and two in the Altitude series fired at AEDC under simulated altitude conditions—were instrumented with thermocouples located on the external surface of the chamber. The maximum temperatures recorded during the tests occurred approximately 90 s after motor tailoff. The maximum

motor temperature of 600°F occurs in the elliptical dome sections of the chamber.

The titanium chamber required a different insulation design. Configuration 2, developed for the titanium chamber, contains 12.7 lb of insulation and vulcanizing adhesive. The insulation thickness is 0.200-in. at the chamber openings and tapers to 0.080 in. where the dome sections join the cylindrical section. The cylindrical section requires one layer of 0.030-in. insulation.

Configuration 2 was evaluated by four motor tests. Two steel chambers were instrumented with thermocouples and fired at the JPL site at ETS to confirm the design. The remaining two motors, with titanium chambers, were fired at ambient conditions during the environmental test phase. One titanium unit, instrumented with thermocouples, confirmed the expected chamber temperatures. A maximum chamber temperature of 500°F occurs in the dome sections 90 s after motor tailoff. The second titanium unit was first subjected to test environments (temperature cycle, booster acceleration, and vibration) and then static-fired without any detrimental effects to the insulation or bond interface.

The additional quantity of insulation in the titanium chamber dome sections is required to reduce case temperatures during motor operation. The yield strength of 6Al–4V titanium decreases rapidly at elevated temperatures and is also initially lower (150,000 vs 180,000 psi) than 410 steel. The stress in the titanium chamber at peak motor operating pressure would approach the yield strength of titanium if the unit were allowed to reach the same temperature (350°F) as the steel case. The criterion for evaluating this insulation design is based on the margin of safety between the actual working stress in the chamber and the titanium yield strength at the operating temperature. Figure 14 depicts a typical titanium-yield-strength curve for environmental test G-8T. This figure shows that insulation configuration 2 provides adequate chamber temperature control during the motorburning phase. The additional insulation required for the titanium chamber helps to maintain postfire dynamic balance requirements, since some virgin insulation material remains which tends to adhere symmetrically to the chamber surface. Configuration 2 was used for all Qualification and Flight units.

c. Quality control. The fabrication of the chamber insulation does not involve intricate steps or extremely critical processes. The vendor takes only normal precautions to properly prepare and install the insulation patterns in the required sequence. Precision templates are used in the cutting of each piece of insulation. The most critical process is the cure cycle. The insulation lay-up is evacuated, pressurized, and heated at a given rate to achieve the proper cure and optimum bonding characteristics. Cooling must be gradual, since the bond line is still quite weak during the final part of the cycle, and premature release of autoclave pressure may cause failure of the insulation-to-chamber interface. To ensure the proper cure cycle the entire cure is documented by temperature, pressure, and vacuum recorders.

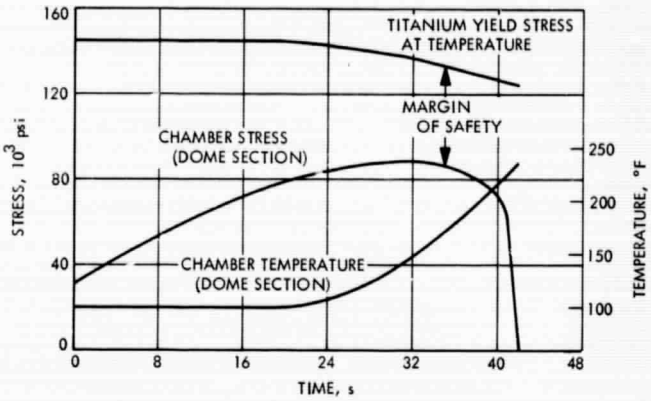

Fig. 14. Chamber temperature, chamber stress, and titanium yield stress

Early in the program numerous chambers showed bond failures between insulation and chamber at the igniter and nozzle openings. These failures were repaired to avoid a possible motor failure mode. Since the bond tensile and shear stress levels are highest at the chamber openings, this is the most probable location for an initial bond failure. If the bond is conceived for maximum strength, this type of failure would not occur. The bond failed as a result of improper preparation of the chamber surface. Cleaning the surface chemically assures optimum bond strength and ensures the removal of all oxidation contaminants. An alkaline (sodium hydroxide) rinse applied to the internal surface of the chamber removes most contaminants. Then an etch solution of nitric acid and hydrofluoric acid is applied to chemically clean the critical titanium chamber openings. The application of the etch solution for 3 min removes less than 0.0003 in. of titanium. Since the introduction of the etching process, all chamber insulations have been securely bonded at the igniter and nozzle openings. Additional details on chamber insulation are given in Ref. 7.

4. Igniter. The ATS igniter is of the controlled-pressure type (shown in exploded and cross-sectional views in

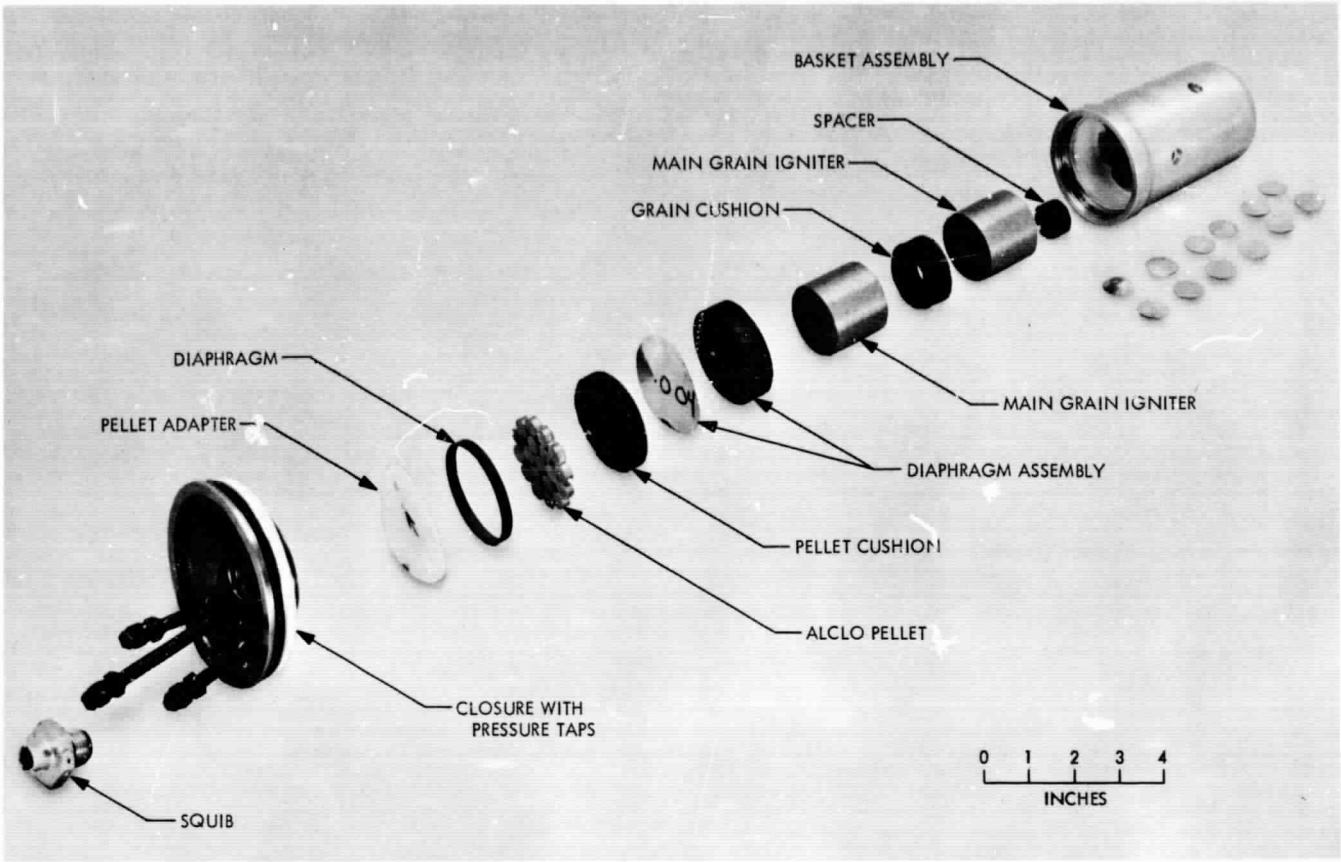

Fig. 15. Igniter with development closure (exploded view)

Figs. 15 and 16); it is assembled as a separate unit and is externally installed into the forward-end of the motor. The igniter is secured by a high-strength nut with the igniter closure acting as the pressure closure for the forward-end motor opening. The ignition material is an aluminum–potassium perchlorate composition whose hot burning mass causes ignition by impinging on, and radiating to, the motor propellant surface. The aluminum igniter basket is designed to withstand only the ignition phase, after which it is consumed and expelled with no detrimental effect on secondary motor hardware. The basket assembly (less closure) weighs approximately 1 lb.

a. Chronological development. At the inception of the ATS program, a scale-up of the flight-proven SYNCOM igniter was attempted. This earlier developed ignition system (Ref. 2) consisted of a highly perforated fiberglass basket filled with 60 g of pelletized ignition material. A single, dual-bridgewire squib initiated the pellets (main charge). The squib body was designed to function as the forward-end closure of the motor. The scaled-up

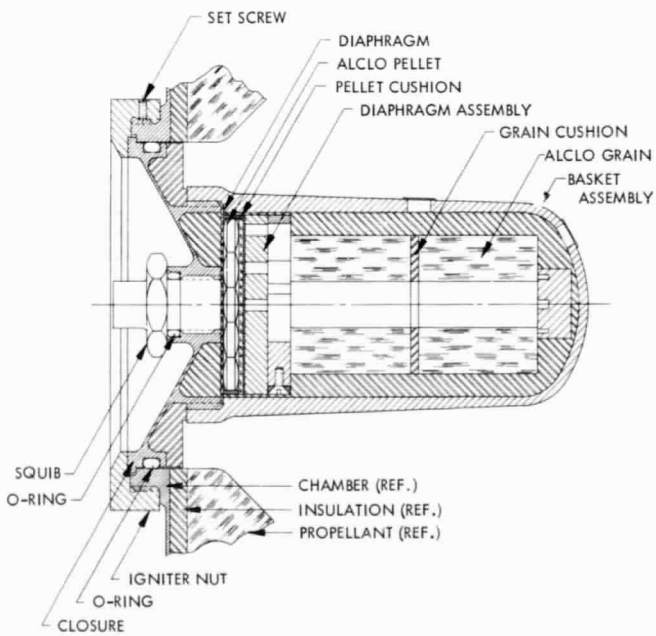

Fig. 16. Igniter

Fig. 17. Components of scaled-up SYNCOM igniter

SYNCOM igniter for ATS use (Fig. 17) consisted of a highly perforated steel basket filled with 200 g of randomly packed pellets and an electrical squib for igniter initiation. Two tests of this scaled-up ignition system resulted in both baskets rupturing during igniter ignition (Fig. 18). Pressure results were also inconsistent between the two tests. These initial tests led to the conclusion that scaling the SYNCOM igniter for ATS use would be extremely difficult if not impossible.

A contract was then let to develop a *Polaris* type of grain (controlled-pressure) igniter. This igniter was to be of heavy hardware type requiring minimum testing to prove the pyrotechnic system only. Figure 19 shows the cross-sectional view. A modification of this igniter was developed at JPL (Fig. 20) by replacing the primary grain with 19 ALCLO pellets and increasing the number of gas ports in the main grain chamber from six to twelve. The additional six holes were spaced 120-deg apart in two planes along the cylindrical section of the basket. For the first Heavyweight motor test (A-2), sufficient igniter testing had been completed to establish the igniter pyrotechnic train as 19 ALCLO 0.052 pellets as the primary charge and 2 ALCLO grains, or slugs, as the main charge. Additional testing with ignition test motors (ITMs) or isolated igniters was continued to optimize basket thickness and number and size of basket gas ports. Internal and external basket insulation were also part of the continued testing. Basket materials tested ran the gamut of steel, fiberglass, nitrocellulose, magnesium, and aluminum.

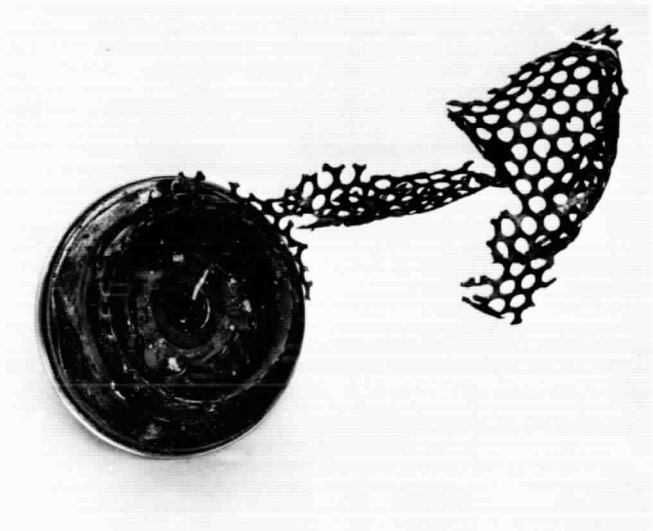

Fig. 18. Scaled-up SYNCOM igniter after firing test

Because of the excellent results achieved with the SYNCOM I squib (Ref. 8), a similar squib was used for the Development Phase of ATS. The internal configuration of the squib was the same as that of the SYNCOM but the squib body was designed to adapt to a threaded closure squib port. Later modifications of the squib were

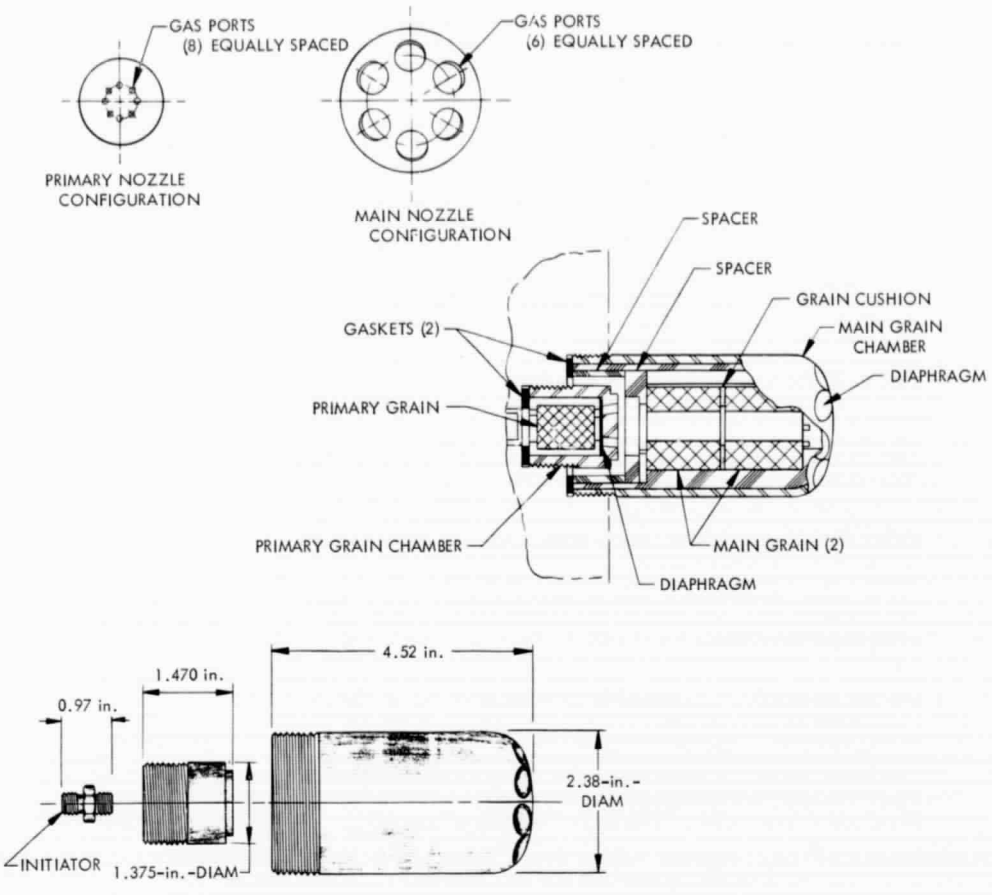

Fig. 19. Aerojet igniter design proposal

made to the bridgewire attachments and resistor heat sinks to improve the reliability of the system.

b. Design details of present igniter. The ATS igniter, as finally designed and proved (Fig. 16), is of the controlled-pressure type. The pyrotechnics consist of a squib that ignites 19 pellets (primary charge). These pellets burn, build up to a desired pressure, burst a soft aluminum diaphragm, and ignite 2 large ALCLO main grains (87 g/grain). The hot gases are then ported into the motor chamber through the twelve gas ports located in the igniter basket. The flame temperature of the pyrotechnics is about 8000°F. For a total igniter burn time of 220 to 270 ms, an internal basket peak pressure in a range of 1800 to 3000 psi (depending on the temperature conditioning of the igniter assembly) and an internal motor peak pressure in a range of 212 to 273 psi are produced. The igniter basket, made of 6061-T6 aluminum, has tapered walls varying in thickness from 0.25 in. at the threaded section to 0.1 in. at the dome. The basket is internally insulated with a silica-fiber-filled polyurethane material in such a manner as to hold and cushion the main grains. The diaphragm assembly (separating the primary charge from the main grain as shown in Fig. 15) is made of laminated plastic (grade LE) and has 31 gas ports with 0.125-in. diameters. A soft aluminum diaphragm of 0.004-in. thickness provides the desired pressure buildup of the igniter pellets. A polyethylene diaphragm holds the pellets in place and acts as a seal (O-ring type) for the basket-to-closure interface. A closure with three pressure taps (as shown in Fig. 15) was used during the Development Phase; it is made of heat-treated stainless steel and insulated for protection from propellant burning. The flight-type closure, with squibs, will be a part of the safe-and-arm device (see Section IV-A-9).

c. Igniter testing and Qualification. A complete series of tests has been run on the igniter as an isolated unit to test the various subcomponents as well as the ability of the unit to withstand only the ignition phase. Hydroburst tests were performed on unported baskets to check

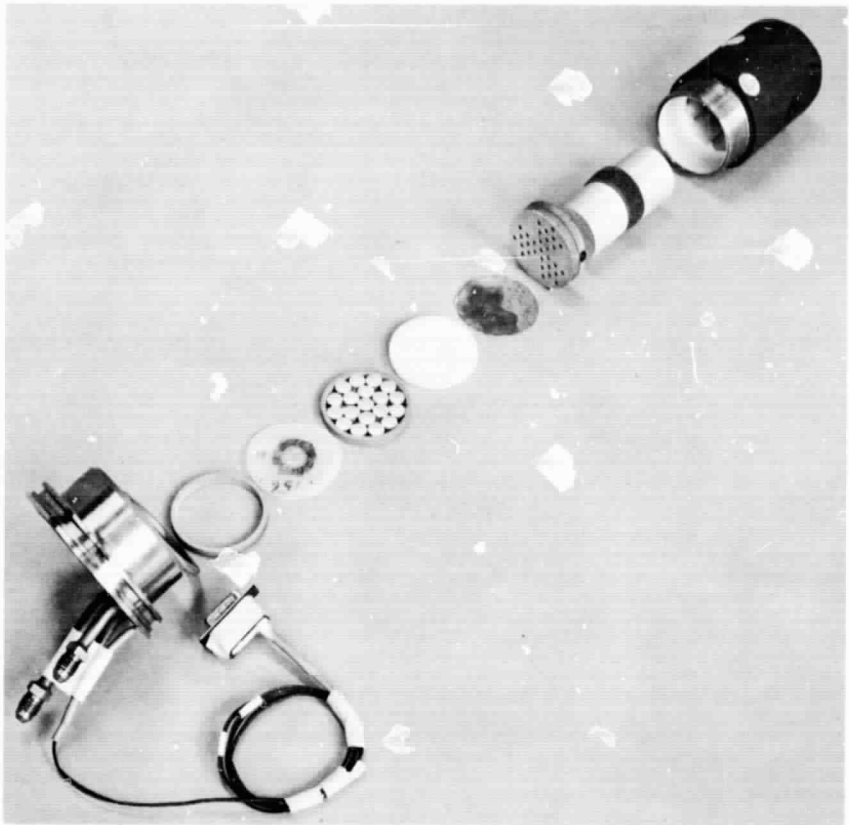

Fig. 20. Modified Aerojet igniter (exploded view)

the difference in various tapered wall thicknesses. Shock tests on baskets with gas ports were run to check possible yield from the ignition phase. Fiberglass and nitrocellulose baskets failed during these tests; but the 6061-T6 aluminum baskets showed little or no yielding after repeated testing with shock pressures in a range of 1800 to 2900 psia. Single igniter firings, with a full pyrotechnic load, were tested to examine the ability of the igniter basket to withstand the burning of the pellets and main grains. High-speed movies were taken to examine flame-spreading characteristics (Fig. 21). Postfire inspection showed the gas ports eroded to about 25% of their original size. Four igniters were subjected to temperature cycling with no noticeable effect on physical characteristics or performance. Three igniters were put through vibration testing and two igniters were centrifuged with no deleterious effects. Two igniters have been through all three environmental tests (centrifuge, vibration, and temperature cycling), inspected, and fired with no effect on performance. Hydroburst tests were run on the igniter closure to check for yield, buckling, and failure. The closure was found to have a margin of safety of 1.45 on buckling and 4.2 on failure (bursting).

ITM testing. Ignition test motors (ITM) were cast and fired with an as-cast surface. An as-cast surface is considered to be fuel-rich and more difficult to ignite than a machined propellant surface. Ten ITM tests were run, including one test with only one main grain in the igniter. All tests, including the one-grain test, showed close relation in pressure and time. All motors ignited satisfactorily. The one-grain test proved, to some degree, the margin of safety in the igniter system.

Motor testing. During the program 30 full-scale developmental motors have been fired with the igniter performing satisfactorily in all tests. The firings have covered temperatures of 10°, 60°, and 110°F. There have been low-pressure and atmospheric starts. Except for ignition delay time, which depends on the firing circuit, all measured parameters within the ignition sequence of the igniter showed a high degree of uniformity.

Qualification testing. In the eight Qualification firings conducted at AEDC, the JPL igniter assembly and the HDL safe-and-arm device (Fig. 22) were used. The results of this formal ignition qualification are summarized

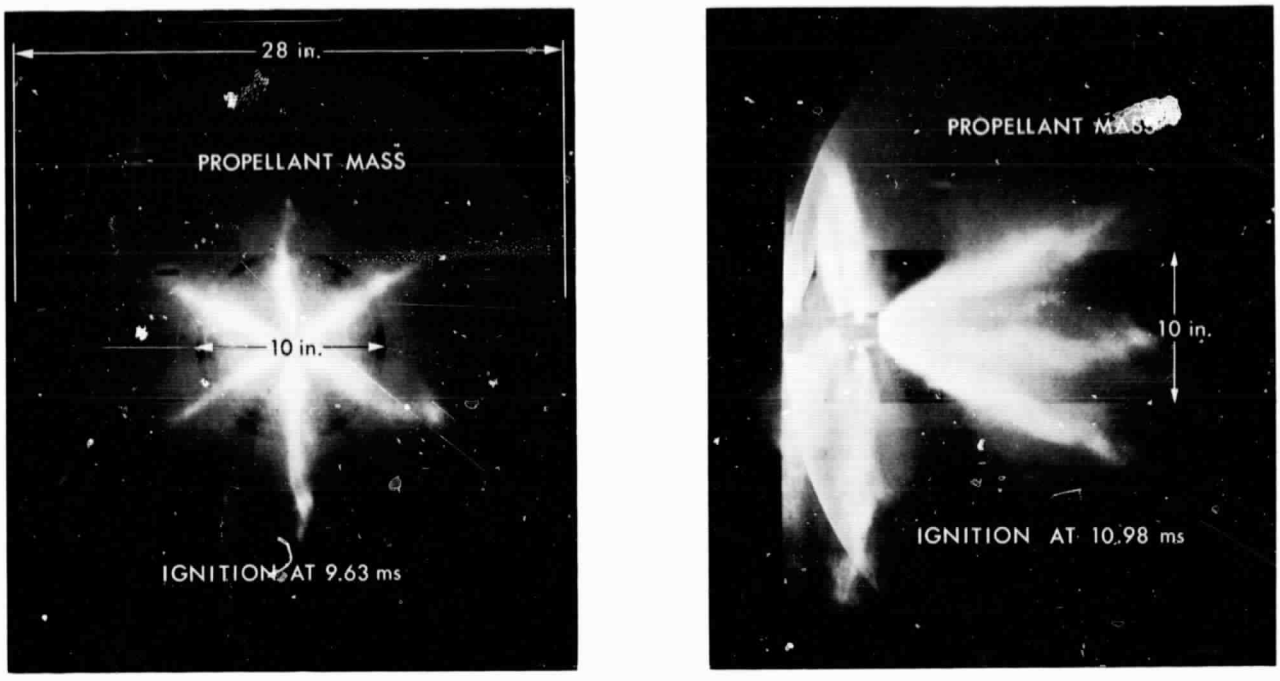

Fig. 21. Flame propagation

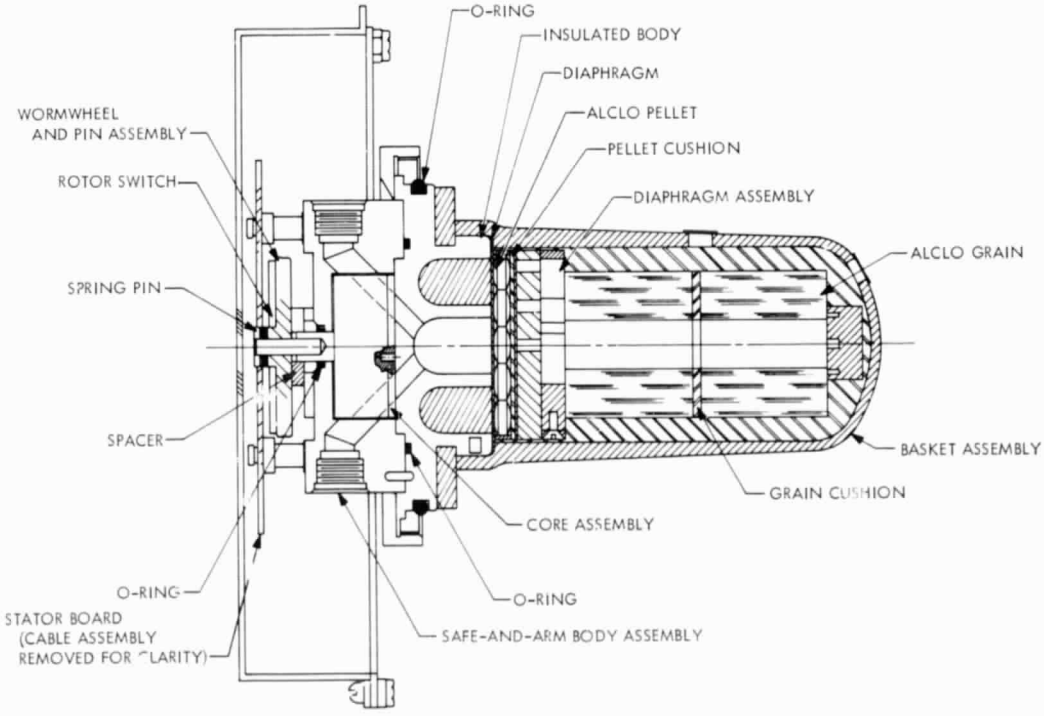

Fig. 22. Igniter and safe-and-arm assembly

Table 7. Motor ignition data, Qualification Phase

Code	Run	Igniter	Test (1966)	Temperature, °F	t_{D_i}	t_{M_i}	t_{m_i}	t_Δ	t_{t_m}	t_{D_m}	P_{t_i}	P_{t_m}	$P_{c_{start}}$
					ms						psia		
Q-8T	1	QIG-8	Jul 29	100	4	33	37	11	48	28	1693	250	101
Q-6T	2	QIG-6	Aug 3	100	3	31	34	9	43	23	1874	257	101
Q-2T	3	QIG-2	5	100	3	32	35	10	45	28	1923	250	100
Q-4T	4	QIG-4	9	100	1	39	40	5	45	23	1879	272	100
Q-5T	5	QIG-5	15	40	2	42	44	9	53	25	1215	234	102
Q-7T	6	QIG-7	18	40	2	34	36	12	48	25	1821	221	101
Q-1T	7	QIG-1	19	40	2	41	43	11	54	33	1362	213	101
Q-3T	8	QIG-3	Aug 23	40	3	37	40	10	50	28	1578	230	100

See Appendix for ignition events index.

in Table 7. A separate JPL Technical Memorandum has been written on the ATS ignition system (Ref. 9).

5. Balance weights. To maintain spin stability throughout the mission, stringent balance requirements have been placed on the motor before and after propellant expulsion. The allowable dynamic and static imbalance before propellant loading and at motor burnout are shown in Fig. 6.

Static imbalance, alone, shifts the principal axis parallel to, but not collinear with, the spin axis of the motor. In mathematical terms, static imbalance can be defined as

$$S = Wr$$

where

S = static imbalance, lb-in.

W = motor weight, lb

r = principal axis shift, in.

Dynamic imbalance, alone, tilts the principal axis with respect to the spin axis. Therefore, the principal axis will generate a double cone about the motor spin axis, whose apex is at the center of gravity of the unit. Dynamic imbalance can be defined as

$$D = g\,\alpha\,(I_x - I_z)$$

where

D = dynamic imbalance, lb-in.^{2}

α = principal axis tilt, rad

g = acceleration due to gravity, ft/s^2

I_x = mass moment of inertia about pitch axis, lb-in.-s^2

I_z = mass moment of inertia about spin axis, lb-in.-s^2

In a realistic case of imbalance there will be a combination of static and dynamic imbalance. Therefore, the principal axis will be shifted and tilted with respect to the spin axis.

It is not possible to have the motor in static and dynamic balance both before and after propellant expulsion. The more critical balance requirement is after motor burnout, since the unit stays with the spacecraft during its life span. Therefore, to minimize the motor imbalance at burnout the empty assembly is balanced before loading takes place. For this purpose a vertical balancing machine (from MB/Trebel Machine, subsidiary of MB Electronics, New Haven, Connecticut) that operates on a hard bearing-force measurement (transducer) system is used for the inert units.

The empty motor assembly is placed in the vertical position on the balance machine within 0.001 in. of the spin axis. Static and dynamic balance are then achieved in one operation. The required location and thickness of balance weights are determined by direct console readout. Table 8 summarizes the weights and the amounts of imbalance removed from the empty Qualification motors.

Balance weights of lead (1/8- or 3/16-in.-thick) are permanently affixed to the motor with an epoxy adhesive. The two selected balance planes are located 1.5 in. from the motor attachment surface (inside of the mounting ring) and 26.25 in. aft of the attachment surface on the nozzle adapter ring. The weights, their location in azimuth—as well as distance from the center of gravity,

Table 8. Prefire motor balance data, Qualification Phase

Code	Imbalance removed				Imbalance remaining	
	Static, lb-in.	Dynamic, lb-in.^{2}	Chamber balance weight, g	Nozzle balance weight, g	Static, lb-in.	Dynamic, lb-in.^{2}
Q-1T	0.9	14.6	19.4	73.7	0.3	4.0
Q-2T	0.8	30.2	42.9	88.3	0.2	5.0
Q-3T	1.4	9.7	18.1	79.2	0.2	5.0
Q-4T	1.7	27.8	48.6	44.2	0.1	3.0
Q-5T	1.0	19.9	33.4	45.0	0.1	4.0
Q-6T	0.8	14.0	21.5	52.4	0.1	2.0
Q-7T	1.1	8.7	17.8	47.9	0.2	4.0

and their distance from the motor centerline are recorded. It is then possible to calculate the amount of static and dynamic imbalance removed by the addition of the weights. Before the motor is removed from the balance table, a residual imbalance determination is made to ensure that the unit has been balanced within 0.5 lb-in. static and 5.0 lb-in.^{2} dynamic imbalance.

Static and dynamic imbalance have been determined on six motors loaded with live propellant. These units were initially balanced in the empty configuration. The imbalance of each unit did not exceed the specification requirements (see Table 9). The imbalance of live units was tested on a vertical balance machine (from Gisholt Machine Company, Madison, Wisconsin) at Vandenberg Air Force Base, California, because this facility is designed for hazardous operations.

It is impossible to determine accurately the amount of postfire imbalance after static or spin–fire testing. The presence of gravity and the handling–removing from test cell, transporting, and setting up in the balance machine–of the fired hardware causes the loosening and nonsymmetric redistribution of the charred insulation. Only one unit from the Altitude series was subjected to a postfire imbalance determination. This unit met the maximum specification requirements. However, most of the charred insulation had to be removed from the chamber because it had fallen from the walls during shipment from AEDC. The remaining, intact insulation was unsymmetrically distributed, so provided nonconclusive balance data.

Table 9. Loaded motor imbalance data, Development Phase

Code	Imbalance remaining	
	Static, lb-in.	Dynamic, lb-in.^{2}
G-2	1.8	31.8
E-2	6.8	31.7
D-2T	0.4	3.3
F-1	3.5	36.8
F-2	2.1	15.4
F-3	3.0	30.8

6. Propellant and grain configuration. The propellant for the ATS apogee motor, JPL 540, is a composite system containing polyurethane fuel binder, ammonium perchlorate oxidizer, and aluminum fuel additive (Ref. 10). This system is the same as that used in the SYNCOM and EARLYBIRD programs. The propellant is mixed in a vertical sigma-blade mixer in 1200-lb quantities. This batch is sufficient to cast a single apogee unit, ten batch check units, tensile specimens, and peel test samples. Propellant mixing and casting are carried out under a pressure of 5 torr or less. The ATS unit is cured at 140°F for 5 days. The quality control charges are cured at 140°F for only 72 hours.

The ten 12-lb batch-check units (Fig. 23) verify each propellant batch for ballistic properties. Two units are fired, each at temperatures of 10° and 110°F. Six units are fired at 60°F. Excellent agreement between batch-check data and ATS firings has been achieved (Ref. 11).

The grain design of the ATS motor is basically a straight cylinder with a small web of propellant at the forward-end. The geometric configuration is such that propellant burnout occurs in the two ellipsoidal ends before taking place in the cylindrical section. Theoretically, a sliverless configuration is attained; however, because of possible erosive burning, minor chuffs occur after motor tailoff. These chuffs, which have been reproducible, amount to only one-quarter percent of the total thrust integral. Close quality control of insulation dimensions and post-cure machining of the propellant surface has greatly reduced the amount of motor chuffing.

The propellant is completely case-bonded. No release boots are used. To achieve reliable bonding of propellant to chamber insulation, the insulation is treated a day before propellant casting with a solution of 75% methylene chloride and 25% toluene-2,4-diisocyanate (TDI). Methylene chloride, which is caustic, attacks the insulation and allows the TDI curing agent to penetrate the

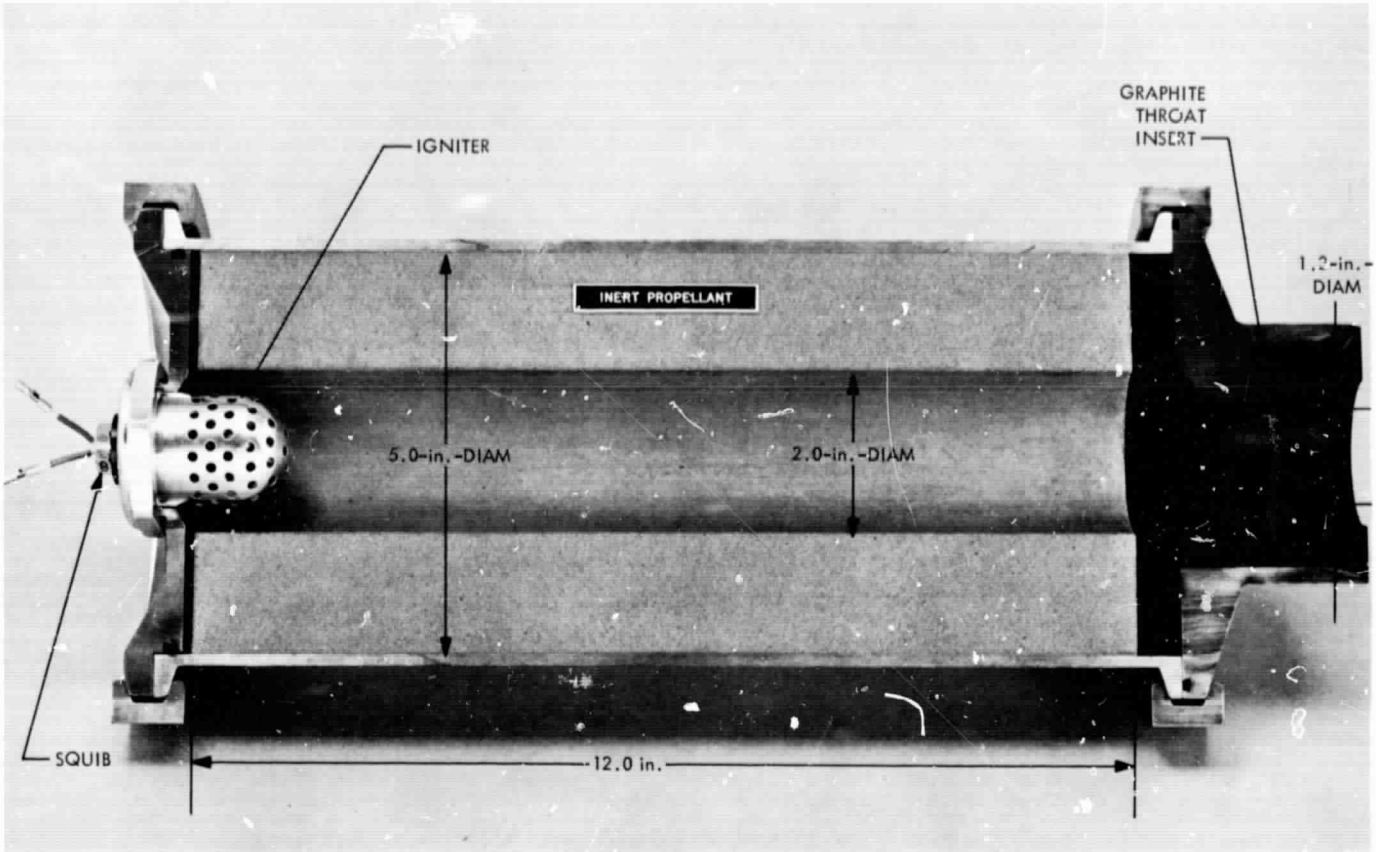

Fig. 23. Sectional photograph of the 5 × 13 batch-check motor

insulation surface. The insulation is exposed to this solution for only 3 min. The removal of the methylene chloride is then accomplished by oven drying, leaving only the curing agent (TDI). The propellant is also cured with TDI; therefore, during curing, an effective chemical bond between propellant and insulation is achieved. Peel tests have shown that the propellant–insulation bond strength is greater than the strength of the cured propellant. The polyurethane propellant has a nominal tensile strength of 140 psi and an elongation of 80% when measured at maximum tensile strength.

7. ***Propellant trimming.*** In view of the impulse requirement for the spacecraft, whose weight can vary from 1300 to 1550 lb, the propellant weight in the apogee motor must be alterable within relatively wide limits. The ATS motor case and perforation mandrel were designed to allow the motor to be cast with an overweight of propellant when considering even the maximum spacecraft weight. Consequently, because it is advantageous to be able to alter the perforation surface by a suitable means of trimming, a remote propellant-trimming facility was designed and installed at ETS. The hazardous nature of the trim operation necessitated that the trimming machine be housed remotely from the operator controls.

The trimmer is analogous to a hydraulically fed and template-controlled boring machine with the boring bar or ram, in this case, being fed upward. The machine is shown in Fig. 24. Trimming the core diameter is achieved in the following sequence. The boring tool is set to a precalculated diameter after consideration of the volume and density of propellant to be removed. The motor is placed aft-end-down on the trimmer turntable, centered, and secured by bolts. Then, operated from the control building, the motor-turntable assembly is rotated by an electric motor that effects the proper cutting speed. In sequence, the boring ram, which is raised hydraulically at the proper feed rate, is radially controlled by a hydraulic servomechanism that traces the shape of a precut template. The template controls the shape and height of the cut; the cutting tool radius, which can be adjusted independently, produces the port diameter. The scrap

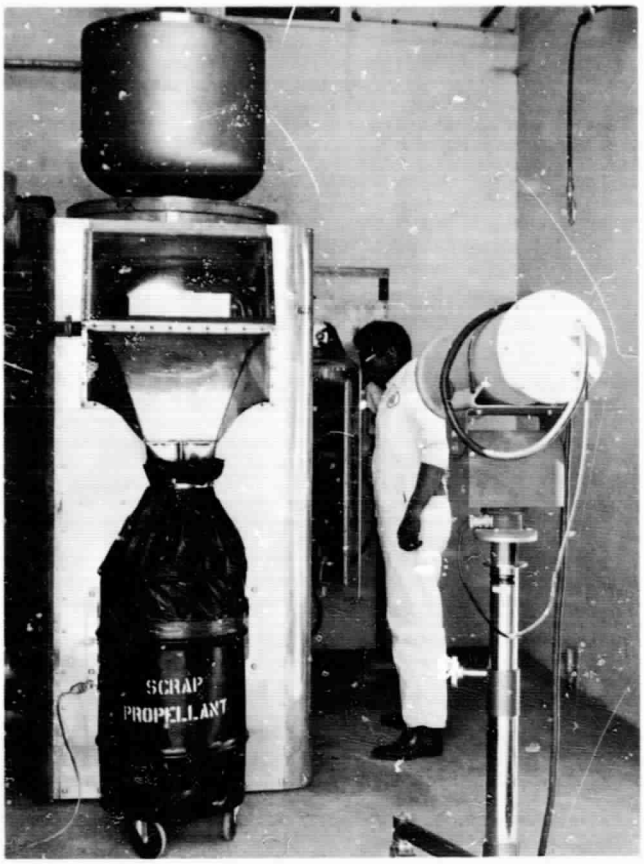

Fig. 24. Remote propellant trimmer

propellant drops continuously into a chute through which it is discharged into a partially evacuated hopper that eliminates airborne dust hazards and enables the scrap to be weighed for a final propellant weight calculation. The entire operation is viewed over closed-circuit television from the control building.

The steps in the actual cutting are threefold. The first cut along the entire perforation length acts as a clean-up cut, removing the taper generated by the casting mandrel; the original perforation diameter of about 9.1 in. is enlarged to 9.9 in. by this cut. The second cut, located at the aft-end of the grain, provides an entrance perforation to fit the submerged nozzle. The combined weight removed by these first two cuts decreases the as-cast, approximately 787-lb propellant weight by nearly 22 lb, leaving around 5 lb to be trimmed by the third, and final, cut. The third cut lies parallel to the first, along the entire port length. Before this cut is made, the final diameter is calculated to establish the final propellant weight. When trimming is complete, the motor is taken to an assembly and inspection building. The perforation diameter and core concentricity are measured for conformity, and the final propellant weight is determined.

To date, the results show an accuracy of prediction of the propellant weight to within ± 1 lb at the present design weight of 760 lb, and an ability to determine and report the final weight to within ±0.5 lb. The sum of these conservative figures yields an accuracy, from prediction to reporting, of ±0.2%.

IV. Motor Development and Qualification Phases

To produce the ATS solid propellant rocket motor, a normal sequence of events has been followed. These include the following phases:

(1) Design of motor hardware and auxiliary equipment.

(2) Fabrication of hardware.

(3) Development testing of motor.

(4) Qualification testing of motor.

(5) Loading and delivery of flight unit.

(6) Engineering flight support.

Throughout the Development Phase test results were evaluated, and the motor component hardware was redesigned when necessary.

A. Development Phase

The Development Phase for the apogee motor consists of 47 primary tests. These tests are cataloged into the 11 major subgroups shown in Table 10. The subgroups and the units contained in each subgroup are arranged in an approximately sequential testing order. Each unit has been designated by a code. Principal test conditions and environments are specified for each unit. This table is intended only as a general summary of the Development Phase. Basic test C-3A was a repeat of C-3. Test C-3 was the only ATS test that was not of full duration. At approximately 17 s after motor ignition, the nozzle body was expelled from its retaining ring, causing the motor to drop in pressure, at which time it continued to burn to propellant completion. Test E-4T, which was to evaluate the apogee motor and synchronous-altitude gravity-gradient-spacecraft combination, was cancelled by GSFC.

1. Heavyweight series. Because of the lengthy procurement time involved in producing the flight-weight

Table 10. Motor Development Phase

Series	Code[a]	Test conditions					Test environment				
		Temperature, °F			Location	Test stand type	Temperature cycle	Shipping temperature	Booster acceleration	Booster vibration	Vacuum start
		10	60	110							
A Heavyweight (J3901512)	A-1	Inert propellant loading to check motor casting fixtures, casting procedures and charge preparation									
	A-2		√		ETS	Single component					√
	A-3		√								√
	A-4		√								√
	A-5		√								√
B Hydroburst (J3901513) 410 Steel	B-1	Ambient			JPL	None required		Hydroburst to destruction			
	B-2										
	B-3F										
(J3901790) Titanium	B-4T										
	B-5T										
	B-6TF										
C Basic	C-1		√		ETS	Single component					√
	C-2		√								√
	C-3		√			Diffuser					√
	C-3A		√								√
	C-4	√				Single component					√
	C-5			√							√
	C-6		√								
	C-7			√							
D Dynamic model JPL	D-1	Ambient			ETS/JPL/Vendor	None required			√	√	
	D-2T									√	
HAC	D-3				HAC						
	D-4										
	D-5T										
Thermal model HAC	D-6F										
	D-7F										
	D-8TF										
E Altitude	E-1		√		AEDC	Single component					√
	E-2		√								√
	E-3T		√			Soft, HAC payload					√
	E-4T[b]		√								√
F Storage	F-1	√			ETS	Spin—150 rev/min	√		√	√	
	F-2	√					√		√	√	
	F-3	√					√		√	√	

[a]T stands for titanium chamber, F for fired chamber, and A for repeat test.

[b]Cancelled by Goddard Space Flight Center.

Table 10 (contd)

Series	Code[a]	Test conditions					Test environment				
		Temperature, °F			Location	Test stand type	Temperature cycle	Shipping temperature	Booster acceleration	Booster vibration	Vacuum start
		10	60	110							
G Environment	G-1			√	ETS	Single component	√	√			
	G-2	√					√	√			
	G-3		√		AEDC	Spin—100 rev/min					√
	G-4		√							√	√
	G-5		√		ETS	Spin—150 rev/min					
	G-6			√			√		√	√	
	G-7	√					√		√	√	
	G-8T			√		Single component					
	G-9T	√				Spin—150 rev/min	√		√	√	
H Minimum propellant load	H-1	√			ETS	Single component					
I Safe and arm	I-1		√		ETS	Single component					
J Omnidirectional antenna	J-1		√		ETS	Spin—100 rev/min					
Z Flight acceptance	Z-7T	√			ETS	Spin—150 rev/min	√				

chambers, JPL designed and had fabricated six boilerplate ATS motor chambers. These units were made from ¼-in.-thick mild steel; they duplicated, within reasonable limits, the internal volume, dimensions at the aft and forward openings, and overall length of the flight chamber. This 260-lb chamber hardware (Fig. 25) was used for the five Heavyweight tests (A-1 through A-5). These tests allowed JPL to evaluate early in the program the design of the propellant-casting fixtures, the motor processing and handling procedures, and the design of various motor subcomponents. The first unit (A-1) was loaded with an inert polyurethane propellant to ensure the compatibility of motor and casting hardware. This series of tests was a prerequisite for the Basic test series.

2. *Hydroburst series.* Six motor chambers, three each of steel and titanium, were designated for hydrostatic destructive prooftesting to determine if design objectives had been met. Two new and one used chamber of each material were tested. Results of the titanium chamber tests are listed on page 11.

3. *Basic series.* The first of the flight-designed 410 steel chambers were used for the Basic tests (C-1 through C-7).

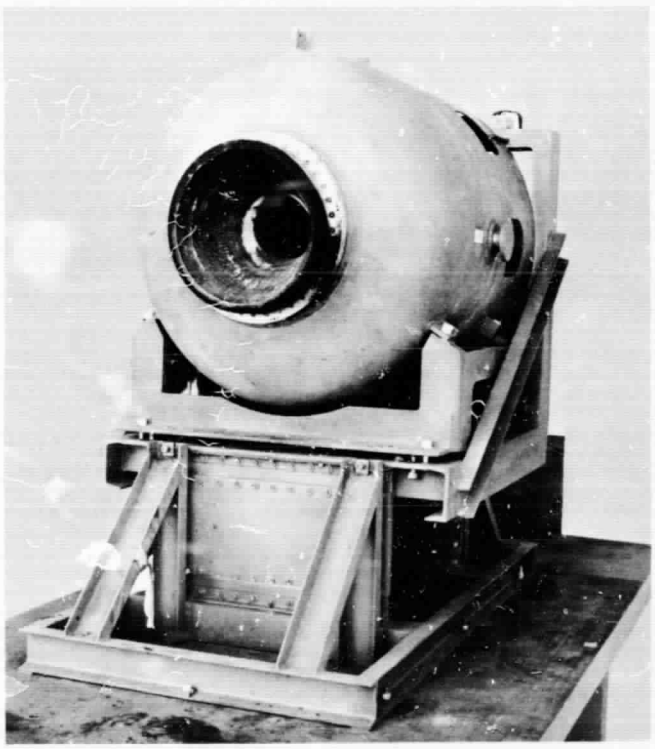

Fig. 25. Heavyweight chamber hardware

The objectives for the series were (1) to verify compatibility of the flight chamber with casting fixtures and handling equipment, (2) to verify motor firing at temperature extremes of 10° and 110°F, (3) to further evaluate flight components under static test conditions, and (4) to further establish procedures for motor processing.

This series was originally assigned five units for testing. Three initial units were to be tested at 60°F, after which one unit each was to be tested at temperature extremes of 110° and 10°F. After the five Basic tests were completed, a loaded unit capable of being fired over a known temperature range would be ready for environmental testing. The Basic tests were considered prerequisite for the Environment series. Because a nozzle failure occurred on test C-3, caused by external heating to the nozzle ring, the test was repeated as C-3A. Tests C-6 and C-7 were assigned to evaluate the chamber insulation required for the titanium design. Therefore, eight tests, instead of five, were conducted during the Basic series.

4. Dynamic and thermal series. Motor hardware loaded with an inert JPL polyurethane propellant was used to verify the structural design of the loaded motor assembly to withstand booster acceleration and vibration loads. The physical parameters—density, tensile strength, elongation—of the inert propellant composition duplicated those of the live propellant. Five dynamic models were fabricated. Three units (two steel and one titanium) were delivered to the ATS spacecraft contractor for dynamic testing of the combined spacecraft and apogee motor. Three fired motor assemblies (two steel and one titanium) were also delivered to Hughes Aircraft Company (HAC) for thermal testing of the spacecraft–apogee motor.

5. Altitude series. Program planning called for the early static testing of two motor units at simulated altitude conditions to establish vacuum motor performance. The JPL static-test facility at ETS was used for the majority of the developmental firings. Most of the ETS tests were conducted at atmospheric conditions, making accurate motor vacuum performance data only a reasonable approximation. Two apogee units (E-1 and E-2) were tested under simulated high-altitude conditions at AEDC. A simulated altitude of slightly greater than 100,000 ft was maintained during motorburn. Vacuum performance agreement between the two tests was excellent (Refs. 12 and 13).

The two remaining tests in this series (E-3T and E-4T) were also scheduled for AEDC testing. Test E-3T, fired during June 1966, was a combined spacecraft–apogee motor test. The synchronous-altitude spin-stabilized spacecraft and apogee unit were soft-mounted in test cell J-5. Thermal and vibration data were obtained from the spacecraft during and after motorburn (Ref. 14). The last test in this series (E-4T), tentatively scheduled for the synchronous-altitude gravity-gradient spacecraft–apogee motor combination, was cancelled by GSFC.

6. Storage series. Three motor units, cast in September 1965, were placed in long-term ambient storage at ETS. These units were processed to flight-standard procedures, and all hardware components are of flight design with the exception of the 410 steel chambers. Before being placed in storage, the units received grain alignment and final hardware alignment inspections, center-of-gravity determination, moment-of-inertia determination, and x-ray and ultrasonic inspections. The units were removed from storage at designated intervals for physical reinspection. The original plan called for one unit to be fired after one year of ambient storage and the remaining two units fired after two years of storage. All storage units were subjected to test environments of temperature cycle, booster acceleration, and booster vibration after storage and before static-testing. The units were tested at ETS with a grain temperature of 10°F while spinning at 150 rev/min.

The same propellant-insulation system was used on the earlier SYNCOM unit as on the present ATS unit. The SYNCOM motor has been aged for two and a half years at ambient conditions with no apparent degradation of hardware, propellant, or performance. No real problems were expected with storage of this larger unit, but periodic inspections of the units were made during the storage periods. Two ATS apogee units (G-3 and G-4) as old as six months have been fired successfully under simulated altitude conditions at AEDC.

The first storage unit (F-1) was tested after 16 months of storage, on the last day of January 1967. This unit appeared to operate normally during its 45-s burn. A complete analysis of all prefire and postfire data revealed that the motor survived the 16 months of storage and subsequent simulated launch environments. The remaining two storage units, F-3 (20 months) and F-2 (24 months), have also been successfully static-tested. The results of this storage program have verified that after withstanding at least two years of ambient storage the apogee

motor can then be subjected to booster launch environments and successfully static-tested. No degradation in motor performance was observed from the prolonged storage. Additional details of the storage program are given in Ref. 1 (SPS 37-48).

7. Environment series. The Development program was considered complete with this series of nine tests. Originally only seven tests, with the 410 steel chambers, were assigned to this series. Because of the introduction of the titanium chamber two tests were added—G-8T and G-9T. Individual units are subjected to separate test environments before they are inspected and static-tested. The final tests include units first being subjected to all test environments, in sequence, and then static-tested at grain temperature extremes of 10° and 110°F. Units G-6 and G-7 represent the final Environment tests with the 410 steel chamber. Titanium unit G-9T was subjected to the test environments before being tested at 10°F. With the successful completion of test G-9T the apogee unit was considered ready for the formal Qualification Phase. Two units in this series (G-3 and G-4) were static-tested at AEDC under simulated altitude conditions. The results are given in a separate AEDC report (Ref. 15).

8. Minimum propellant load test. A single ATS unit (H-1) was processed, trimmed to a propellant weight of 644 lbs, and static-tested (10°F) at ETS. This unit demonstrated the ability to off-load the apogee motor to provide the required velocity increment for a 1300-lb (minimum weight) spacecraft. The apogee unit, as cast, contained 785 lb of propellant; 141 lb of propellant was removed by the JPL remote trimming process. The H-1 unit performed as predicted.

9. Safe-and-arm test. During the Development program, GSFC established the requirement that the apogee unit would require a safe-and-arm (S&A) device. The development of the flight igniter, as discussed in Section III-B-4, had been completed by JPL. Discussion between GSFC and JPL established a mutually agreeable interface between the igniter and the S&A device. This unit, both mechanically and electrically, blocks the squibs (dual squibs–single bridgewire) from the primary charge of the igniter. Development test I-1 at ETS was a 10°F, single-component test to confirm the dimensional fit and the compatibility of only the mechanical part of the S&A device to the apogee unit. The S&A temperatures and the integrity of the five O-ring seals were confirmed during this motor firing. The development phase for the HDL S&A device is covered in Ref. 16.

10. Omnidirectional antenna tests. Development test J-1 was the fourth and final test in a series conducted to evaluate the design and release mechanism of an omnidirectional antenna to be used on the ATS-C spacecraft. The design and fabrication of the antenna was assigned to Hughes Aircraft Company by GSFC. Hughes was supported by JPL with three apogee motor ignition tests and one full duration test (J-1). As shown in Fig. 26 the antenna is located at the apex of a fiberglass dome, which in turn is mounted to the nozzle exit cone of the apogee motor. During launch the antenna–dome will be used until motor ignition at which time it is expelled.

The first three tests, with only the ignition pulse used to expel the antenna–dome, established final design release times and flight path of the test article. Test J-1 used a live motor (full duration) as a final confirmation of antenna design and release mechanism.

The setup for test J-1, which was basically the same for all tests, consisted of the equipment pictured in

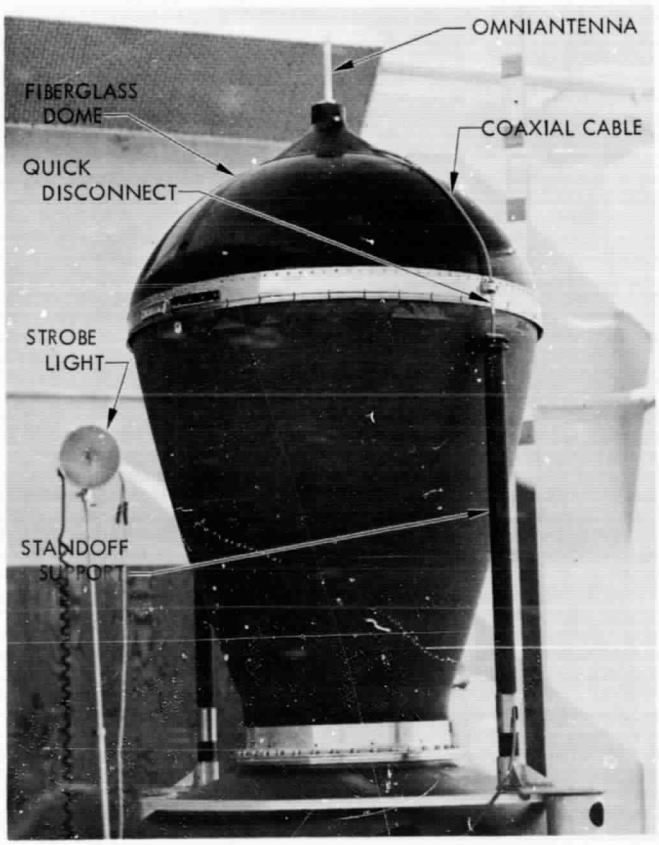

Fig. 26. Omniantenna–dome combination on apogee motor

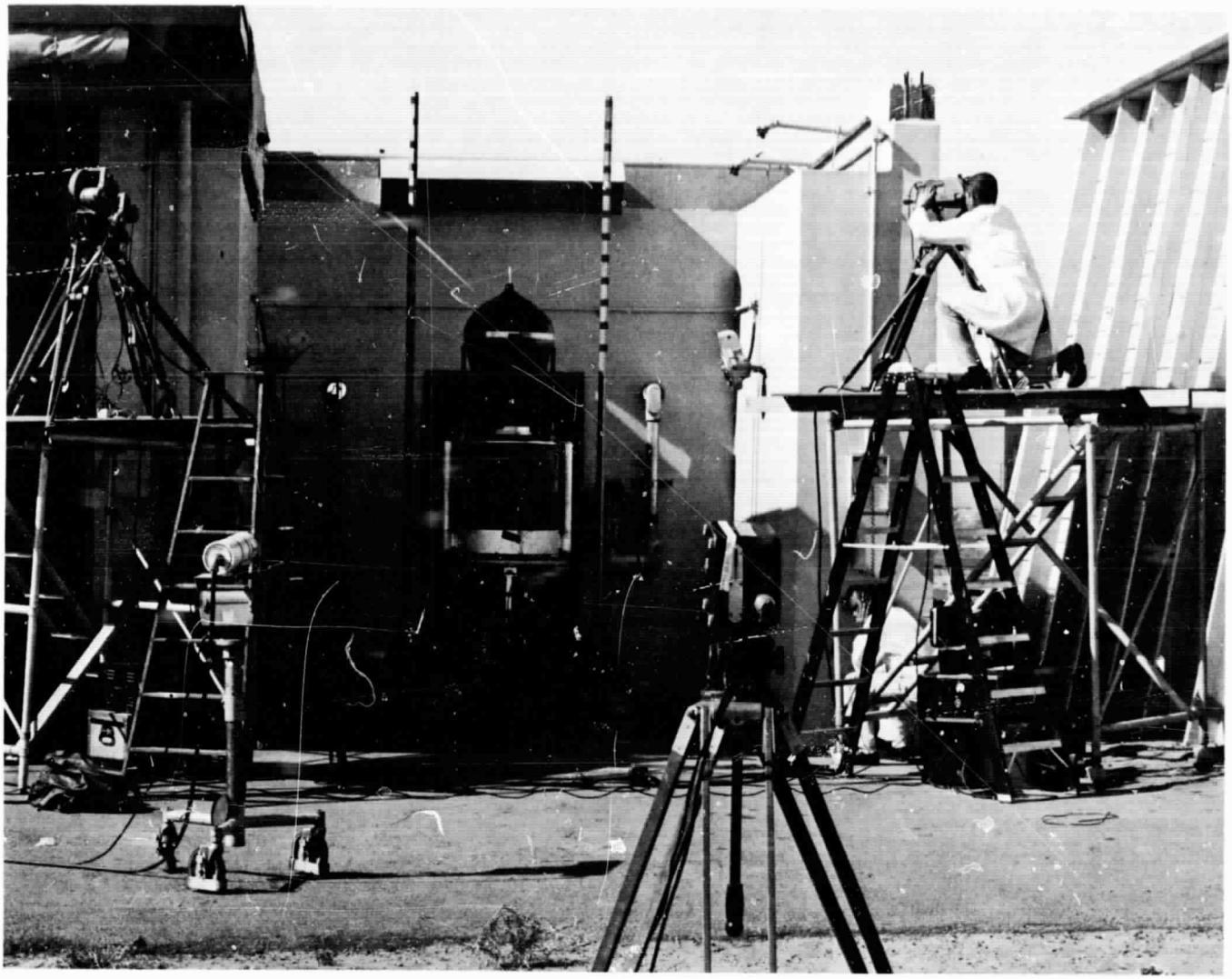

Fig. 27. Pretest installation of test article and high-speed cameras

Fig. 27. The motor was mounted on the vertical spin test stand located in the north test bay of building E-60 at ETS. During the test, the motor and antenna were spinning at 100 rev/min. Four 16-mm Fastax cameras, operating at approximately 2000 frames/s, photographed the release and initial free flight of the antenna–dome combination. A single 16-mm Milliken camera, operating at 500 frames/s, was used for overall test coverage. Figure 28 shows the five camera positions. Two transducers measured chamber pressure, while a single transducer measured igniter basket pressure. The output of all transducers was recorded on an oscillograph. A special circuit was created to indicate the release of the coaxial cables. The signal indication, which occurs after the antenna has traveled 0.25 in., was also recorded on the oscillograph. Temperature-indicating paint was applied to the antenna standoff supports. The paint was applied in three colors that indicated temperatures of 500°, 700°, and 900°F.

The Fastax camera does not have the capability of incorporating a timing mark on the film; therefore, a stroboscopic light was placed in view of all Fastax cameras. When the light was triggered at the same time that current was supplied to the squib, a positive indication of ignition sequence start was produced on the film. Figure 29 shows, by means of a block diagram, the electrical circuits for the high-speed cameras, igniter ignition, and strobe light. The firing of the squib and strobe light and starting of each camera were controlled by a Fastax power control unit. The test was initiated by actuating the start switch on each control unit box.

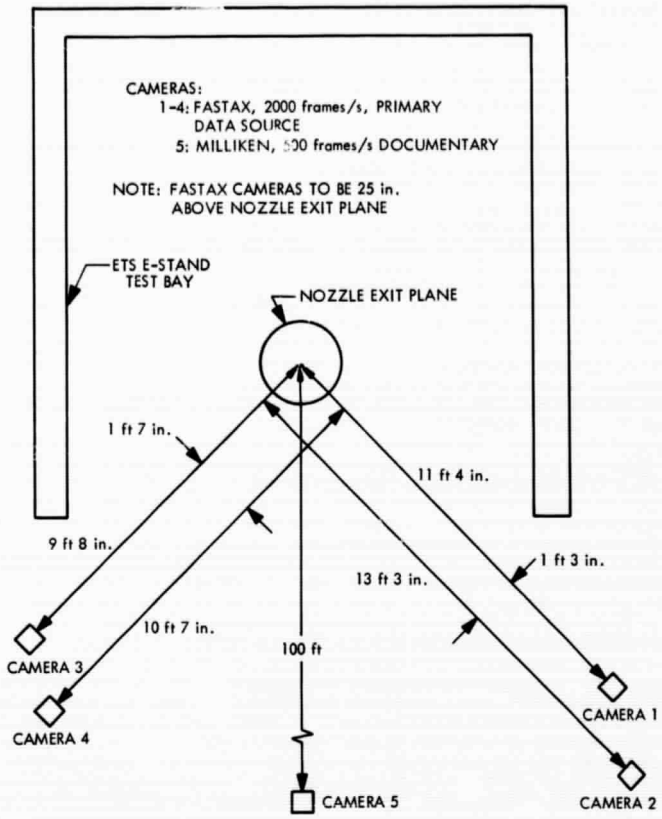

Fig. 28. Camera positions for omniantenna tests

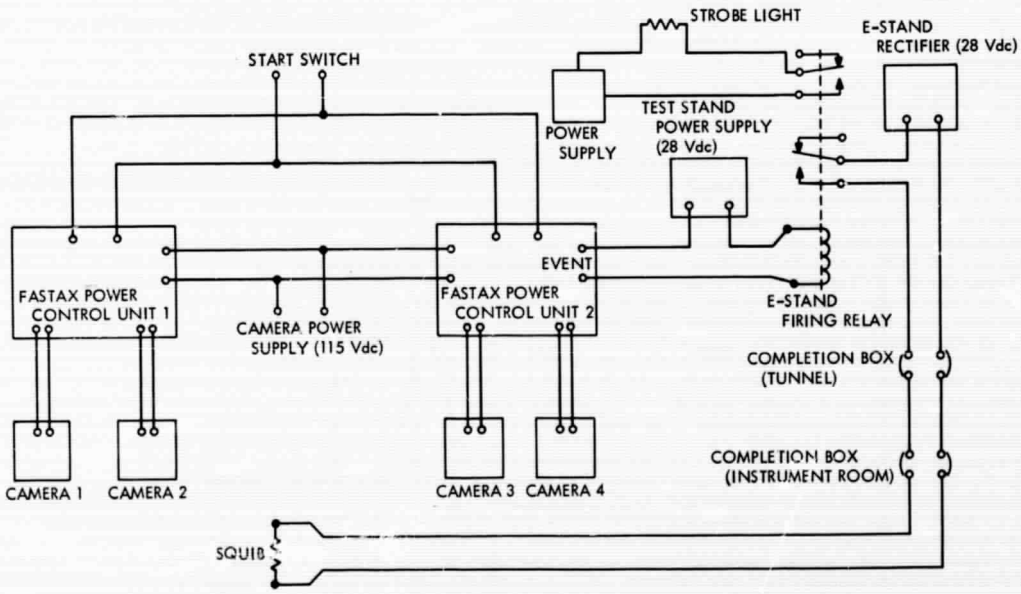

Fig. 29. Electrical diagram of high-speed cameras and igniter ignition circuit

Following a dry run that included the testing of all five cameras, test J-1 was performed. All data were adequately recorded except for ignition current. A close examination of the oscillograph revealed that the start of the ignition sequence could still be correlated without an ignition current trace. At the time current was applied to the squib circuit a slight noise signal was generated in all pressure transducer circuits. This noise signal is discernible on all transducer traces recorded on the oscillograph (Fig. 30) and corresponds to zero time t_0, or first indication of squib current.

The results of the recorded pressures of the motor chamber and igniter basket are given in Fig. 30. The oscillograph trace also shows the results of the antenna disconnect circuit. The ignition parameters on test J-1 are nominal when compared with previous apogee motor firings at similar conditions. Figure 31 and Table 11 summarize the critical ignition phase pressure levels and corresponding times for the four omniantenna tests. The summary includes the coaxial cable disconnect response time and corresponding chamber pressure.

A visual inspection of the temperature-sensitive paint on the antenna standoff supports and brackets revealed that the temperature was below 500°F during the live motor firing. This result has been documented by color photographs. The antenna standoff brackets, which are bonded to the nozzle exit cone, achieve a temperature at the bracket interface of 1100°F, while the bonding adhesive is serviceable to 350°F. The antenna disconnect circuit showed *open* (Fig. 30) at 14 ms after the application

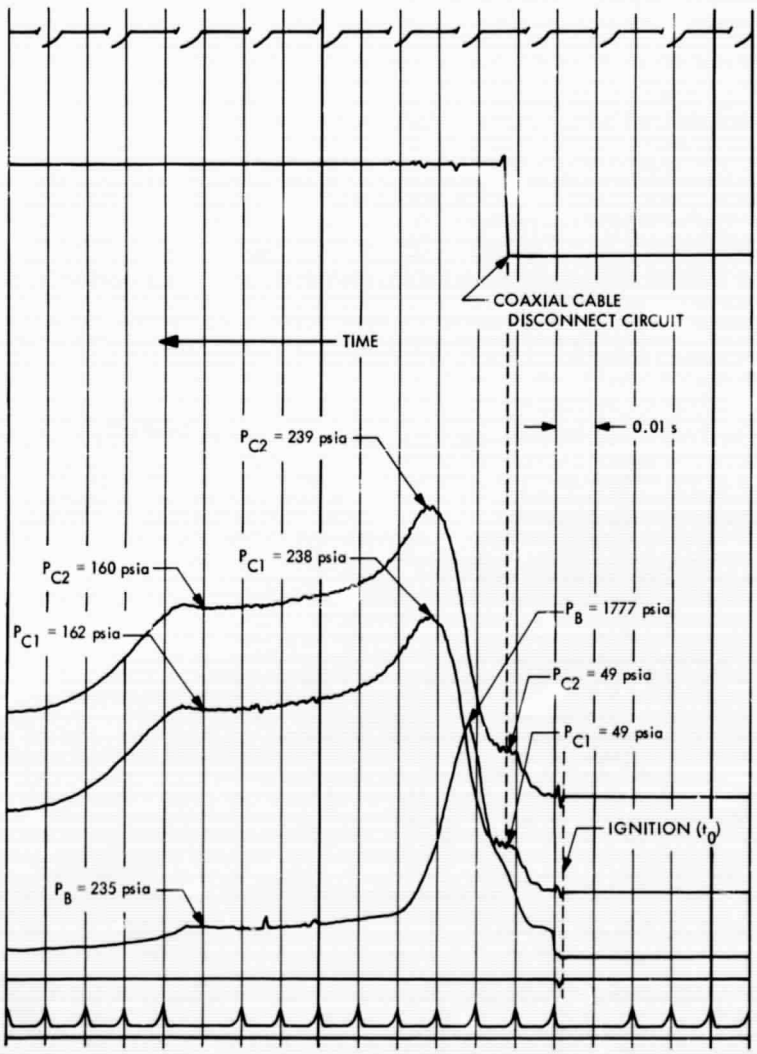

Fig. 30. Motor ignition characteristics—omniantenna test J-1

Table 11. Igniter data, omnidirectional antenna tests

Code	Test date (1967)	Temperature, °F	Vacuum start	t_{D_i}	t_{M_i}	t_{I_i}	t_Δ	t_{I_m}	t_{D_m}	t_{coax}	P_{I_i}	P_{I_m}	P_{coax}
				ms							psia		
0–1	Dec 15, 1966	Ambient, 60	No	—	—	39	4	43	17	—	1693	122	—
0–2	Feb 17, 1967	Ambient, 60	No	2	28	30	8	38	15	24	1781	127	57
0–3	Mar 9, 1967	Ambient, 60	No	2	28	30	6	36	16	25	1863	119	62
J–1	Mar 10, 1967	Ambient, 60	No	2	23	25	9	34	5	14	1777	239	49

See Appendix for ignition parameter definitions except:
t_{coax} = delay time from t_0 until indication of coaxial cable disconnect.
P_{coax} = motor chamber pressure at time of coaxial cable disconnect.

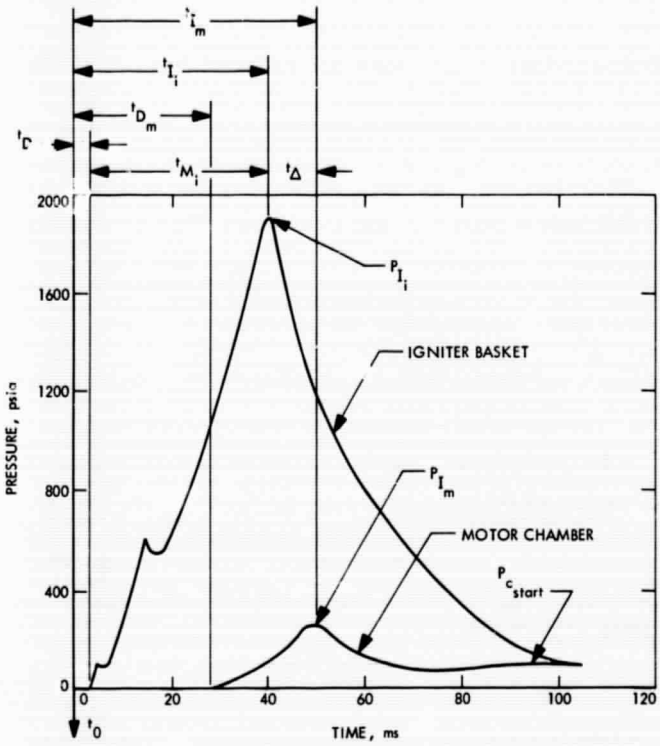

Fig. 31. Motor ignition parameters

of squib current. At this time the antenna had traveled approximately a quarter of an inch from its original position. Similarly, the motor chamber pressure was 49 psia, which closely corresponds to the nozzle diaphragm rupture pressure. The antenna is apparently released from the motor within milliseconds after the nozzle diaphragm ruptures, and thus never sees the peak chamber pressure during the ignition phase of the motor.

In summary, the igniter impulse was more than sufficient to separate the antenna–dome from the motor without producing structural damage. Visual and photographic coverage showed that the antenna released and maintained a free flight path along the centerline of the motor well beyond the region of the VHF antennas of the spacecraft. A comparison of apogee motor ignition parameters shows excellent agreement between the four tests and previous motor firings. The overall results from the four antenna tests indicate that the antenna design and its release mechanism are completely reliable for flight application, and no future antenna tests are planned. Reference 17 covers this effort in a separate HAC report.

11. Flight acceptance test. The final unit tested in the Development Phase, designated Z-7T, was used as an acceptance unit for the three flight units loaded in March–April 1968. The first flight units (Z-1T, Z-2T, and Z-3T) were loaded in September 1966. Because of the relatively long time between flight loadings (approximately 18 months) the processing and testing of an ATS apogee unit before committing the remaining flight hardware was considered necessary.

Unit Z-7T was cast during February 1968. It was subjected to standard processing and inspection techniques. Before being static-tested, the unit was subjected to a temperature cycle of 10°, 110°, and 10°F and returned to ambient temperature for visual and radiographic inspection. The unit was static-fired at ETS with a grain temperature of 10°F while spinning at 150 rev/min. Postfire inspection of motor hardware indicated normal operation and performance during its 43-s run. Flight units Z-4T, Z-5T, and Z-6T were loaded after the successful testing of unit Z-7T.

12. Motor ballistic summary. During the development of the ATS apogee motor, static firings were conducted at ETS; simulated altitude tests were performed at

AEDC. The ETS test area has facilities that allow either horizontal or vertical motor firings. The apogee motor in general has been fired under the following test conditions:

(1) Atmospheric tests in a single-component thrust stand with nozzle area ratios of 8.5 and 35.0.

(2) Constant-area self-pumping diffuser tests in a single-component thrust stand to fully expand the exhaust gases to an area ratio of 8.5.

(3) Atmospheric vertical spin tests with only pressure measurements being made.

(4) Pressure altitude tests at AEDC in a nonspinning single-component thrust stand.

(5) Horizontal spin tests at AEDC in a test stand capable of measuring both the axial thrust and side forces.

The basic instrumentation required for any test includes two transducers to measure the motor chamber pressure from independent pressure taps, a single transducer to measure the igniter basket pressure, and a dual-bridge load cell to measure thrust. In addition, various tests included the installation of thermocouples on the external surface of the motor case and the nozzle for temperature measurements. In tests at AEDC, a low-range transducer was also used to measure the motor chamber pressure during motor tailoff.

The pressure transducers for any test at ETS were calibrated on a high-accuracy deadweight calibrator accurate to within 0.04%. A similar deadweight calibrator was used for AEDC tests. For thrust measurements made at ETS, the load cell was calibrated in the laboratory, but not after installation. The seeming lack of accuracy in the thrust measurement made at ETS can be explained by the fact that the nozzle would not flow full at any time during the run, even though it was cut off as short as physically possible ($\epsilon = 8.5$). For the thrust measurements made at AEDC, the load cells (two dual-bridge cells) were first calibrated in the laboratory. After the load cells and the apogee motor were installed in the test stand, calibration was performed at both sea-level and altitude conditions.

The data acquisition system at ETS consists mainly of a 60-channel digital system. For integral data the test signal is fed into a voltage-to-frequency converter and then into the flow registers. When high-frequency analog data are to be recorded, various oscillographs and magnetic tape decks are available. The static-test data, recorded on magnetic tapes, are reduced at JPL with standard data-reduction computer programs. Listed in Table 12 are the test conditions and important performance results for all the ATS static firings.

B. Qualification Phase

Eight units were tested for the formal Qualification Phase of the apogee motor. Details of the prefire test environments and static-test conditions are shown in Table 13. The units were fired at simulated altitude at the AEDC T-3 facility during July and August 1966. Four units were fired at each temperature of 40° and 100°F while spinning at 100 rev/min. Pressure, thrust, and temperature measurements were recorded. All units were of flight-quality hardware and processed to established quality control loading and inspection procedures. Critical prefire and postfire inspection, and alignment, weight, and balance data were determined for these units.

The pertinent data obtained on the motor during the Qualification Phase (Table 14 and Fig. 32) were used to predict the flight performance of the apogee motor. This phase of the motor program is detailed in reports both by JPL and AEDC (Refs. 18 and 19).

V. Test Environment

To verify that the apogee motor could withstand environments of shipping, storage, launch, and orbiting, tests were performed to subject certain units to simulated conditions. With the exception of vacuum start, all the environmental test levels are more severe than the predicted, flight environments.

A. Vacuum Start

During motor ignition, ten units tested at ETS were subjected to low-pressure starts. An internal motor pressure of 5 torr (112,000 ft) was achieved. The motor nozzle was pressure-sealed by means of an aluminum plate with a rubber gasket placed over the expansion cone (Fig. 33). The vacuum plate was expelled during motor ignition. The five development units fired at AEDC (E-1, E-2, E-3T, G-3, and G-4) were subjected to a simulated altitude of 120,000 ft (3.5 torr) during motor ignition. The nozzle diaphragm was purposely ruptured so that motor ignition was subjected to cell pressure conditions. A comparison of vacuum and atmospheric ignition test data shows no deleterious effects from low-pressure starts. The Qualification units were also subjected to vacuum starts.

Code	Casting data		Test conditions						Physical ha	
	Batch number	Casting date	Type	Location	Test date	Run number	Temperature, °F	Propellant weight, lbm	Chamber	Nozzle
									Serial nu	
C-1	221/222/223	Jan 27, 1964	Atmospheric	ETS	Feb 26, 1964	E-127	60	760.8	P-2	F-13 ε = 8.5
C-2	224/225/226	Feb 18, 1964	Atmospheric	ETS	Mar 5, 1964	E-129	60	761.3	P-7	F-7 ε = 8.5
C-3	233/234/235	May 5, 1964	Diffuser	ETS	Jun 4, 1964	E-174	60	762.2	P-7F	F-6 ε = 8.5
C-3A	236/237/238	May 21, 1964	Diffuser	ETS	Jun 12, 1964	E-175	60	765.8	P-2F	F-5 ε = 8.5
C-4	242/243/244	Jun 25, 1964	Atmospheric	ETS	Jul 15, 1964	E-218	10	764.8	P-13	F-11 ε = 8.5
C-5	245/246/247	Jul 7, 1964	Atmospheric	ETS	Jul 23, 1964	E-237	110	769.3	P-12	F-12 ε = 8.5
C-6	263	Jun 10, 1965	Atmospheric	ETS	Jul 9, 1965	E-416	60	765.7	P-24	F-30 ε = 8.5
C-7	265	Jul 8, 1965	Atmospheric	ETS	Aug 10, 1965	E-435	110	767.0	P-22	F-29 ε = 8.5
E-1	239/240/241	Jun 9, 1964	Diffuser	AEDC	Jul 16, 1964	1426-01	60	765.6	P-9	F-9 ε = 35
E-2	252	Aug 6, 1964	Diffuser	AEDC	Oct 13, 1964	1511-01	60	764.4	P-18	F-15 ε = 35
E-3T	293	Mar 10, 1966	Diffuser	AEDC	Jun 2, 1966	1603-01	75	759.7	T-20	F-42 ε = 35
F-1	273	Sep 23, 1965	Spin, 150 rev/min	ETS	Jan 31, 1967	E-781	10	764.4	P-32	F-26 ε = 35
F-2	274	Sep 30, 1965	Spin, 150 rev/min	ETS	Sep 29, 1967	E-829	10	766.6	P-34	F-27 ε = 35
F-3	275	Sep 17, 1965	Spin, 150 rev/min	ETS	May 10, 1967	E-792	10	764.7	P-23	F-28 ε = 35
G-1	248/249/250	Jul 16, 1964	Atmospheric	ETS	Dec 16, 1964	E-342	110	766.8	P-11	F-16 ε = 35
G-2	251	Jul 28, 1964	Atmospheric	ETS	Dec 16, 1[illegible]	E-343	10	766.1	P-10	F-17 ε = 35
G-3	255	Nov 10, 1964	Diffuser and spin 100 rev/min	AEDC	May 2[illegible]	1540-02	75	765.3	P-[illegible]4	F-24 ε = 35
G-4	257	Feb 4, 1965	Diffuser and spin 100 rev/min	AEDC	M[illegible] 1965	1540-01	75	768.6	P-15	F-20 ε = 35
G-5	254	Nov 3, 1964	Spin, 150 rev/min	ETS	[illegible]v 24, 1964	E-326	60	768.7	P-16	F-14 ε = 8.5
G-6	259	Feb 11, 1965	Spin, 150 rev/min	ETS	Jul 16, 1965	E-431	110	767.2	P-19	F-21 ε = 35
G-7	260	Feb 18, 1965	Spin, 150 rev/min	ETS	Aug 6, 1965	E-434	10	759.6	P-20	F-19 ε = 35
G-8T	280	Oct 21, 1965	Atmospheric	ETS	Nov 9, 1965	E-485	110	759.8	T-4	F-36 ε = 35
G-9T	281	Oct 27, 1965	Spin, 150 rev/min	ETS	Jan 4, 1966	E-515	10	759.6	T-6	F-23 ε = 35
H-1	227/228/229	Apr 16, 1964	Atmospheric	ETS	Nov 4, 1964	E-314	10	640.4	P-5	F-10 ε = 8.5
I-1	264	Jul 1, 1965	Atmospheric	ETS	May 3, 1966	E-637	60	708.2	P-21	F-50 ε = 35
J-1	291	Mar 3, 1966	Spin, 100 rev/min	ETS	May 10, 1967	E-784	60	75[illegible].8	T-18	F-37 ε = 35
Z-7T	308	Feb 14, 1968	Spin, 150 rev/min	ETS	May 16, 1968	E-84	10	760.4	T-23	F-49 ε = 35

For definitions of motor ballistic parameters see Appendix.

[a]Time from t_0 to occurrence of event.

[b]Nozzle expelled about 17 s after motor ignition; all performance data voided.

[c]SDI part number 101120. (All others are SDI part number 100728.)

[d]Measurements not recorded.

[e]Data unavailable because of electrical noise during motor ignition phase.

[f]Thrust measurement was not r

[g]Data unavailable because of

[h]Vacuum correction does not a

FOLDOUT FRAME 1

hardware			Pressure									Time					
	Igniter	Squib	Characteristic velocity $\overline{W}^*$, ft/s	Chamber pressure integral $\int_{t_0}^{t_r} P_c dt$, psia-s	Igniter basket peak pressure P_{T_i}		Chamber ignition peak pressure P_{i_m}		Chamber starting pressure $P_{c_{start}}$		Chamber run peak pressure $P_{c_{peak}}$		Motor delay time t_{D_m}, ms	Action time t_a, s	Run time t_r, s	Vacuum peak thrust $F_{vac_{peak}}$	
number					psia	ms[a]	psia	ms[a]	psia	s[a]	psia	s[a]				lbf	s
	SYC-231	9	4981.3	8918.0	1997	52	255	63	103.9	0.23	265.2	32.1	34	42.31	42.42	5888	32.9
	SYC-233	10	4982.0	8921.1	1620	50	173	60	98.6	0.27	260.6	33.0	29	42.96	43.04	5746	33.0
	SYC-234	11	—[b]	—[b]	1828	59	249	71	115.2	0.22	—[b]	—[b]	40	—[b]	—[b]	—[b]	—[b]
	SYC-235	12	4972.6	8952.2	2289	48	270	63	99.6	0.21	264.4	34.1	35	42.76	42.89	5766	34.2
	SYC-241	18	4960.3	8944.5	1853	34	228	45	98.0	0.25	252.3	34.6	17	44.45	44.52	5563	33.3
	SYC-243	20	4972.3	9012.2	3292	21	273	29	98.8	0.21	274.6	32.8	9	41.68	41.76	6034	32.8
	SYC-255	30	4957.8	8951.2	1950	22	269	29	96.1	0.25	254.8	33.7	11	44.08	44.18	5686	33.8
	SYC-265	9[c]	4982.4	8999.2	3000	12	320	16	96.2	0.20	272.3	33.4	3	42.35	42.57	6018	33.4
	SYC-240	6	4982.9	8960.4	1524	59	239	69	98.1	0.24	263.4	34.0	26	42.93	43.42	6338	34.2
	SYC-242	26	4984.4	8937.8	1832	38	233	49	89.9	0.20	261.5	34.6	27	43.32	43.59	6319	34.0
	SYC-279	13719 13748	—[d]	—[d]	—[d]	—[d]	—[d]	—[d]	—[d]	—[d]	—[d]	—[d]	—[d]	—[d]	—[d]	—[d]	—[d]
	SYC-257	56	4896.0	8846.0	—[e]	—[e]	230	—[e]	103.0	0.20	242.2	34.3	—[e]	—[d]	44.96	—[f]	—[f]
	SYC-258	34	4962.0	8992.0	1892	15	225	38	99.0	0.21	248.1	32.9	16	—[d]	44.53	—[f]	—[f]
	SYC-259	35	4902.6	8865.4	1607	35	235	44	98.0	0.21	244.6	33.3	20	—[d]	44.54	—[f]	—[f]
	SYC-253	38[c]	4975.3	8997.2	—[g]	—[g]	—[g]	—[g]	99.4	0.21	277.4	33.0	—[g]	—[g]	—[g]	—[h]	—[h]
	SYC-252	58[c]	4951.2	8945.5	1527	22	212	32	92.4	0.25	242.7	36.0	2	45.48	45.74	—[h]	—[h]
	SYC-260	36	4965.2	8970.1	1626	33	241	44	99.5	0.25	261.7	32.3	16	42.52	43.09	6233	33.0
	SYC-261	31	4965.1	9042.7	1826	32	233	45	96.6	0.25	261.0	33.1	22	42.99	43.56	6226	33.2
	SYC-245	28	4964.6	9002.8	1930	33	225	42	98.6	0.25	258.9	33.0	—[e]	—[e]	—[g]	—[f]	—[f]
	SYC-262	59[c]	4978.5	9021.9	3485	16	276	23	100.4	0.23	268.5	30.3	—[e]	—[e]	41.74	—[f]	—[f]
	SYC-263	60[c]	4958.6	9019.7	1650	14	217	23	99.3	0.27	245.7	33.9	—[e]	—[e]	45.09	—[f]	—[f]
	SYC-264	61[c]	4967.2	8898.8	2863	12	296	22	99.3	0.25	262.7	30.8	3	41.76	41.92	—[h]	—[h]
	SYC-256	40[c]	4959.2	8901.4	1592	17	234	30	100.4	0.34	243.8	33.3	—[e]	—[e]	44.91	—[f]	—[f]
	SYC-244	27	4965.6	7514.3	2005	20	224	40	191.1	0.36	264.2	20.3	12	31.74	31.81	5774	21.3
	SYC-280	13640 13686	—[d]	—[d]	—[d]	—[d]	—[d]	—[d]	—[d]	—[d]	—[d]	—[d]	—[d]	—[d]	42.33	—[d]	—[d]
	SYC-278	13637	4933.6	8817.6	1777	06	239	34	97.0	0.21	257.4	31.6	—[e]	—[d]	42.61	—[f]	—[f]
	SYC-288	13717	4959.0	8905.0	2032	18	259	28	103.0	0.18	251.0	33.5	6	—[d]	43.44	—[f]	—[f]

made during spin tests.
malfunction of oscillograph recorder.
pply because of incomplete expansion of exhaust gases.

FOLDOUT FRAME 2

Table 12. Motor static-test data, Development Phase

	Time			Thrust						Nozzle					Code
	Motor delay time t_{D_m}, ms	Action time t_a, s	Run time t_r, s	Vacuum peak thrust $F_{vac_{peak}}$		Measured total impulse I_{mea}, lbf-s	Vacuum total impulse I_{vac}, lbf-s	Measured specific impulse $I_{sp_{mea}}$, lbf-s/lbm	Vacuum specific impulse $I_{sp_{vac}}$, lbf-s/lbm	Throat diameter, in.			Exit diameter (initial), in.	Throat erosion (area), %	
				lbf	s					Initial	Final	Average			
.1	34	42.31	42.42	5888	32.9	138,450	197,640	182.0	259.8	4.083	4.123	4.103	11.907	1.97	C-1
.0	29	42.96	43.04	5746	33.0	137,560	196,580	180.7	258.2	4.083	4.125	4.104	11.907	2.07	C-2
[b]	40	—[b]	—[b]	—[b]	—[b]	—[b]	—[b]	—[b]	—[b]	4.083	—[b]	—[b]	11.906	—[b]	C-3
1	35	42.76	42.89	5766	34.2	181,110	193,320	236.5	252.4	4.083	4.127	4.105	11.906	2.17	C-3A
.6	17	44.45	44.52	5563	33.3	137,560	197,510	179.9	258.2	4.084	4.114	4.099	11.905	1.47	C-4
.8	9	41.68	41.76	6034	32.8	140,850	198,100	183.1	257.5	4.083	4.118	4.100	11.907	1.72	C-5
.7	11	44.08	44.18	5686	33.8	138,710	199,620	181.1	260.7	4.084	4.114	4.099	11.907	1.47	C-6
.4	3	42.35	42.57	6018	33.4	140,690	200,080	183.4	260.9	4.083	4.120	4.101	11.908	1.82	C-7
.0	26	42.93	43.42	6338	34.2	205,060	214,740	267.9	280.2	4.085	4.124	4.105	24.134	1.92	E-1
.6	27	43.32	43.59	6319	34.0	210,730	214,360	275.7	280.2	4.090	4.124	4.107	24.135	1.67	E-2
[d]	—[d]	—[d]	—[d]	—[d]	—[d]	—[d]	—[d]	—[d]	—[d]	4.083	—[d]	—[d]	24.137	1.67	E-3T
.3	—[e]	—[d]	44.96	—[f]	—[f]	—[f]	—[f]	—[f]	—[f]	4.083	4.106	4.094	24.137	1.13	F-1
.9	16	—[d]	44.53	—[f]	—[f]	—[f]	—[f]	—[f]	—[f]	4.083	4.104	4.094	24.134	1.20	F-2
.3	20	—[d]	44.54	—[f]	—[f]	—[f]	—[f]	—[f]	—[f]	4.083	4.103	4.093	24.137	0.98	F-3
0	—[g]	—[g]	—[g]	—[h]	—[h]	131,360	—[h]	171.3	—[h]	4.083	4.114	4.098	24.137	1.52	G-1
0	2	45.48	45.74	—[h]	—[h]	127,400	—[h]	166.3	—[h]	4.083	4.115	4.099	24.135	1.57	G-2
3	16	42.52	43.09	6233	33.0	212,190	214,760	277.3	280.6	4.083	4.110	4.096	24.135	1.33	G-3
1	22	42.99	43.56	6226	33.2	213,240	215,740	277.4	280.7	4.082	4.112	4.097	24.106	1.48	G-4
0	—[e]	—[e]	—[g]	—[f]	—[f]	—[f]	—[f]	—[f]	—[f]	4.083	4.113	4.098	11.904	1.48	G-5
3	—[e]	—[e]	41.74	—[f]	—[f]	—[f]	—[f]	—[f]	—[f]	4.082	4.108	4.095	24.127	1.28	G-6
9	—[e]	—[e]	45.09	—[f]	—[f]	—[f]	—[f]	—[f]	—[f]	4.082	4.105	4.094	24.126	1.13	G-7
8	3	41.76	41.92	—[h]	—[h]	129,498	—[h]	170.3	—[h]	4.084	4.114	4.099	24.138	1.47	G-8T
3	—[e]	—[e]	44.91	—[f]	—[f]	—[f]	—[f]	—[f]	—[f]	4.083	4.106	4.094	24.136	1.13	G-9T
3	12	31.74	31.81	5774	21.3	117,080	163,930	182.8	256.0	4.084	4.105	4.094	11.904	1.03	H-1
[d]	—[d]	—[d]	42.33	—[d]	—[d]	—[d]	—[d]	—[d]	—[d]	4.082	4.122	4.102	24.133	1.99	I-1
6	—[e]	—[d]	42.61	—[f]	—[f]	—[f]	—[f]	—[f]	—[f]	4.081	4.104	4.093	24.138	1.13	J-1
5	6	—[d]	43.44	—[f]	—[f]	—[f]	—[f]	—[f]	—[f]	4.085	4.106	4.096	24.134	1.51	J-7T

Table 13. Motor Qualification Phase

Code[a]	Test conditions			Test environment
	Temperature, °F	Location	Test stand type	
Q-1T	40	AEDC	Spin-100 rev/min	(1) Temperature cycle (2) Booster acceleration (3) Booster vibration (4) Vacuum start
Q-2T	100			
Q-3T	40			
Q-4T	100			
Q-5T	40			
Q-6T	100			
Q-7T	40			
Q-8T	100			

[a]T stands for titanium chamber

B. Shipping Temperature

The test environment for shipping temperature is extremely severe when actual shipping temperature conditions are considered. Two Development units (G-1 and G-2) were subjected to a 10-day shock temperature cycling. The temperature exposures were 24-h periods at 10° and 110°F. Both units survived this environment and were successfully static-fired at grain temperatures of 10° and 110°F.

C. Temperature Cycle

Exposure to temperature cycle test environment verifies that the apogee unit is capable of withstanding conditioning over a range of 10° to 110°F. Periods of exposure are 72 h at each extreme. This time period

Table 14. Motor data, Qualification Phase

Data[a]	Q-8T	Q-6T	Q-2T	Q-4T	Q-5T	Q-7T	Q-1T	Q-3T
Test conditions								
Motor firing order	1	2	3	4	5	6	7	8
Test date (1966)	Jul 29	Aug 3	Aug 5	Aug 9	Aug 15	Aug 18	Aug 19	Aug 23
AEDC altitude chamber	T-3	T-3	T-3	T-3	T-3	T-3	T-3	T-3
Average test altitude, ft	104,000	106,000	105,000	104,000	104,000	103,000	104,000	107,000
Motor conditioning temperature, °F	100	100	100	100	40	40	40	40
Time data								
Igniter delay time t_{D_i}, ms	4	3	3	1	2	2	2	3
Motor delay time t_{D_m}, ms	28	23	28	23	25	25	33	28
Motor action time t_a, s	41.92	41.85	42.35	42.02	43.33	43.03	43.27	43.61
Pressure data								
Igniter basket peak pressure P_{I_i}, psia	1693	1874	1923	1879	1215	1821	1362	1578
Motor chamber ignition peak pressure P_{I_m}, psia	250	257	250	272	234	221	213	230
Motor chamber starting pressure $P_{c_{start}}$, psia	101	101	100	100	102	101	101	100
Motor chamber run peak pressure $P_{c_{peak}}$, psia	264.2	262.2	259.8	262.8	251.6	255.7	250.5	248.2
Chamber pressure integral $\int_{t_0}^{t_r} P_c\, dt$, psia-s	8909.6	8904.5	8925.8	8924.5	8891.1	8900.1	8876.6	8897.1
Characteristic velocity $\bar{W}^*$, ft/s	4974.3	4986.0	4983.4	4985.2	4965.5	4967.3	4955.4	4960.2
Thrust data								
Vacuum peak thrust $F_{vac_{peak}}$, lbf	6397	6362	6279	6355	6074	6180	6065	6012
Vacuum total impulse I_{vac}, lbf-s	213,957	214,119	213,860	214,021	213,087	213,533	213,189	213,797
Vacuum specific impulse $I_{s_{Pvac}}$ (based on JPL loaded W_p), lbf-s/lbm	281.52	281.92	281.51	281.61	280.78	281.19	280.81	281.02
Vacuum specific impulse $I_{s_{Pvac}}$ (based on AEDC weight difference), lbf-s/lbm	278.22	278.40	278.15	278.26	277.66	277.78	277.55	277.71

[a]See Appendix and Figs. A-1 and A-2 for definition of performance parameters.

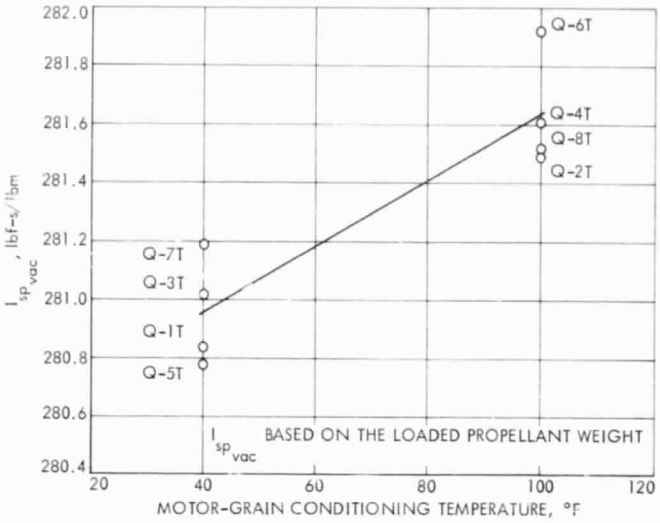

Fig. 32. Vacuum specific impulse vs motor temperature

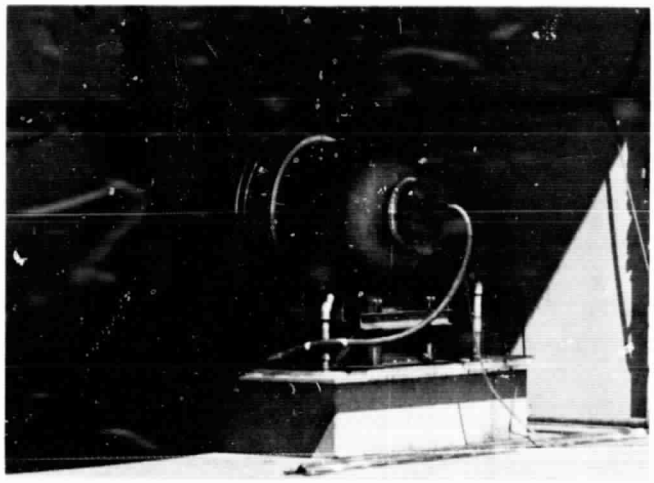

Fig. 33. Motor test setup showing vacuum plate

allows the complete unit (including grain) to stabilize at the conditioning temperature. Two different temperature cycles were used during this program (Table 15). A total of nine developmental units have been successfully subjected to these temperature exposures. The eight Qualification units were also exposed to this test environment before being static-tested at AEDC.

Table 15. Temperature cycle

Cycle A		Cycle B	
Time, h	Temperature, °F	Time, h	Temperature, °F
72	110	72	10
72	10	72	110
72	110	72	10
48	60	48	60
(Alignment, x-ray, and visual inspection)		(Alignment, x-ray, and visual inspection)	
72	10	72	110
(Static firing at 10)		(Static firing at 110)	

D. Booster Acceleration

Centrifuge testing demonstrates that the apogee unit loaded with live propellant is adequate to withstand the static acceleration levels associated with the *Atlas/Agena* launch phase and the motorburning phase of the ATS flight. Table 16 gives the schedule of static acceleration testing. Figure 34 shows a typical unit mounted on the centrifuge boom.

Seven units have been subjected during the Development Phase to static acceleration testing. The first unit (D-1) was loaded with an inert polyurethane propellant to assure complete operational safety. The three Storage units (F-1, F-2, and F-3) were placed in this environment after long-term ambient storage. The Qualification units were also subjected to this test environment before being static-tested at AEDC. No observable or measured effects were noted for any of the units tested.

Table 16. Schedule of motor static acceleration testing

Test position	Acceleration				Centrifuge, rev/min
	Level, g	Duration, min	Attachment point	Distance from centrifuge axis, in.	
Lateral (nozzle up)	2.3	10	Motor axis	216.0	19.3
Axial tension (nozzle out)	12.0	10	Chamber attachment skirt plane	205.2	45.4
Axial compression (nozzle in)	12.0	10	Chamber attachment skirt plane	226.9	43.2

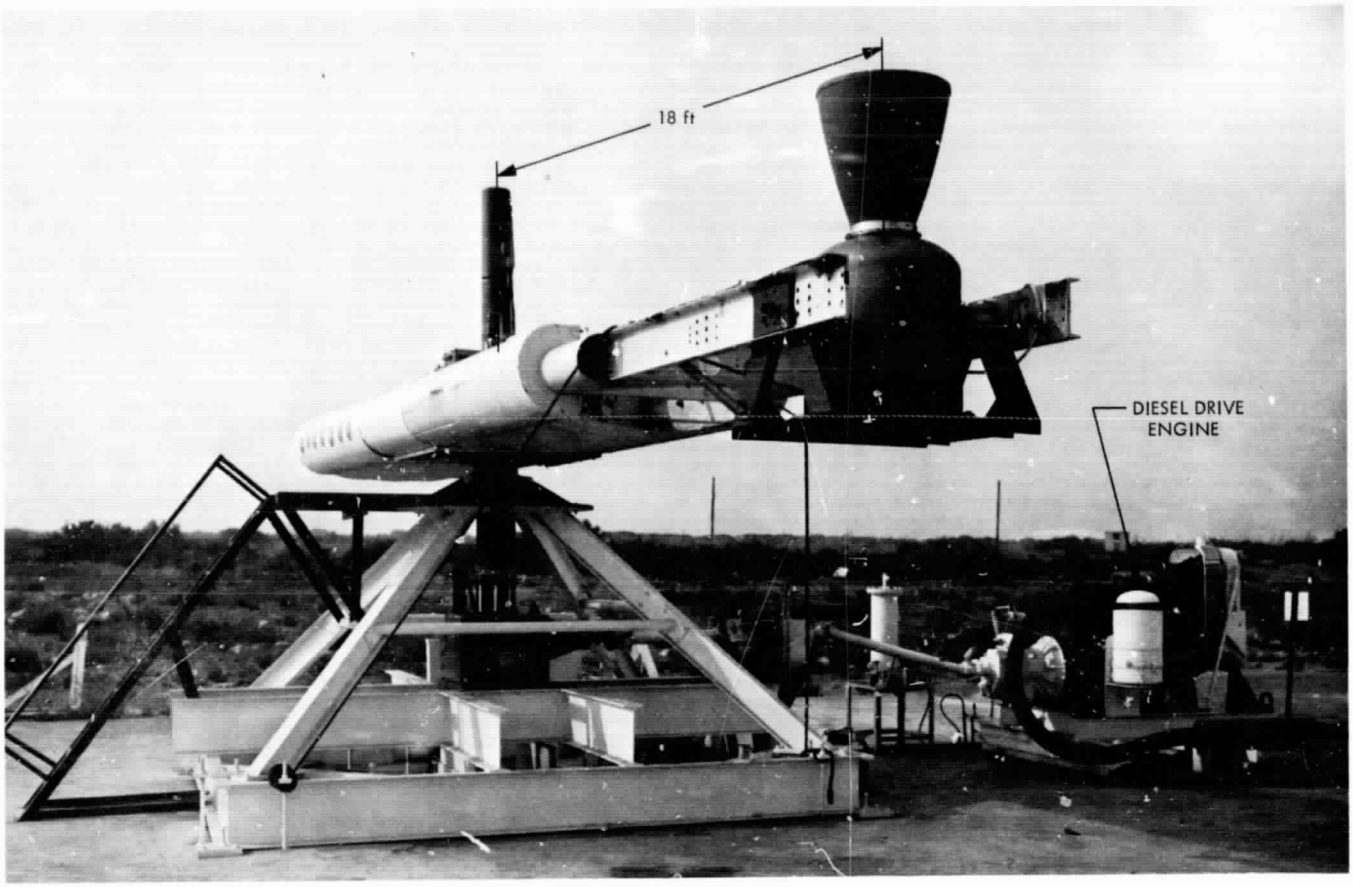

Fig. 34. Centrifuge with motor assembly installed (lateral mode)

E. Booster Vibration

The ATS apogee motor is required to withstand a prescribed vibration environment. This environment exceeds the predicted input requirements of the *Atlas/Agena* booster system. The vibration specification that has been presented (Section III) gives the required input levels at the motor–spacecraft attachment plane. The frequency range of 5 to 15 Hz has been deleted because the shaker used for the vibration tests could not handle the weight of the loaded motor in that range.

The first motor vibration test (D-1), performed at JPL on a stainless steel chamber loaded with inert propellant, was conducted primarily to evaluate the vibration equipment and the response of the motor to the required input levels. At this time, a remote vibration facility was being built at ETS that would have capabilities of vibrating a live ATS motor. In May 1965 the remote facility was completed. During the 3 months that followed, each of three live motors (G-4, G-6, and G-7) was successfully vibrated to input requirements. These motors have since been static-tested with each motor performing properly.

Because the ATS program requirements had changed to include a titanium motor chamber, two additional vibration tests were scheduled during November and December 1965. The vibrational test of a titanium chamber loaded with inert propellant was performed to evaluate the changes in motor response caused by the change in case material and to establish detailed testing procedures to be used in the environmental test phase for the nine Qualification motors. One additional motor cast during the Environment series of the Development program was used to verify that the titanium chamber loaded with live propellant could survive vibration. The tests on this unit were performed during December 1965; all data received from both the vibration environmental test and the static-firing indicated that the motor performed normally.

Detailed vibrational test procedures were established during the titanium chamber tests. Of the eighteen

channels of data recorded per test axis, two were control, two control monitor, four fixture response, and eight motor response accelerometers; in addition, one channel recorded the armature current used to evaluate the shaker performance, and one recorded a constant-sine signal used for data analysis. All of these channels are recorded on magnetic tape. The control accelerometers and various motor response accelerometers are monitored on an oscillograph for instantaneous data.

Vibrational input is controlled by a servo system which, during the sinusoidal part of the test, uses the quadratic mean of two control accelerometer signals. During the random noise portion of the test, output from only one accelerometer is used to control the shaker. The control accelerometers are located in the motor–spacecraft attachment plane to simulate the input flight conditions as closely as possible. Figure 35 shows the installation of the motor in the lateral test mode. The accelerometers are mounted to the test article with micarta blocks that are then cemented to the motor. The blocks are located in specified positions on the motor. The shaker is rotated to a horizontal position for the lateral test mode and connected to a slider plate that rides on a granite block. An oil film is maintained between the slider plate and the granite block to reduce sliding friction. For the axial test mode the shaker is rotated to a vertical position and the motor, with adapting fixture, is mounted on top (Fig. 36). The shaker is remotely controlled from a special console as shown in Fig. 37.

The environmental vibration testing of the nine Qualification motors started on March 8, 1966. The test procedures developed by the titanium chamber tests were used for the Qualification motors. All channels of accelerometer data were recorded on magnetic tape.

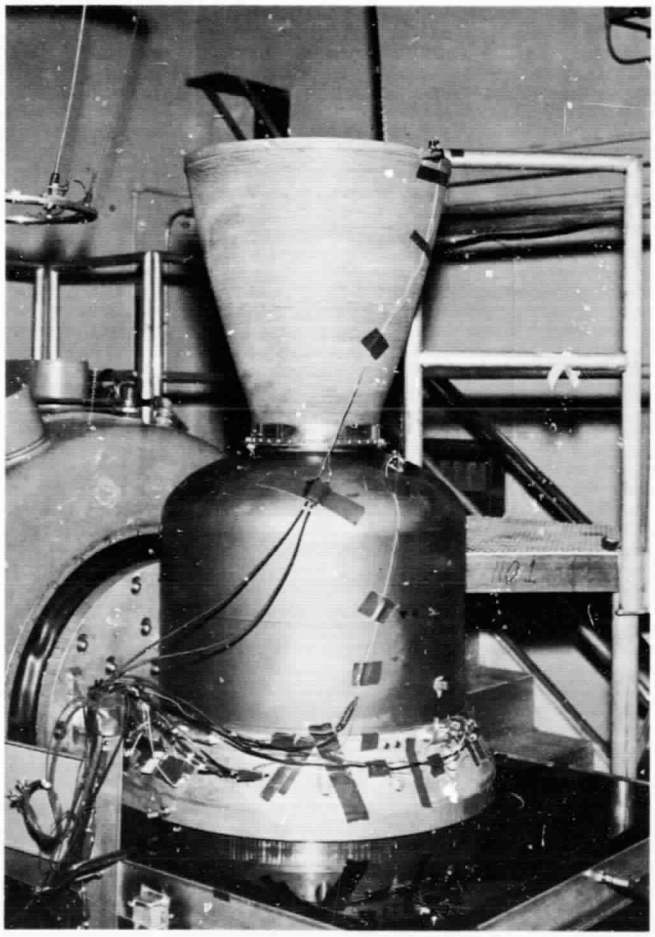

Fig. 35. Vibration test (lateral mode)

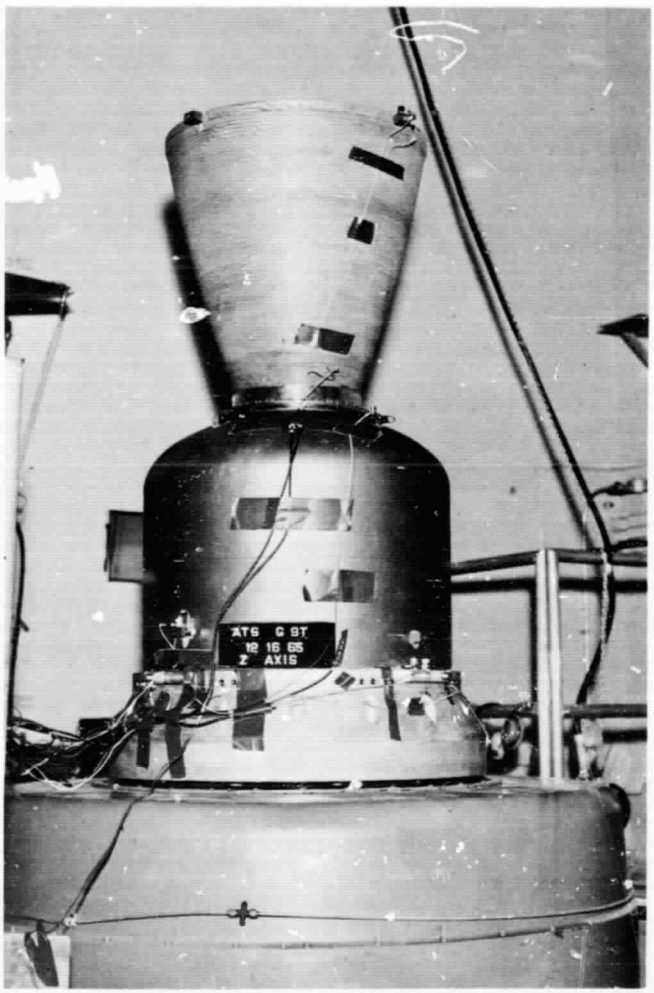

Fig. 36. Vibration test (axial mode)

Fig. 37. Vibration control console

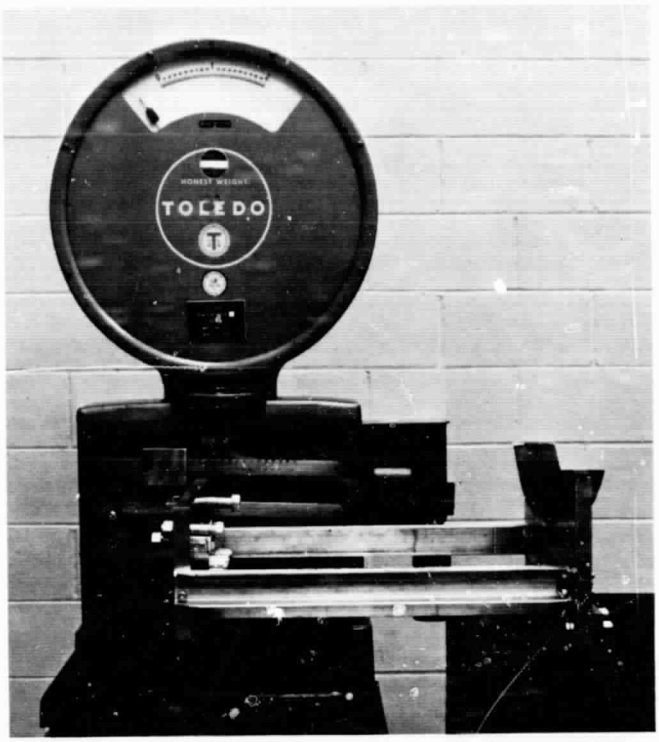

Fig. 38. Center-of-gravity fixture

VI. Motor Physical Parameters

A. Center of Gravity

The center of gravity of the motor has been determined for the loaded and empty (prefire) configurations. Fired Qualification units were used to determine a more realistic spent motor center-of-gravity to be used for spacecraft flight analysis. To permit determination of the center of gravity, the unit is set in a cradle (Fig. 38) and the weight component reaction, which is transmitted through a knife-edge support, is measured by a platform scale. The motor is then rotated 180 deg in the cradle, and the weight component reaction at the nozzle-end measured. This method is used to calculate the center-of-gravity location from either end of the motor. The center-of-gravity measurements, as determined by a summation of the moments about either knife-edge support, agree to within 0.050 in.

The center of gravity of the 75-lb empty motor assembly is 21.0 in. from the motor attachment plane, and of the flight motor loaded with the maximum propellant weight of 760 lb the center of gravity is 11.5 in. from the motor attachment plane.

B. Moment of Inertia

A bifilar pendulum method is used to determine the moment of inertia of the motor in the loaded and empty configurations. Fired Qualification units were used to determine the postfire moment of inertia. These data are required for spacecraft spin stabilization analysis. The bifilar pendulum method uses two 14-ft rods to suspend the motor during moment-of-inertia tests. To calculate the moment of inertia, weight component reactions are taken at each suspension point by load cells, and the period of oscillation is measured while the motor is suspended by the two rods.

All moment-of-inertia determinations for loaded motor assemblies have been conducted with the maximum propellant weight of 760 lb. Figure 39 shows a typical determination test. The moments of inertia of the flight configuration motor are listed in Table 17.

C. Motor Alignment

Because of spacecraft attitude control requirements, the thrust vector of any rocket on board must be rigidly defined. The thrust vector of the apogee motor is collinear with the spacecraft spin axis. The following requirements were specified by GSFC for the apogee

Table 17. Motor moment-of-inertia data

Motor configuration	Moment of inertia, lb-in.^{2}	
	Pitch axis	Roll axis
Loaded	101,000	84,000
Empty, prefire	17,000	8,000

The S&A–igniter assembly was not included for these determinations.

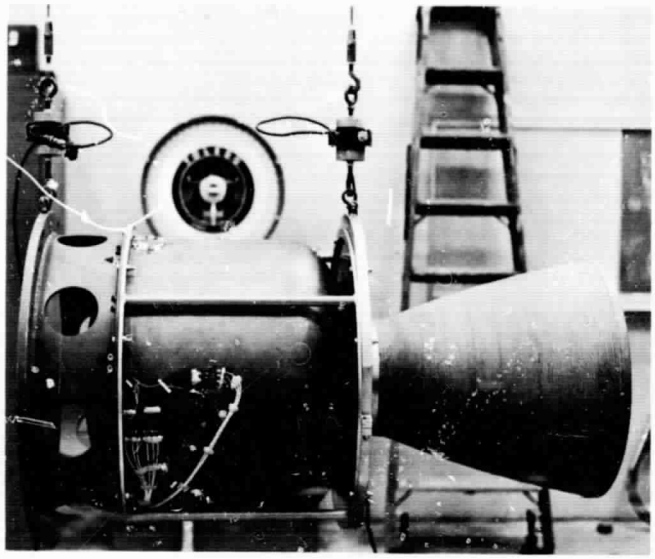

Fig. 39. Moment-of-inertia fixture

motor. The slope of the thrust vector (the line connecting the centroids of the nozzle throat and exit areas) may not be in misalignment with the spin axis by more than 0.001 in./in. Further, when the measured thrust vector is projected to intersect the plane of the motor-spacecraft attachment ring, the vector may not deviate from, nor be offset to, the plane center by more than 0.030 in. The chamber and nozzle were designed to these requirements so that if all component tolerances were maximum and additive the specification limits would not be exceeded. A dimensional analysis on the chamber and nozzle drawings, with consideration of the worst-case conditions, showed a maximum possible thrust misalignment of 0.0009 in./in. and an offset of 0.027 in.

After fabrication each of the chambers, steel and titanium, and each of the nozzles underwent a precision mechanical inspection for (1) determination of drawing conformity, (2) comparison of parts data for quality control purposes, and (3) data for thrust misalignment and offset calculations. The dimensional data then became a factor in determining the assignment of each component to Development test, Qualification test, flight, or flight backup.

The dimensional inspections concerned the following: the circumferential out-of-roundness, which is defined as the difference between maximum and minimum radii about the centroid of the measured profile; the centroidal offset, which is the horizontal deviation of the centroid of the profile in question from a vertical line originating from the centroid of a reference diameter; and flatness, which is the vertical distance between the maximum peak and minimum valley of the surface (vertical is parallel to the axis of symmetry).

Thirty-six flight design nozzles were fabricated and accepted by JPL. The A-5 nozzle attachment ring diameter, used to center the nozzle (refer to Fig. 40) during motor assembly, was the reference diameter of the part; the centroidal offset and circumferential out-of-roundness

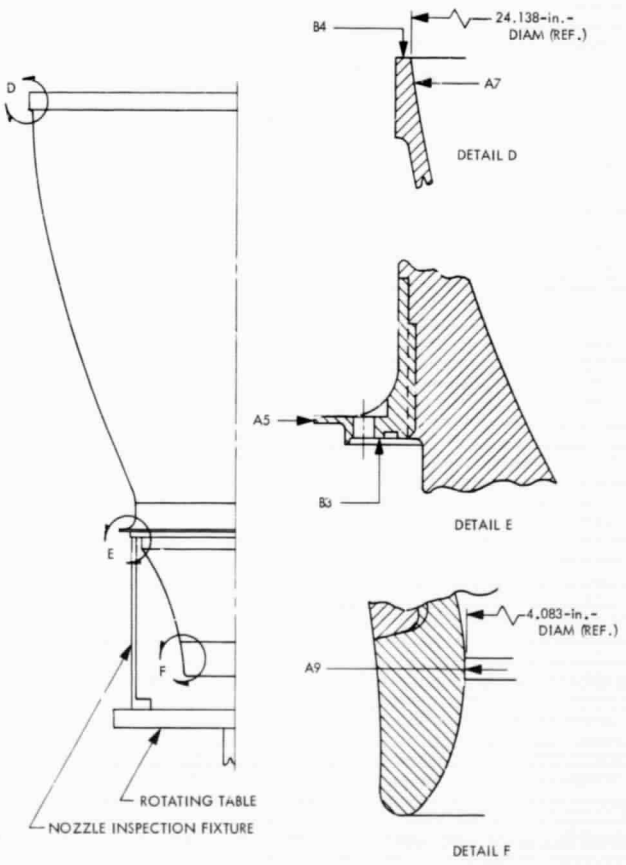

Fig. 40. Alignment inspection positions

of all the A diameters were measured with respect to the A-5 reference. The B-3 surface is the mating plane with the chamber, the reference with which all the parallel measurements of the B surfaces were compared. The flatness of the B-3 surface was used to evaluate possible nozzle misalignment before nozzles were installed on a chamber. To permit inspection of all the aforementioned positions, the nozzle was placed on a rotating table and was supported by a precision inspection fixture.

Figure 41 depicts the locations of the alignment inspections performed on the 53 chambers (23 of which were titanium) that have been accepted by JPL. The A-1 diameter and the B-1 surface were designated references of the chamber, since they constitute the motor–spacecraft attachment. The A-2 diameter and B-2 surface are critical because they are the surfaces to which the nozzle is attached. The A-3 diameter, which is also measured for alignment, is less critical; its only function is to provide a mating surface for the igniter whose alignment does not need to be so precise as that of the nozzle. As with the nozzle, the chamber, mounted to a precision inspection fixture, is inspected on a rotating table. It was found that changing the chamber material from stainless steel to titanium did not disrupt the precision to which the chambers were being fabricated. Table 18 shows the precision to which the individual chambers and nozzles were manufactured. The data given represent the inspection results of seven sets of hardware assigned to flight status.

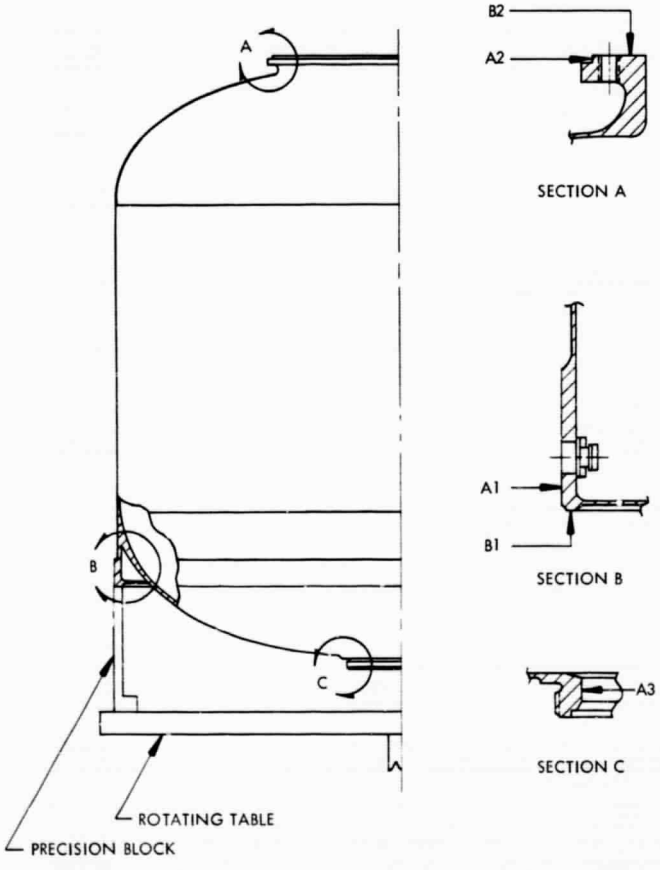

Fig. 41. Chamber alignment inspection positions

To confirm that the precision of the motor chamber was not affected by various processing steps, several chambers were inspected after each major processing operation. These operations included (1) proof-pressure testing, (2) chamber insulating, (3) propellant casting and curing, and (4) propellant machining. Only minor changes in chamber out-of-round and flatness readings were due to chamber processing. An evaluation of all measurements revealed no deleterious effects due to chamber processing. A comparison of prefire and postfire chamber measurement data also showed little or no change due to static testing. The ATS chamber has been cleaned, pressure-tested, dimensionally inspected, and reused as a precision solid propellant motor component.

Prefire and postfire alignment measurements on most of the nine Qualification motors were performed (Table 19). To measure the alignment of the motor assembly, the assembly is placed in a precision fixture on a rotating table. Figure 42 shows a motor so mounted and defines the inspection positions. Both thrust alignment and offset were degraded by motor static-testing, although all postfire measurements were well within specification limits.

VII. Motor Nominal Data

Reference 20 is a separate JPL document that lists the ATS apogee motor performance characteristics in a condensed form. This publication was prepared for the Chemical Propulsion Information Agency for inclusion in the Rocket Motor Manual, CPIA/M1. One additional JPL document (Ref. 21) was generated during the ATS program that describes the handling equipment required for the apogee motor.

VIII. Flight of the *Applications Technology Satellite*

The first *Applications Technology Satellite* (ATS-B) was launched successfully by an *Atlas/Agena* booster on

Table 18. Motor alignment summary, flight hardware

Chamber			Surface and inspection description, in.						
Code	Serial No.	Weight, lb	A-1 Out-of-round	A-2 Out-of-round	A-2 Offset from A-1	A-3 Out-of-round	A-3 Offset from A-1	B-1 Flatness	B-2 Flatness
Z-1T	T-15	23.92	0.0005	0.0010	0.0004	0.0016	0.0012	0.0008	0.0018
Z-2T	T-16	23.71	0.0006	0.0012	0.0011	0.0010	0.0016	0.0008	0.0024
Z-3T	T-17	23.83	0.0007	0.0006	0.0007	0.0014	0.0010	0.0005	0.0024
Z-4T	T-19	23.74	0.0005	0.0018	0.0006	0.0025	0.0020	0.0005	0.0016
Z-5T	T-21	24.63	0.0003	0.0020	0.0007	0.0007	0.0014	0.0008	0.0022
Z-6T	T-22	24.34	0.0002	0.0010	0.0015	0.0007	0.0019	0.0005	0.0029
Z-7T	T-23	24.20	0.0004	0.0008	0.0010	0.0014	0.0007	0.0005	0.0029
Nozzle			**Surface and inspection description, in.**						
Code	Serial No.	Weight, lb	A-5 Out-of-round	A-7 Out-of-round	A-7 Offset from A-5	A-9 Out-of-round	A-9 Offset from A-5	B-3 Flatness	B-4 Flatness
Z-1T	F-45	37.86	0.0008	0.0090	0.0027	0.0003	0.0010	0.0035	0.0045
Z-2T	F-40	37.77	0.0004	0.0035	0.0020	0.0004	0.0007	0.0013	0.0017
Z-3T	F-46	37.94	0.0008	0.0030	0.0015	0.0002	0.0005	0.0016	0.0023
Z-4T	F-33	37.95	0.0005	0.0045	0.0018	0.0005	0.0003	0.0006	0.0010
Z-5T	F-48	37.24	0.0012	0.0055	0.0015	0.0003	0.0004	0.0021	0.0034
Z-6T	F-47	37.50	0.0010	0.0065	0.0015	0.0004	0.0006	0.0023	0.0033
Z-7T	F-49	37.70	0.0010	0.0120	0.0030	0.0006	0.0008	0.0032	0.0050

Table 19. Motor alignment data, Qualification Phase

Measurement data	Code							
	Q-1T	Q-2T	Q-3T	Q-4T	Q-5T	Q-6T	Q-7T	Q-8T
Thrust misalignment, prefire, in./in.	0.00001	0.00005	0.00009	0.00005	0.00002	0.00004	0.00002	0.00005
Thrust misalignment, postfire, in./in.	0.0005	0.0002	0.0002	0.0006	—	0.0003	0.0004	—
Thrust offset, prefire, in.	0.0006	0.0017	0.0022	0.0001	0.0004	0.0008	0.0011	0.0009
Thrust offset, postfire, in.	0.013	0.003	0.004	0.014	—	0.007	0.008	—

Note
Specification requirement (GSFC-S2-0153)
Misalignment (maximum) 0.001 in./in.
Offset at attachment plane (maximum) 0.030 in.

December 6, 1966 at 9:12 p.m. EST. Approximately 16½ h after launch (1:46 p.m. EST), a ground signal was sent from Mojave, California to the spacecraft, commanding the JPL apogee rocket motor to fire. The 840-lb solid propellant apogee motor transferred the spacecraft from a highly elliptical to a near synchronous 22,300-mi equatorial orbit. At the time of this report, the satellite is on-station above Christmas Island in the Central Pacific Ocean. All spacecraft components and experiments functioned as planned.

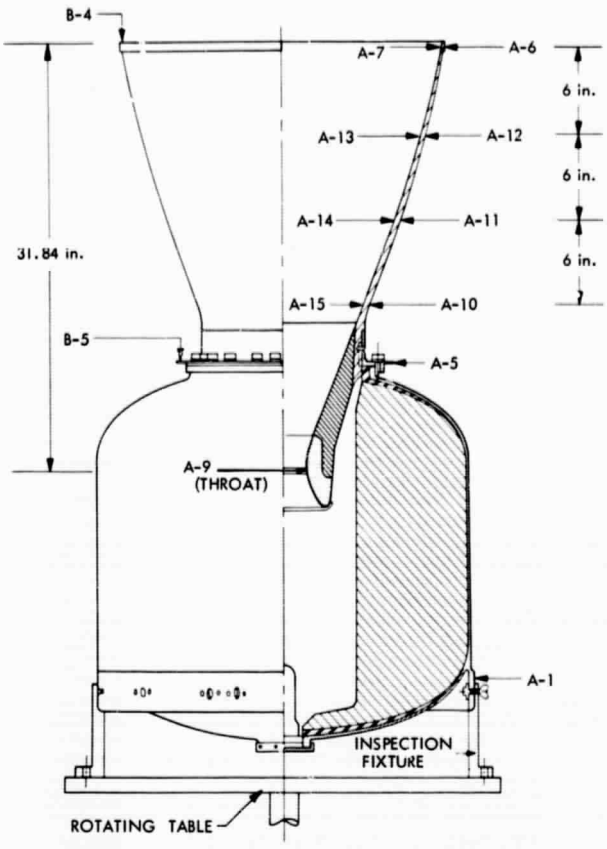

Fig. 42. Motor assembly alignment inspection

The second satellite (ATS-A) was launched April 5, 1967. The payload was to be placed in a medium-altitude 6000-mi circular orbit, so that the principle of gravity-gradient spacecraft stabilization could be studied. The satellite was launched by an *Atlas/Agena* vehicle. At the first apogee position, the *Agena* was to re-ignite and transfer the payload from a highly elliptical orbit to a circular one. The second *Agena* burn did not occur, and the spacecraft was left in its original elliptical orbit. The use of the spacecraft at its present position is doubtful and its lifetime unknown. The ATS-A did not require a JPL apogee motor.

The third satellite (ATS-C) was launched November 5, 1967. At 10:37 a.m. EST on November 6, the apogee motor was fired, placing the spacecraft into the planned synchronous orbit. This spin-stabilized satellite was positioned at longitude 47° W over the Atlantic Ocean near the mouth of the Amazon River in South America. Nine major meteorological and communication experiments were carried.

The fourth satellite (ATS-D) was launched from the AFETR on August 10, 1968. This was the first use of the *Atlas/Centaur* for an ATS launch. The *Centaur* launch vehicle failed to provide a second burn at the second equatorial crossing. As a result, the spacecraft was never separated from the *Centaur* vehicle and was left in a low-altitude parking orbit (100 by 413 nmi with a 36-deg inclination). Most of the subsystems and experiments were turned on and operated normally. The combined *Centaur*/ATS-D vehicle reentered the atmosphere of the earth in late October 1968.

On August 12, 1969 the fifth and final satellite was launched from the AFETR. The ATS-E spacecraft was positioned above the equator at about longitude 110° W (600 mi west of Quito, Ecuador). The primary ATS-E experiment is a gravity-gradient stabilization system.

The performance of the booster (*Atlas/Centaur*) was as planned, placing the spacecraft and apogee motor into a highly elliptical orbit (22,728 by 1,336-mi transfer ellipse). Shortly after separation of the spacecraft from the booster, the spacecraft began to wobble around its Z axis (0.5 to 1.0 deg total angle). Because of this wobble the JPL apogee motor was fired at the first, instead of the planned second, apogee position. Shortly after the completion of motor firing, the spacecraft, rather than spinning at 100 rev/min about the Z axis, tumbled about the Z axis. Because the spacecraft's roll-to-pitch moment-of-inertia ratio after motor firing is approximately 1.0, any small disturbing force can transfer the spacecraft's spin to a new axis. This apparently occurred.

The spacecraft released the spent motor hardware while in this tumbling mode. Some structural damage to the spacecraft occurred during this separation maneuver. Indications are that solar cell damage to the extent of 12–17% has occurred. The ATS-E spacecraft without the spent motor returned to a spinning mode around its Z axis. The major problem with the mission at present is that the spacecraft is now spinning in the wrong direction, making the deployment of the gravity-gradient booms impossible.

The spacecraft has been brought to station over the equator. Meanwhile possible methods of correcting the negative spin condition are being considered. All indications are that the JPL apogee unit performed its required task of placing the ATS-E spacecraft into a synchronous earth orbit.

Table 20. Flight motor data

Code	Flight number	Flight date	Casting data		Component serial number			
			Batch number	Casting date	Chamber	Nozzle	Igniter	Safe-and-Arm
Z-1T	—	—	296	Sep 7, 1966	T-15	F-45	—	—
Z-2T	ATS-B (ATS-I)	Dec 6, 1966	297	Sep 14, 1966	T-16	F-40	Fig. 1	31
Z-3T	ATS-C (ATS-III)	Nov 5, 1967	298	Sep 21, 1966	T-17	F-46	Fig. 3	32
Z-4T	—	—	304	Mar 6, 1968	T-19	F-33	—	—
Z-5T	ATS-D (ATS-IV)	Aug 10, 1968	305	Mar 20, 1968	T-21	F-48	Fig. 7	22
Z-6T	ATS-E (ATS-V)	Aug 12, 1969	307	Apr 10, 1968	T-22	F-47	Fig. 6	19

	Weight data, lb							
	Chamber[a]	Nozzle[b]	Miscellaneous[c]	Igniter	Safe-and-Arm	Total inert hardware	Propellant	Total motor assembly
Z-1T	36.80	37.69	0.37	1.00	5.00	80.86	757.30	838.16
Z-2T	36.76	37.71	0.37	1.00	5.00	80.84	758.30	839.14
Z-3T	36.65	37.75	0.37	1.00	5.00	80.77	758.10	838.87
Z-4T	36.69	38.10	0.37	1.00	5.00	81.16	759.50	340.66
Z-5T	37.36	37.15	0.37	1.00	5.00	80.88	760.00	840.88
Z-6T	37.06	37.43	0.37	1.00	5.00	80.86	759.90	840.76

[a]*Chamber* includes chamber insulation, TDI, and lead balance weight.
[b]*Nozzle* includes diaphragm and balance weight.
[c]*Miscellaneous* includes 36 screws and washers, O-ring, and nozzle lock wire.

For each ATS mission that requires an apogee unit for final synchronous orbit spacecraft insertion, JPL supplies at least two apogee units for mission support. Table 20 lists the pertinent parameters for the six apogee units cast specifically for flight use. Two units, Z-1T and Z-4T, were not used for flight and are stored at ETS at ambient conditions. Approximately two to four weeks before launch the apogee units are inspected and motor preparation is completed. Motor operations performed at AFETR included visual receiving inspection of motors and igniters, motor grain x-ray, and motor pressure test; and the mating of igniter to HDL's safe-and-arm device, the installation of the ignition assembly into the apogee motor, and the integration of the complete apogee unit into the spacecraft. Both apogee units at AFETR receive visual inspection, and x-ray and pressure testing, after which one unit is returned to storage while only one unit is then prepared for final flight. The ATS apogee unit has supplied precise velocity increments to three ATS spacecraft (Table 21).

Table 21. ATS apogee motor velocity data

Spacecraft	Velocity increment ΔV, ft/s	
	Predicted	Measured
ATS-B	6150	6157
ATS-C	6026	6026
ATS-A	Apogee unit not required	
ATS-D	*Centaur* second burn failure	
ATS-E	4668	4684

Appendix

ATS Apogee Motor Parameter Definitions

(1) t_0 = zero time, or time at which current is applied to squib (Figs. A-1 and A-2), s

(2) t_{D_i} = the delay time from t_0 until first indication of squib pressure (Fig. A-1), ms

(3) t_{D_m} = delay time from t_0 until first indication of motor chamber pressure (Fig. A-1), ms

(4) t_{I_i} = time from t_0 until igniter peak pressure (Fig. A-1), ms

(5) t_{I_m} = time from t_0 until chamber ignition peak pressure (Fig. A-1; this is not the same as run peak pressure), ms

(6) t_Δ = time from igniter basket peak pressure P_{I_i} until chamber ignition peak pressure P_{I_m} (Fig. A-1), ms

(7) t_{M_i} = time from initial squib pressure until igniter basket peak pressure; total igniter reaction time (Fig. A-1), ms

(8) P_{I_i} = igniter basket peak pressure during ignition phase (Fig. A-1), psia

(9) P_{I_m} = motor chamber peak pressure during ignition phase (Figs. A-1 and A-2), psia

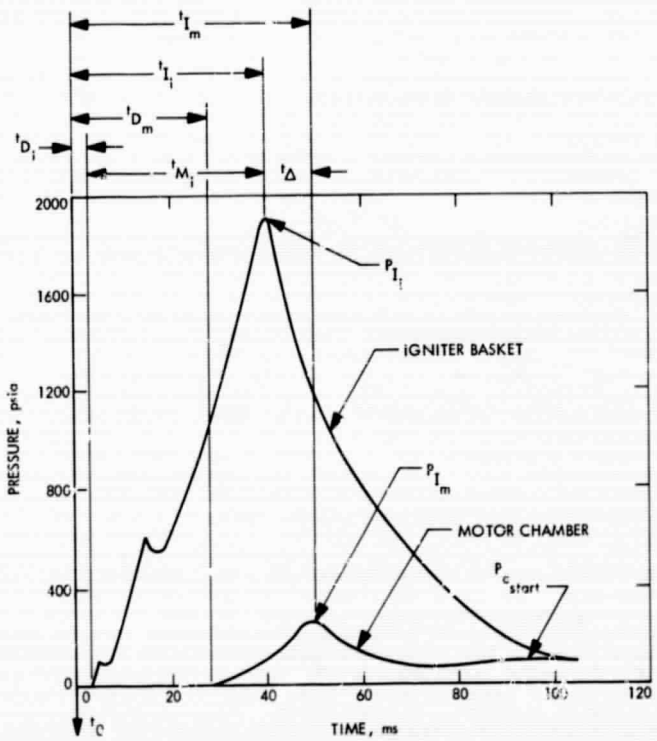

Fig. A-1. Motor ignition parameters

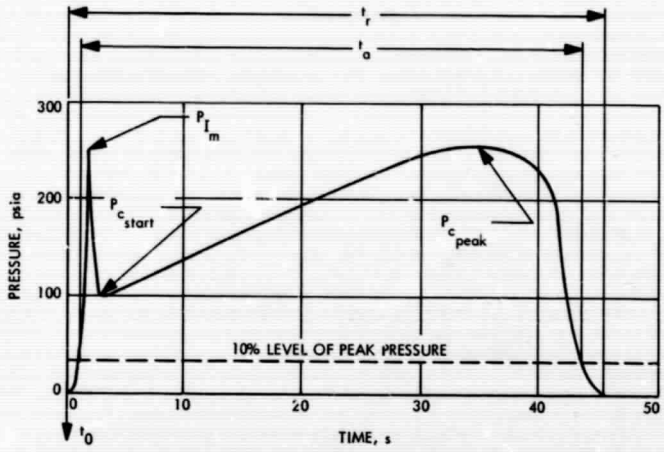

Fig. A-2. Motor parameters

(10) $P_{c_{start}}$ = motor chamber starting pressure (Fig. A-1), psia

(11) $P_{c_{peak}}$ = motor chamber run peak pressure (excluding ignition phase) (Fig. A-2), psia

(12) t_a = action time, or time from motor chamber pressure at 10% of its run peak value ($P_{c_{peak}}$) at ignition until its decrease to 10% of the run peak value during motor tailoff (Fig. A-2), s

(13) t_r = run time, or time from application of electrical current to squib t_0 until motor chamber pressure returns to ambient conditions following motor tailoff (Fig. A-2), s

(14) I_{mea} = measured total impulse, lbf-s

(15) $I_{sp_{mea}}$ = measured specific impulse, lbf-s/lbm

(16) $\int_{t_0}^{t_r} P_c\, dt$ = motor chamber pressure integral, psia-s

(17) $\overline{W}^*$ = characteristic velocity, ft/s

$$\overline{W}^* = \frac{g_0 A_{t_{ave}}}{W_p} \int_{t_0}^{t_r} P_c\, dt$$

where

g_0 = acceleration due to gravity (32.14 lbm-ft/lbf-s^2)

$A_{t_{ave}}$ = average nozzle throat area (based on prefire and postfire measurements)

W_p = loaded propellant weight

t_0 = zero time (item 1)

t_r = run time (item 13)

(18) $F_{vac_{peak}}$ = vacuum peak thrust, measured at the same time as $P_{c_{peak}}$, lbf

$$F_{vac_{peak}} = F_{mea} + A_e P_{cell}$$

where

F_{mea} = measured thrust

A_e = nozzle exit area (initial)

P_{cell} = cell pressure at time F_{mea} is maximum.

(19) Evaluation of vacuum total impulse (I_{vac}) must be corrected because of diffuser flow breakdown occurring during motor tailoff. For impulse data following flow breakdown (t_1), a calculated nozzle vacuum thrust coefficient ($C_{F_{vac}}$) is used. This $C_{F_{vac}}$ value is calculated approximately 1.0 s prior to flow breakdown by the following expression:

$$C_{F_{vac}} = \frac{\int_{t_1-1}^{t_1} F_{mea}\, dt + A_e \int_{t_1-1}^{t_1} P_{cell}\, dt}{A_{t_{final}} \int_{t_1-1}^{t_1} P_c\, dt}$$

(20) With the use of the calculated $C_{F_{vac}}$ value, vacuum total impulse (I_{vac}) is calculated by the following expression:

$$I_{vac} = \int_{t_0}^{t_1} F_{mea}\, dt + A_e \int_{t_0}^{t_1} P_{cell}\, dt + C_{F_{vac}} A_{t_{final}} \int_{t_1}^{t_r} P_c\, dt$$

(21) $I_{sp_{vac}}$ = vacuum specific impulse, lbf-s/lbm

$$I_{sp_{vac}} = \frac{I_{vac}}{W_p}$$

where

W_p = either JPL loaded propellant weight or AEDC weight difference between prefire and postfire measurements.

References

1. *Supporting Research and Advanced Development*, Space Programs Summaries 37-20 to 37-33, Vol. V. Jet Propulsion Laboratory, Pasadena, Calif., covering period of Feb. 1, 1963 to May 31, 1965 (Confidential).

   Supporting Research and Advanced Development, Space Programs Summaries 37-34 to 37-41, Vol. IV. Jet Propulsion Laboratory, Pasadena, Calif., covering period of June 1, 1965 to Sept. 30, 1966.

   Supporting Research and Advanced Development, Space Programs Summaries 37-43 to 37-45, Vol. IV. Jet Propulsion Laboratory, Pasadena, Calif., covering period of Dec. 1, 1966 to May 31, 1967.

   Supporting Research and Advanced Development, Space Programs Summaries 37-47 to 37-49, Vol. III. Jet Propulsion Laboratory, Pasadena, Calif., covering period of Aug. 1, 1967 to Jan. 30, 1968.

   Supporting Research and Advanced Development, Space Programs Summary 37-53 Vol. III. Jet Propulsion Laboratory, Pasadena, Calif., Oct. 31, 1968.

2. Anderson, R. G., Gin, W., and Kohorst, D. P., *The SYNCOM I JPL Apogee Rocket Motor*, Technical Memorandum 33-143, Revision 1. Jet Propulsion Laboratory, Pasadena, Calif., Sept. 16, 1963 (Confidential).

3. Haserot, R. L., *SYNCOM Apogee Rocket Motor (Description and Performance Characteristics)*, Technical Memorandum 33-176. Jet Propulsion Laboratory, Pasadena, Calif., July 1, 1964 (Confidential).

4. Fordyce, D. V., *Apogee Rocket Motor*, ATS No. S2-0153. Goddard Space Flight Center, Greenbelt, Md., June 10, 1965.

5. Lardenoit, V. F., Wada, B. K., and Kohorst, D. P., *Design, Fabrication, and Testing of the Applications Technology Satellite Apogee Motor Chamber*, Technical Memorandum 33-309. Jet Propulsion Laboratory, Pasadena, Calif., Nov. 1, 1966.

6. Grippi, R. A., *Design, Fabrication, and Testing of the Applications Technology Satellite Apogee Motor Nozzle*, Technical Memorandum 33-333. Jet Propulsion Laboratory, Pasadena, Calif., July 15, 1967.

7. Grippi, R. A., *Design, Fabrication, and Testing of the Applications Technology Satellite Apogee Motor Insulation*, Technical Memorandum 33-341. Jet Propulsion Laboratory, Pasadena, Calif. (to be published).

8. Cork, J. M., *SYNCOM I Igniter Squib Development and Qualification*, Technical Report 32-444. Jet Propulsion Laboratory, Pasadena, Calif., June 3, 1963.

9. Lee, T. P., *Ignition System for the ATS Rocket Motor*, Technical Memorandum 33-317. Jet Propulsion Laboratory, Pasadena, Calif., Feb. 1, 1967.

10. Anderson, F. A., *Properties and Performance of JPL 540 Propellant*, Technical Memorandum 33-131. Jet Propulsion Laboratory, Pasadena, Calif., Apr. 30, 1963 (Confidential).

11. Frank, D. R., *Factors Affecting the Reproducibility of Small Solid-Propellant Batch-Check Rocket Motors for Quality-Control Purposes*, Technical Memorandum 33-260. Jet Propulsion Laboratory, Pasadena, Calif., Oct. 15, 1965.

References (contd)

12. Lee, B. J., *Altitude Testing of a JPL-SR-28-1 Apogee Rocket Motor for the Advanced Technological Satellite Spacecraft (Preliminary Test Phase—Part I)*, AEDC-TDR-64-207. Arnold Engineering Development Center, Arnold Air Force Station, Tenn., October 1964.

13. Cimino, A. A., and Stevenson, C. W., *Altitude Testing of a JPL-SR-28-1 Apogee Rocket Motor for the Advanced Technological Satellite Spacecraft (Preliminary Test Phase—Part II)*, AEDC-TDR-64-259. Arnold Engineering Development Center, Arnold Air Force Station, Tenn., December 1964.

14. Domal, A. F., *Thermal and Dynamic Investigation of the Hughes ATS Spacecraft and Apogee Motor System at Simulated High Altitude (S/S Synchronous Spacecraft Thermal Model S/N T-4)*, AEDC-TR-66-170. Arnold Engineering Development Center, Arnold Air Force Station, Tenn., October 1966.

15. Stevenson, C. W., and Nelius, M. A., *Results of Testing Two JPL-SR-28-1 (S/N's P-14 and P-15) Solid-Propellant Rocket Motors Under the Combined Effects of Simulated Altitude and Rotational Spin*, AEDC-TR-65-186. Arnold Engineering Development Center, Arnold Air Force Station, Tenn., September 1965.

16. Nelson, M., *Report on Evaluation Program for Safety Ignition Device for Applications Technology Satellite Rocket Motor*. Harry Diamond Laboratories, U.S. Army Materiel Command, Washington, D.C.

17. Fisher, W. T., *Results of the Developmental Test Program for ATS-C Omni-Directional Antenna Support Dome*, SSD 70265R. Hughes Aircraft Company, Space Systems Div., El Segundo, Calif., June 9, 1967.

18. Frank, D. R., and Anderson, R. G., *Qualification Phase for the Applications Technology Satellite Apogee Rocket Motor*, Technical Memorandum 33-339. Jet Propulsion Laboratory, Pasadena, Calif., Sept. 15, 1967.

19. Cimino, A. A., and Stevenson, C. W., *Results of the Qualification Test of Eight JPL SR-28-3 Rocket Motors at Simulated Altitude*, AEDC-TR-66-221. Arnold Engineering Development Center, Arnold Air Force Station, Tenn., November 1966.

20. Anderson, R. G., *Applications Technology Satellite Apogee Motor (Description and Performance Characteristics)*, Technical Memorandum 33-340. Jet Propulsion Laboratory, Pasadena, Calif., Jan. 1, 1968.

21. Lee, T. P., *Handling Equipment for the Applications Technology Satellite (ATS) Rocket Motor*, Technical Memorandum 33-337. Jet Propulsion Laboratory, Pasadena, Calif., July 1, 1967.

NASA — JPL — Coml., L.A., Calif.